THESIS FOR THE DEGREE OF DOCTOR OF PHILOSOPHY (Ph.D.)

Adaptor proteins in the vascular endothelium

by Anita Boratkó

Supervisor: Csilla Csortos, Ph.D.

UNIVERSITY OF DEBRECEN

DOCTORAL SCHOOL OF MOLECULAR MEDICINE

Debrecen, 2013

Table of contents

Abbreviations

AJ - adherens junction

ALI - acute lung injury

ANK - ankyrin

ARDS - acute respiratory distress syndrome

bFGF - basic fibroblast growth factor

BPAEC - bovine pulmonary artery endothelial cells

BSA - bovine serum albumin

cAMP - cyclic adenosine monophosphate

CD31 - cluster of differenctiation 31

Cdk1 - cyclin dependent kinase 1

CPI-17 - C-kinase potentiated protein phosphatase-1 inhibitor

DAPI - 4’,6-diamidino-2-phenylindole

DMEM - Dulbecco's Modified Eagle Medium

DTT - dithiothreitol

E3KARP - Na^+/H^+ exchanger type 3 kinase A regulatory protein

EBP50 - ERM binding phosphoprotein of 50 kDa

EC - endothelial cell

ECIS - electric cell-substrate impedance sensing

ERM - ezrin-radixin-moesin

FBS - fetal bovine serum

FL - full length

FNTA - farnesyltransferase, CAAX box, alpha

GFP - green fluorescent protein

GNB2L1 - guanine nucleotide binding protein, beta polypeptide 2-like 1

GSK3β - glycogen synthase kinase 3 β

GST - glutathione S-transferase

HEAT motif - (Huntingtin, elongation factor 3, protein phosphatase 2A, yeast kinase TOR1)

HPAEC - human pulmonary artery endothelial cell

HRP - torma peroxidáz

HSP27 - heat shock protein 27

HUVEC - human umbilical vein endothelial cells

IKEPP - intestinal and kidney-enriched PDZ protein

IP - immunoprecipitation

IPTG - isopropyl β-D-1-thiogalactopyranoside

LAMR1 - non-integrin laminin receptor 1

LB - Luria-Bertani broth

LC-MS/MS - liquid chromatography-tandem mass spectrometry

M20 - 20 kDa small subunit of myosin phosphatase

MAPK - mitogen-activated protein kinase

MEM - minimal essential medium

MBS – myosin binding subunit

MLC20 - myosin light chain

MLCK - myosin light chain kinase

MP - myosine phosphatase

MT - microtubule

MYPT - myosin phosphatase target subunit

NHERF - Na^+/H^+ exchanger regulatory factor

NLS - nuclear localization signal

NMDA - N-methyl D-aspartate receptor

NR2B - subunit of NMDA receptor

PAGE - polyacrylamide gel electrophoresis

PECAM-1 : CD31, platelet endothelial cell adhesion molecule

PBS - phosphate buffered saline

PCR - polymerase chain reaction

PDZ - PSD-95; post-synaptic density protein 95 kDa, Dlg; *Drosophila* discs large protein, ZO1; zonula occludens 1

PDZK1 - PDZ-containing kidney protein 1

Pin1 - peptidylprolyl cis-trans isomerase

PKA - protein kinase A

PKC - protein kinase C

PMA - phorbol 12-myristate 13-acetate

PP1 - protein phosphatase 1

PP1c - catalytic subunit of PP1

PP2A - protein phosphatase 2A

PP2Aa - A subunit of PP2A

PP2Ac - catalytic subunit of PP2A

PP2B - protein phosphatase 2B, calcineurin

PP2C - protein phosphatase 2C

PPM - metal ion-dependent protein phosphatases

PPP - phosphoprotein phosphatases

PPP1R16B - protein phosphatase 1, regulatory subunit 16B

PR - phosphatase regulator

PTP - phosphotyrosine and dual specificity protein phosphatases

RACK1 - receptor for activated C kinase 1

S, Ser - serine

SDS - sodium dodecyl sulfate

SG2NA - S/G2 nuclear autoantigen

SLC9A3R1 - solute carrier family 9, subfamily A, member 3 regulator 1

SOC - super optimal broth with catabolite repression

T, Thr- threonine

TBS - Tris buffered saline

TER - transendothelial electrical resistance

TGF-β1 - transforming growth factor β1

TIMAP - TGF-β inhibited membrane-associated protein

TJ - tight junction

VEGF - vascular endothelial growth factor

WD repeat - tryptophan-aspartic repeat

WT - wild type

Y, Tyr - tyrosine

Introduction

Endothelial barrier function and endothelial cytoskeleton

Vascular endothelium is the layer of closely connected cells lining the inner surface of blood vessels. The major function of vascular endothelium is to provide a semipermeable barrier that controls exchange of fluids, nutrients, and metabolic wastes between blood and tissues while preventing pathogens from entering the latter. It regulates a variety of processes including blood perfusion, angiogenesis or metabolic and synthetic functions. Integrity of the endothelial cell (EC) monolayer as well as proper cytoskeletal structure of individual cells are required for appropriate EC barrier function. Cell-cell as well as cell-extracellular matrix interactions are crucial in the physiological role of EC. Two types of intercellular junctions have been characterized as cell–cell adhesive barrier structures in the vascular endothelium: adherens junctions (AJ) and tight junctions (TJ) [1-3].

Healthy endothelium is able to respond to physical and chemical signals by production of a wide range of factors that regulate vascular tone, cellular adhesion, thromboresistance, smooth muscle cell proliferation, and vessel wall inflammation. The well-established vascular endothelial barrier function is indicated by the balance of contractile and tensile forces. The shifted balance towards the contractile forces results in gap formation between the cells. Endothelial barrier dysfunction occurs in a variety of diseases and injurious conditions, including inflammation, trauma, ischemia, diabetes mellitus, multiple sclerosis, thrombosis and metastatic tumor development [4-6]. Loss of structural integrity of pulmonary endothelium plays a key role in the development of acute lung injury (ALI) and its most severe form, the acute respiratory distress syndrome (ARDS) [7, 8]. Lost ability of the alveoli to exchange oxygen and carbon dioxide, collapsion and fluid leakage (edema) into the alveoli are trademarks of these diseases [9].

Angiogenesis occurs in the early stages of carcinogenesis in response to vascular endothelial growth factor (VEGF) and basic fibroblast growth factor (bFGF) produced by the tumor or stromal cells. Unlike the normal processes, tumor-induced neovasculature produces a more fenestrated, thin-walled endothelium, partially due to

underdeveloped endothelial cell–cell junctions [10, 11]. In diabetes, a group of metabolic and inflammatory disorders are associated with the defects of insulin production. Diabetes is accompanied by cardiomyopathy and peripheral vascular diseases that originate from microcirculatory disturbances [12, 13]. Even though endothelial barrier dysfunction is a key element underlying many diseases, our knowledge is still limited about the precise mechanisms that regulate the endothelial barriers.

Endothelial cytoskeleton, microfilaments (or actin filaments), microtubules, and intermediate filaments, beside providing cells with shape, mechanical strength, polarity, and movement, are essential in the maintenance of EC barrier function. Each of the filaments are formed by polymerization. Dynamics, stability and function of EC cytoskeleton are highly dependent on a large number of accessory and regulatory proteins that control the localized assembly, connect filaments to each other and to other cellular components. Rearrangement of the cytoskeletal elements changes the shape of endothelial cells, and eventually, modifies vascular permeability. Treatment of EC with various bioactive agents, such as a thrombin-challenge, may induce dysfunction characterized by increased vascular permeability and the appearance of intercellular gaps. Cytoskeletal and cytoskeleton-associated proteins which are regulated by a phosphorylation/dephosphorylation dependent manner play a pivotal role within this process [2, 14, 15]. Many of these signaling pathways are not yet completely explored, despite the research already done on the topic.

Reversible protein phosphorylation

Reversible phosphorylation of proteins can be found almost in all biological activities of eukaryotic cells, such as controlling gene expression, protein complex formation, lipid raft assembly/disassembly, protein degradation, etc. It is one of the most important mechanisms influencing the activity of proteins. The enzymes that play a key role in reversible phosphorylation are protein kinases, responsible for the phosphorylation of proteins and protein phosphatases, which catalyze the cleavage of phosphate groups. There are more than 500 protein kinases in the human genome that catalyze the transfer of inorganic phosphate supplied by ATP onto serine (Ser; S), threonine (Thr; T) or tyrosine (Tyr; Y) amino acid residues of numerous proteins [16].

The specificity of protein phosphorylation is determined by the local amino acid sequence, consensus sequence, surrounding the S/T/Y residue to be phosphorylated [17]. These consensus amino acid sequences are unique recognition sequences for phosphorylation by individual kinases. In contrast, protein phosphatases do not strictly require such amino acid consensus sequences to identify substrates for dephosphorylation. The actual phosphorylation state of a protein is determined by the relative activities of a kinase and an opposing phosphatase. Activation of kinases may occur through phosphorylation or release from autoinhibition. Cofactors (e.g., Ca^{2+}, Mg^{2+}), inhibitory proteins, or recruitment to proximity of phospho-accepting substrates by scaffolding proteins can enhance or inhibit kinase activity. In addition, sub-cellular localization can also be an important factor in activation, for example, when protein kinase C (PKC) is activated, it translocates from the cytosol to the cell membrane [18].

Molecular and functional analyses of protein kinases and protein phosphatases in EC are equally important for the better understanding of the regulation of EC barrier function. The next chapter provides a brief overview on Ser/Thr specific protein phosphatases involved in EC barrier regulation.

Characterization of the Ser/Thr-specific protein phosphatases

Previously, classification of the Ser/Thr-specific protein phosphatases was based on their biochemical substrate specificity and sensitivity towards specific inhibitors [19, 20]. By recognition of the primary structures of phosphatases, the number of members increased, and also several new types of phosphatases were found. The new classification is based on molecular biological aspects, the amino acid sequence homology and the three-dimensional structure. Based on the structure of the catalytic subunit, three families of protein phosphatases were created: phosphoprotein phosphatases (PPP), metal ion-dependent protein phosphatases (PPM) and the phosphotyrosine and dual specificity protein phosphatases (PTP) [21]. Protein phosphatase 2A, 2B (PP2A and PP2B) and protein phosphatase 1 (PP1) catalytic subunits have similar amino acid sequences, while the protein phosphatase 2C (PP2C) is different. Accordingly, PP1, PP2A and PP2B belong to the phosphoprotein phosphatases group, while PP2C is a PPM group member. With exception of PP2C,

Ser/Thr specific phosphatases exist in oligomeric form, consisting of the catalytic subunit and one or more additional regulatory/targeting subunits.

In the next section the properties of PP1, PP2A and PP2B will be discussed.

Protein phosphatase 1

PP1 is one of the most conserved eukaryotic proteins and one of the most significant Ser/Thr phosphatases. It has been found in all cell types examined so far. Due to its broad substrate specificity it plays a major role in many physiological processes such as the cell cycle, apoptosis, and protein synthesis. The PP1 catalytic subunit has three isoforms: PP1α, PP1β (also known as PP1δ), and PP1γ. The isoforms show high amino acid sequence homology and they can not be distinguished by their substrate specificity *in vitro* [22]. The PP1γ isoform has two splice variants, PP1γ1 and PP1γ2. With the exception of the testis-specific PP1γ2, all isoforms are commonly expressed, but they have different subcellular localizations [23]. The crystal structure of PP1c was determined in a complex with its inhibitors or regulatory subunits [24-29].

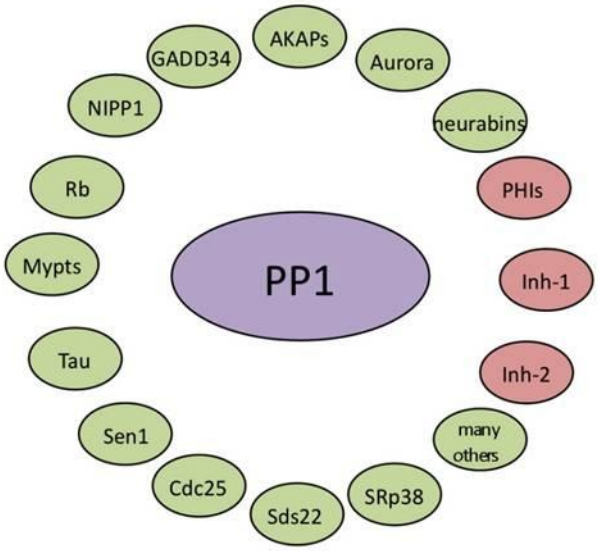

Figure 1. Protein phosphatase 1 is controlled by regulatory interactions (green) and inhibitors (red). *(Virshup et al, 2009, Molecular Cell [30])*

The catalytic subunit is able to catalyze the dephosphorylation of many proteins itself, however, in cells it exists as a holoenzyme, mostly in dimer form with one or more of the regulatory subunit(s). These regulatory subunits target the catalytic subunit

to the phosphoproteins, and control the substrate specificity of the holoenzyme [31, 32] (Fig. 1). The interaction between the catalytic and regulatory subunits of PP1 plays an important role in the regulation of the enzyme [21]. The primary structure of the more than 50 potential regulatory subunits shares no apparent similarities. Still, during mapping of the PP1 binding sites, a consensus (R/K)V*x*F sequence was found in the regulatory subunits, where *x* can be any residue [26, 31-33]. Binding of the catalytic subunit of PP1 to the (R/K)V*x*F motif is not associated with major conformational changes and does not have significant effects on the catalytic activity. This data suggests that this PP1-binding motif serves as an anchor for the initial binding of the regulatory subunits and promotes the binding of secondary sites, which often bind with lower affinity but affect the activity and substrate specificity of PP1 [33, 34].

Protein phosphatase 2A

PP2A is a heterotrimeric holoenzyme with a very diverse structure. As a consequence of this diversity, PP2A is involved in many biological processes, including cell cycle, growth, heat shock process, signal transfer, cell transformation, DNA replication or apoptosis [35-37]. The PP2A trimer consists of a catalytic subunit and two regulatory proteins, PR65 (or A) and the B subunit (Fig. 2).

The catalytic C subunit (PP2Ac) has two isoforms (α and β) in mammalian tissues [38]. In the early embryonic stage of development, the two isoforms have different intracellular localizations and expression levels, but have the same catalytic activity [39]. Expression of the catalytic subunit is regulated by an autoregulatory process, which keeps the amount of protein at a constant level. The autoregulation exist at the translational level and does not affect transcription [40]. Nonetheless, overexpression of PP2Ac became possible by addition of an N-terminal influenza hemagglutinin peptide modification [41].

The PR65 or A subunit has a structural function, it is strongly bound to the catalytic subunit of the enzyme and thereby forms a core dimer of PP2A which is connected to the third variable component, the B subunit. In mammals, two isoforms of the A subunit have been identified, which are 86% identical in their primary sequence. Northern analysis, using RNA isolated from several human cell lines, indicated that the Aβ isoform has a lower expression level than the Aα [42]. However, Aβ has been

shown to be mutated in several human cancers [43]. The cancer associated mutant Aβ isoform is unable to bind to the B or the C subunit [44]. These results suggest that the Aβ isoform may have a specific role in the regulation of cell growth/proliferation. The A subunit can associate with other proteins as well, engaging PP2A in specific signaling pathways [45-47]. It should also be mentioned, the substrate specificity of the dimer form of PP2A (A and C subunit) is determined by the A subunit [48].

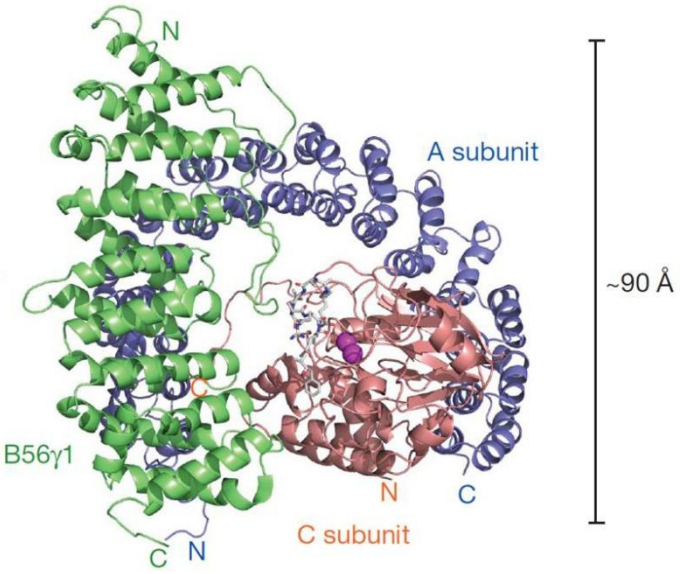

Figure 2. Crystal structure of the Aα-B56γ1-Cα heterotrimeric PP2A holoenzyme.
The scaffold Aα subunit, catalytic Cα subunit and regulatory B56γ1 subunit are coloured in blue, orange and green, respectively.
(Uhn Soo Cho & Wenqing Xu, 2007, Nature [49])

Within the amino acid sequence of the 65 kDa subunit, 15 repeat units have been identified, which are called HEAT motifs [50]. Data obtained from the crystal structure of the protein confirmed the previous hypothesis, that the α-helical structures in the 2-2 repeating units are arranged so that the tertiary structure of the protein is elongated and asymmetric, similar to the letter C [51]. Regulatory B subunits and viral antigens associate with the N-terminal 1-10 HEAT motifs, while the catalytic C subunit binds to the repeating units 11-15 at the C-terminus [45, 46].

The third subunit of the holoenzyme occurs in many molecular weight forms and it is generally called B subunit (Fig. 3). Individual B subunits are classified as members of one of four subfamilies B, B', B" or B'". Protein structure or function of the subfamilies do not show any similarities. The diversity is further increased by the multiple isoforms that can be found within the subfamilies. The various B subunits

determine the substrate specificity and intracellular localization of the PP2A holoenzyme. Within each B subfamily, the members contain a highly conserved region (80% identity), which is located at the central part of the proteins, whereas the C- and N-terminals are different. This implies that the conservative regions play a role in the binding of the A and C subunit, while the various ends are responsible for the divers functions.

The 55 kDa B subfamily or PR55 is encoded by four genes in mammals, therefore four isoforms α, β, γ, and δ are known. The PR55α and PR55δ isoforms are found in most tissues, while the PR55β and PR55γ are mainly found in the brain. PR55α and PR55β are localized in the cytosol, while PR55γ and PR55δ in the cytoskeleton [52-55].

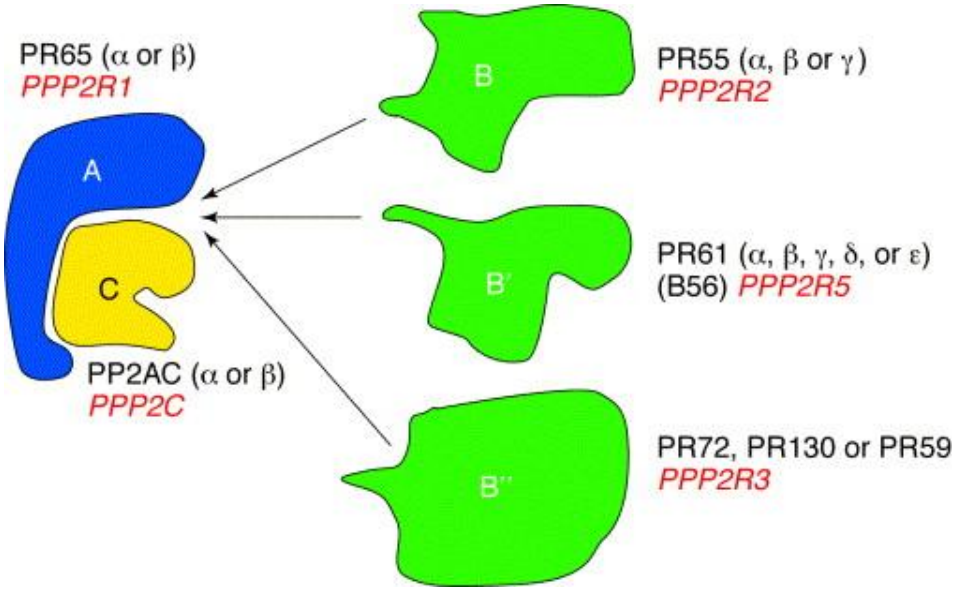

Figure 3.Mammalian protein phosphatase 2A holoenzymes.
(Millward et al, 1999, Trends in Biochemical Sciences [56])

The B' or PR61 subfamily (also named as B56) consists of at least five different gene products, which are indicated by α, β, γ, δ, and ε [57-63]. The human gene B'β encodes two isoforms, β1 and β2, while B'γ has at least three different splice variants. PR61α, PR61β and PR61ε are found in the cytoplasm, while PR61γ1, PR61γ2, PR61γ3 are in the nucleus. PR61δ is localized both in the nucleus and the cytoplasm. PR61α and PR61γ1-3 occur in large quantities in the heart and in the skeletal muscle, PR61β and PR61δ are primarily present in the brain [57-59]. All PR61 proteins but PR61γ1 are phosphoproteins [64].

PR72, PR130, and PR59 belong to the B" family [65-67]. It is likely that PR72 and PR130 are alternative splicing products of the same gene. PR130 was originally cloned from human brain cDNA library [68]. PR59 shares sequence homology with PR72, but differs in its expression pattern and its functional properties. *In vivo* studies revealed that PR59 associates specifically with a phospho-retinoblastoma associated protein [67].

Striatin and S/G2 nuclear autoantigen (SG2NA) are highly related WD40 repeat proteins and belong to the B"' family [69]. Striatin has been reported to associate with the post-synaptic densities of neurons, whereas SG2NA is a nuclear protein expressed primarily during the S and G2 phases of the cell cycle.

Protein phosphatase 2B

PP2B (also called calcineurin) is a Ca^{2+}-dependent enzyme and belongs to the PPP family of phosphatases. The enzyme is a heterodimer, it consists of two tightly connected subunits, a catalytic subunit (calcineurin A) and a Ca^{2+}-binding regulatory subunit (calcineurin B) [70, 71]. Calcineurin A has three isoforms produced by three different genes, while calcineurin B is highly conserved and encoded by a single gene [72]. The A subunit contains the catalytic domain in its N-terminal region, while its C-terminal region contains binding sites for the B subunit and calmodulin, and an autoinhibitory domain as well. Calcineurin is involved in the regulation of several cellular events, such as apoptosis, gene regulation, T-cell activation, etc. [73].

Role of reversible phosphorylation in EC cytoskeleton regulation

The fast and flexible change of the cytoskeleton is crucial in many cellular events such as cell motility and cell division. The organization and the plasticity of the cytoskeleton is determined primarily by the forces or tension generated within the cytoskeleton. Reversible phosphorylation of cytoskeletal and cytoskeleton-associated proteins is a significant element of cytoskeletal changes and endothelial barrier function regulation.

Phosphorylation of the myosin light chain (MLC20) at Ser19 side chain results in cell contraction, stress fiber formation, and intercellular gap formation. The phosphorylation is catalysed by the high molecular weight (210 kDa) Ca^{2+}-calmodulin dependent myosin light chain kinase (MLCK), which is highly homologous with the smooth muscle MLCK. In endothelial cells dephosphorylation of MLC20 is catalysed by myosin phosphatase, a type 1 phosphatase [74, 75]. Binding of thrombin to the protease activated receptor 1 increases the intracellular Ca^{2+} level, the calcium calmodulin complex binds to and activates MLCK that catalyzes the phosphorylation of MLC20. In addition, the level of MLC20 phosphorylation may increase by the activation of the Rho/Rho-kinase pathway, which inhibits the myosin phosphatase and consequently disrupts the equilibrium between kinase-phosphatase activities [76].

Myosin phosphatase (MP)

Myosin phosphatase is a key regulator of endothelial barrier function. It was originally purified from chicken gizzard myofibrils and was shown to be composed of three subunits - the delta isoform of the PP1 catalytic subunit (PP1cδ), the 130 kDa myosin binding subunit (MBS) and a 20 kDa small subunit (M20) which form a heterotrimer [77]. MBS is also called MYPT1, myosin phosphatase targeting subunit 1. It has two isoforms (110 kDa and 130 kDa) encoded by the same gene [78]. The MYPT gene seems to be a housekeeping gene since it is widely expressed in many tissues, although it is present at higher concentrations in smooth muscle [79, 80]. MYPT1 interacts with PP1cδ via its N-terminal PP1c binding motif, and the C-terminus binds M20. Two nuclear localization signals (NLS) and seven further ankyrin repeats were identified within the sequence [81].

Several proteins have been identified to bind to MYPT1, from these the phosphorylated myosin-MYPT1 interaction is one of the most well studied. One binding site for myosin is within the C-terminal half of the ankyrin repeats [82]. Phosphorylation of the ankyrin repeats by PKC was shown to attenuate binding of phosphorylated MLC20 to the N-terminal fragment of MYPT1, implying that the interaction may be regulated via phosphorylation [83]. Phosphorylation of an inhibitory Thr696 site on the C-terminal half of MYPT1 results in inhibition of PP1c activity. Several kinases can phosphorylate Thr696, including Rho-kinase that serves as an

important participant in smooth muscle function [84]. Another well studied regulation of MP is its modulation by small inhibitory proteins. CPI-17 is a phosphorylation-dependent inhibitory protein of MP [85]. It can inhibit the activity of the MP holoenzyme and phosphorylation of CPI-17 by PKC at Thr38 enhances its inhibitory potency [85].

MYPT family proteins

Within the MYPT family there are four other members having high similarity to MYPT1, namely MYPT2, MBS85, MYPT3, and TIMAP (Fig. 4).

MYPT2 was cloned from human brain library using a cDNA probe based on MYPT1 [86]. While MYPT1 is expressed in smooth muscle and in most of the nonmuscle cells, MYPT2 is expressed predominantly in skeletal and cardiac muscles and in brain. MYPT2 has two splicing variants, a smaller MYPT2A and a longer MYPT2B. The two isoforms differ at their C-terminal end [87]. A third, putative regulatory subunit, called myosin binding subunit 85 (MBS85) was cloned from human genomic library [88]. It is ubiquitously expressed, and similarly to other members of the MYPT family it contains a PP1c binding motif, ankyrin repeats, and also an inhibitory phosphorylation site equivalent to Thr696 in human MYPT1.

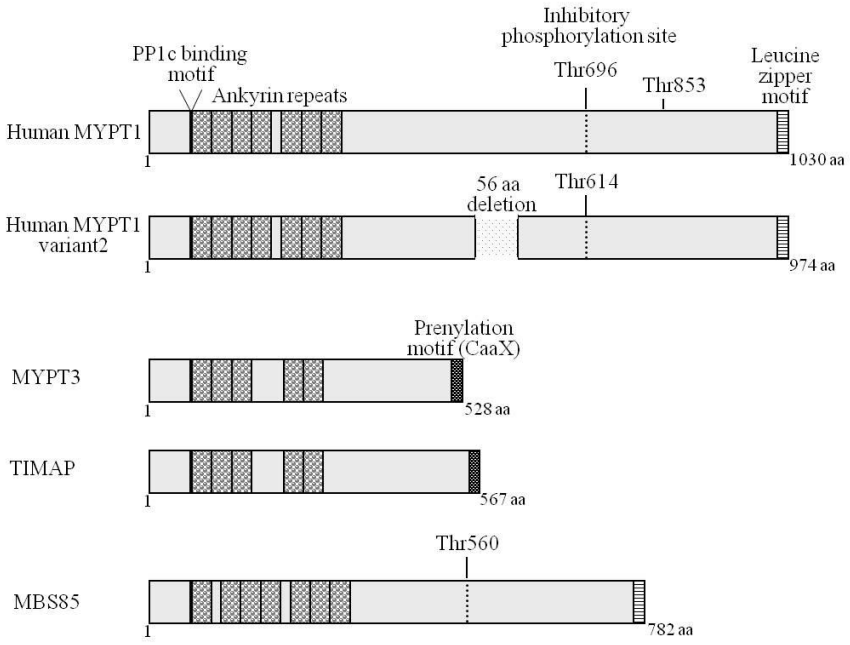

Figure 4. Structural features of MYPT1 and MYPT1-related proteins.
(Csortos et al., 2007, Am J Physiol Lung Cell Mol Physiol [89])

MYPT3 was cloned from an adipocyte cDNA library [90]. It shares some structural features with MYPT1/2, namely N-terminal ankyrin repeats and preceding PP1c binding motif; on the other hand, its size is considerably smaller, 58 kDa, and it has a C-terminal prenylation motif suggesting possible membrane association. The regulatory phosphorylation site found in other MYPT family members is not present in MYPT3 [90].

MBS85 most closely resembles MYPT2, but little is known about its physiological function [88].

Another regulator of PP1c, TIMAP, will be discussed in the next chapter.

TIMAP, a MYPT family regulator subunit

TIMAP (TGF-β inhibited membrane-associated protein) was originally identified in glomerular endothelial cells by representational difference analysis. It is highly expressed in all cultured endothelial and hematopoietic cells compared to non-endothelial cells. Immunofluorescence studies of rat tissues revealed that the protein mainly localizes in the vascular endothelium. Based on its structural features TIMAP has been considered as a member of the MYPT family of the regulatory subunits of PP1 [91]. TIMAP and MYPT3 are the most closely related members within the family. Both proteins contain ankyrin repeats, a PP1c binding motif and a C-terminal prenylation motif; the latter one mediates their association with the plasma membrane [91]. A bipartite nuclear localization signal is also present in TIMAP; accordingly, it was detected in the nucleus of vascular endothelial cells [92], but its significance is not known yet.

In view of the fact that TIMAP mRNA synthesis is down-regulated by TGF-β1 [91], the transcriptional repression of TIMAP could be an important component of the TGF-β1 pathway, as well as apoptosis and endothelial barrier integrity. Although TIMAP is most abundant in endothelial cells, little is known about its exact function and its interacting partners. Specific protein-protein interaction was demonstrated between TIMAP and PP1cδ; and the effect of TIMAP phosphorylation on this interaction was also characterized [92, 93]. Studies made on TIMAP-depleted human

pulmonary artery endothelial cell (HPAEC) monolayers indicated that TIMAP has a positive regulatory effect on the endothelial barrier function. In the absence of TIMAP the effects of barrier function compromising agents (thrombin and nocodazole) were enhanced and the effects of barrier function protecting agents (sphingosine-1-phosphate and ATP) were attenuated [92]. Further studies revealed that the ERM (ezrin-radixin-moesin) proteins, which connect actin filaments to the plasma membrane, are interacting protein partners of TIMAP and they were identified as TIMAP-PP1c substrates [92, 93]. The involvement of TIMAP in protein kinase A (PKA)-mediated ERM phosphorylation/dephosphorylation as part of endothelial cell barrier protection by TIMAP was also shown [92, 93].

The non-integrin laminin receptor 1 (LAMR1), which is involved in the regulation of cell motility, was described to interact with TIMAP. They co-localize at the plasma membrane of endothelial cells, and TIMAP regulates the dephosphorylation of LAMR1 by PP1c [94]. Several potential TIMAP-binding proteins were identified by bacterial two-hybrid screening. Among them are the cysteine and glycine rich protein 1 and the eukaryotic translation elongation factor 2, which are both involved in the organization of the actin cytoskeleton. However, these interactions in mammalian cells have not been verified yet [95].

Role of PP2A and PP2B in the endothelial cytoskeleton regulation

Much less is known about the involvement of PP2A and PP2B activity in the regulation of cytoskeletal structure compared to PP1, although many data suggest their important role. Some actin-binding proteins (caldesmon, cofilin), the small heat shock protein 27 (HSP27) and the microtubule-associated protein, tau, are cytoskeletal targets of PP2A [96-99]. Co-localization of PP2A with microtubules was shown in unstimulated EC, but exposure to carcinoma-derived angiogenic products resulted in a more diffuse distribution of PP2A and a loss of filamentous tubulin [100]. Overexpression of the A and C subunit of PP2A dramatically reduced thrombin- or nocodazole-induced F-actin stress fiber formation and microtubule (MT) dissolution and attenuated the phosphorylation of HSP27 and tau. It also attenuated thrombin- or nocodazole-induced decrease of transendothelial electrical resistance [101].

In vitro experiments suggest that PP2A is responsible for the dephosphorylation of CPI-17 in smooth muscle [102]. Therefore, PP2A might be involved in the regulation of myosin phosphatase. Furthermore it was observed that inhibition of PP2A by okadaic acid induced phosphorylation and translocation of MYPT1 [103].

Human endothelium expresses all three isoforms of calcineurin A, the catalytic subunit of PP2B [104, 105]. In pulmonary artery EC, PP2B associates with the detergent-insoluble actin-enriched cellular fraction. Thrombin treatment considerably increased the activity of PP2B and the activation was correlating with the phosphorylation of the PP2B catalytic subunit [106]. PP2B is also involved in the recovery from thrombin-induced EC dysfunction. Inhibition of PP2B caused prolonged contractile effect of thrombin, while overexpression of constitutively active calcineurin resulted in reduced thrombin-induced stress fiber formation [105]. Most recently it was shown that PP2B may improve endothelial barrier function via inducing dephosphorylation of cofilin and by interaction with MYPT1. PP2B activates myosin phosphatase through dephosphorylation of MYPT1 at Thr696, thereby affecting actin polymerization and decreasing myosin phosphorylation [107].

Adaptor proteins

The specific and well-constructed response of cells to external stimuli requires the integration of multiple signaling pathways. Stimulation of cell surface receptors initiates cellular signals, which may require recruitment of protein binding partners to specific subcellular domains, such as the membrane. Adaptor proteins mostly function as flexible molecular scaffolds. They tend to lack enzymatic activity, but instead, mediate specific protein-protein interactions and facilitate the formation of larger signaling complexes. By linking specific proteins together, cellular signals can be propagated that produce an appropriate response from the cell to the environment. Some adaptor proteins are expressed in all tissues, while the expression of other adaptor proteins is restricted to specific tissues. Adaptor proteins usually contain several protein binding modules (domains) within their structure. The specificity of signaling is achieved by the type of these domains, which predicts the identity of binding partners, as well as the subcellular localization.

Among the many interaction domains, PDZ domains are one of the most frequently encountered ones. The name PDZ is derived from the first three proteins in which these domains were identified: PSD-95 (post-synaptic density protein 95 kDa), Dlg (*Drosophila* discs large protein), and ZO1 (zonula occludens 1). The PDZ domain is approximately 90 residues long and its function is the mediation of protein-protein interactions by binding to the C-terminus of their target protein in a sequence-specific fashion. It has also been shown that some PDZ domains can bind other PDZ domains, either in a head-to-tail fashion, or in a back-to-back fashion [108-110].

Other widely existing protein motifs are the ankyrin repeats. Each ankyrin repeat consists of 30-34 amino acid residues and exhibits a helix-turn-helix conformation stabilized by intra- and inter-repeat hydrophobic and hydrogen bonding interactions. Ankyrin repeat proteins do not recognize specific sequences, the interacting residues are discontinuously dispersed into the entire molecule of both the scaffold protein and its partner [111, 112].

WD-repeat proteins belong to a large and conservative protein family. They contain several, approximately 40 amino acid repeats that usually end with tryptophan-aspartic acid (WD). All WD-repeat proteins are considered to form a circularized β-propeller structure as established by the crystal structure of the G protein beta subunit [113, 114].

NHERF1/EBP50 adaptor protein

ERM binding phosphoprotein of 50 kDa (EBP50) is a member of the Na^+/H^+ exchanger regulatory factor (NHERF) family which consists of four related PDZ domain containing scaffolding proteins termed as NHERF1/EBP50, NHERF2/E3KARP, NHERF3/PDZK1, and NHERF4/IKEPP [115] (Fig. 5). NHERF1 was originally recognized as Na^+/H^+ exchanger-3 binding partner [116], and it has later been identified as an ERM binding phosphoprotein [117]. NHERFs are highly abundant in the epithelium and their role in Na^+/H^+ exchanger-3 regulation is well established [118], therefore EBP50 was characterized mainly in polarized epithelial cells up to present.

EBP50 has two PDZ domains and a C-terminal ERM-binding domain. It is believed that EBP50 forms bridges among plasma-membrane and cytoskeleton proteins through these

domains. Its function, for example, in microvillar assembly as part of the PDZK1/NHERF3-EBP50-ezrin complex was studied in detail [119]. It seems that EBP50 binds ezrin specifically in epithelial cells and there is an interdependence of EBP50 and ezrin for their apical localization [120, 121]. However, a recent paper also describes the effect of EBP50-moesin interaction in the contractile response of artery [122]. Most of the interacting proteins bind to the first PDZ domain, only a few partners described so far relate with the second PDZ, like beta-catenin [123]. Self association of EBP50 through the PDZ domains [124], and the intramolecular interactions between the PDZ2 and C-terminal domains of EBP50 result in an autoinhibition of complex formation with other protein partners [125]. Protein-protein interactions with the other members of the NHERF family [119, 126] have been described as well.

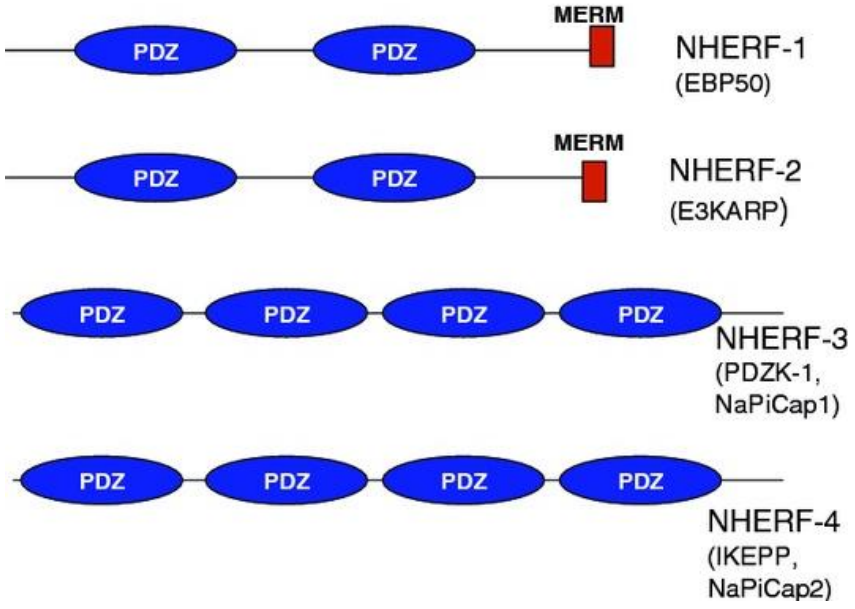

Figure 5. The NHERF family of proteins.
(MERM =Moesin, Ezrin, Radixin, Merlin-binding domain)
(Cunningham et al., 2010, Urol Res [127])

EBP50 is a subject to phosphorylation by several kinases and these modifications have been suggested to alter its binding activity. Oligomerization of EBP50 was shown to be regulated via site-specific phosphorylation. Phosphorylation by PKC on Ser^{337}/Ser^{338} enhances the oligomerization [128]; and G protein-coupled receptor kinase 6 was identified as the kinase responsible for constitutive phosphorylation of Ser^{289} which facilitates PDZ domain mediated interactions [126, 129]. During mitosis EBP50 is phosphorylated on Ser^{279} and Ser^{301} by cyclin dependent

kinase 1 (Cdk1) and that phosphorylation inhibits its oligomerization, but allows association with Pin1, a peptidylprolyl isomerase [130]. In addition, it was shown by S77A and S77D substitutions that phosphorylation of the PDZ1 domain attenuates co-localization of EBP50 with cortical actin [131]. In agreement with the outcome of phosphorylation on oligomerization, it was demonstrated that PKC activation and EBP50 phosphorylation promotes microvili rearrangement [132]. A recent study also showed that phosphorylation of EBP50 by PKC within the PDZ2 domain reduced its association with the cystic fibrosis transmembrane conductance regulator [133]. On the other hand, phosphorylation of EBP50 by Cdk1 inhibits its role in microvilli formation in interphase but not in mitotic cells [132].

Dephosphorylation of the above mentioned sites is an equally important element of the reversible phosphorylation, however, phosphatases specific for EBP50 have not been identified yet.

RACK1 adaptor protein

RACK1 is a highly conserved scaffolding/anchoring protein that contains seven WD repeats predicted to form a seven-bladed propeller structure (Fig. 6). The protein was named Receptor for Activated C Kinase 1, given the association of RACK1 with the active conformation of PKCβII [134-136]. Now it is well known that RACK1 has several other interacting partners [137-141]. Due to its structural features it has the ability to interact simultaneously with several signaling molecules [142] which suggests the possibility for multiple protein interactions. Human RACK1 is encoded by the gene GNB2L1 (guanine nucleotide binding protein, beta polypeptide 2-like 1) [143, 144]. RACK1 is highly expressed in most tissues [145]. It was also observed that changes in the expression level of RACK1 is associated with cancer [146-148].

Figure 6. Crystal structure of RACK1.
Seven-bladed β-propeller structure is indicated, each repeat with different colors
(Adams et al., 2011, Cell Communication & Signaling [149])

The role of RACK1 was identified in many signaling pathways. Upon activation of PKC with PMA, RACK1 co-localizes with the Src tyrosine kinase at the plasma membrane [150] and RACK1 functions as a substrate, as well as a binding partner and inhibitor of the kinase [150, 151]. In response to stress, RACK1 is sequestered into stress granules and inhibits apoptosis by suppressing stress responsive MAPK pathways [152]. The cAMP/PKA signaling pathway is also tightly linked to RACK1 [153-155]. Activation of the pathway in hippocampal neurons leads to the dissociation of RACK1 from Fyn kinase, results in the phosphorylation of the NR2B subunit of N-methyl D-aspartate receptor (NMDA) and the enhancement of the channel's activity [156]. RACK1 interacts with several transmembrane receptors including the insulin-like growth factor receptor I [157, 158], β-integrin receptor [159], androgen receptor [137], as well as several ion channels [160, 161].

Recently, it was also demonstrated that RACK1 is a core component of the eukaryotic 40S ribosomal subunit [162-164]. It is localized on the head region close to the mRNA exit channel, suggesting a physical link between the eukaryotic ribosome and cell signaling pathways *in vivo* [165]. In accord with its structural features, all these recent findings imply the involvement of RACK1 in numerous signaling pathways.

Aims of the study

Endothelial cytoskeleton structure and the vascular barrier are critical in the maintenance of proper lung function. A significant and sustained increase in vascular permeability is a hallmark of acute inflammatory diseases. Approaches designed to understand endothelial cell paracellular gap formation and barrier function have revealed the complexity of these processes as the involvement of various signaling pathways were identified, but our knowledge about their regulation is still limited. ERM proteins are actin-binding linkers connecting F-actin and the plasma membrane, either directly or indirectly via scaffolding proteins. EBP50, an adaptor phosphoprotein, was shown to interact with ERM in epithelial cells, but it has not been studied in the endothelium yet. TIMAP protein is a targeting partner of type 1 protein phosphatase and regulates the phosphorylation level of ERM proteins in pulmonary EC. TIMAP is highly expressed in endothelial cells compared to other cell types suggesting its importance in the endothelium. Indeed, previous results of our research group revealed that it has a crucial role in the regulation of endothelial barrier. Thus, exploring protein-protein interactions of TIMAP is essential to understand its unique role in this cell type.
Our specific aims listed below are divided into two major parts of investigation of EBP50 (part A) and identification of a new protein partner of TIMAP (part B).

Part A: - detection of EBP50 protein in endothelial cells and verification of its phosphorylation during mitosis
- investigation of the effect of phosphorylation on the localization of EBP50
- identification of the phosphatase that plays a role in the dephosphorylation of EBP50

Part B: - identification of a new TIMAP interacting protein in endothelial cells
- structural domain mapping of the interaction
- investigation of the physiological role of the interaction.

Materials and methods

Materials

Chemicals

Materials were obtained from the following sources: thymidine, nocodazole paraformaldehyde, dimethylsulfoxide, bovine serum albumin, Anti-V5 Agarose Affinity Gel antibody produced in mouse, forskolin, anti-FNTA, AR-A014418, sphingosine-1-phosphate: Sigma (St Louis, MO); anti-PP1 catalytic subunit antibody: R&D System (Minneapolis, MN); anti-SLC9A3R1 antibody: Abgent (San Diego, CA); anti-PP2A B subunit (most specific for Bα) and anti-NHERF1(A310) antibodies, anti-rabbit IgG HRP-linked and anti-mouse IgG HRP-linked secondary antibodies, anti-CD31(PECAM-1): Cell Signaling Technology, Inc. (Beverly, MA); anti-PP2A B' subunit, monoclonal anti-PP2Ac, monoclonal anti-β-tubulin antibodies: Upstate Biotechnology (Lake Placid, NY); anti-NHERF2 (C-2), anti-lamin A/C (H-110) antibodies: Santa Cruz Biotechnology, Inc. (Santa Cruz, CA); mouse anti-GFP Invitrogen Corporation (Carlsbad, CA); rabbit anti-GFP: Merck Millipore (Billerica, MA); monoclonal anti-c-myc antibody, custom-made rabbit polyclonal anti-TIMAP antipeptide (NGDIRETRTDQENK) antibody: Zymed laboratories (San Francisco, CA); anti-RACK1 antibody: BD Transduction Laboratories (Heidelberg, Germany); Protease Inhibitor Cocktail Set III EMD Biosciences (San Diego, CA); Alexa 488-, Alexa 594-conjugated secondary antibodies, Texas Red-phalloidin and ProLong Gold Antifade medium with DAPI: Molecular Probes (Eugene, OR), FuGENE® HD Transfection Reagent: Roche (South San Francisco, CA); pCMV-Myc and pcDNA3.1 V5-His, pEGFP-C1, pGEX-4T-2, pGEX-4T-3 vectors: Clontech Laboratories, Inc. (Mountain View, CA); restriction enzymes, T4 DNA ligase, Phire® DNA Polymerase and Phusion® High-Fidelity DNA Polymerase: Thermo Scientific, Inc. (Vantaa, Finland). Substances for cell culturing were from Invitrogen Corporation (Carlsbad, CA). All other chemicals were obtained from Sigma (St Louis, MO).

Buffers, solutions

1xTAE: 4mM Tris, 0.1mM EDTA, 0.114% acetic acid, pH 8.5

2xYTA: 16g/l trypton, 10g/l yeast extract, 5g/l NaCl, pH 7,0

5xSDS sample buffer: 50% glycerin, 10% SDS, 310mM Tris, 100mM DTT, 0.01% bromophenol blue

Blotting buffer: 25mM Tris, 192mM glycine, 0.285mM SDS

IP buffer: 20mM Tris-HCl (pH 7.4), 150mM NaCl, 2mM EDTA, 2mM sodium vanadate, 1% NP-40

LB (Luria-Bertani) agar: 10g/l tryptone, 5g/l yeast extract, 10g/l NaCl, 1.5% agar, pH 7.0

LB medium: 10g/l tryptone, 5g/l yeast extract, 10g/l NaCl, pH 7.0

PBS: 20mM Na_2HPO_4, 115mM NaCl, pH 7.4

SOC: 20g/l tryptone, 2g/l yeast extract, 0.6g NaCl, 10mM $MgCl_2$, 10mM $MgSO_4$, 20mM glucose, pH 7.0

TBS: 25mM Tris-HCl, 150mM NaCl, pH 7.5

TBST: 25mM Tris-HCl, 150mM NaCl, 0.1% Tween-20, pH 7.5

Transfer buffer: 120mM Tris-HCl, 40mM glycine, 20v/v% methanol

Bacterial strains

Esherichia coli BL21 (DE3) suitable for protein expression (Invitrogen Corporation, Carlsbad, CA)

Esherichia coli JM109 suitable for cloning (Invitrogen Corporation, Carlsbad, CA)

Oligonucleotides

Oligonucleotides were synthesized by Integrated DNA Technologies (Coralville, IA).

Construct	**Primers**	**Vector**
TIMAP WT FL	F: 5'-TGGGATCCATGGCCAGTCACGTGG-3' R: 5'-CGCTCGAGTCCTAGGAGATACGGCAAC-3'	pGEX-4T-3
TIMAP 1-290	F: 5'-TGGGATCCATGGCCAGTCACGTGG-3' R: 5'-AACTCGAGCTATGCACTGAGACTAGCTC-3'	pGEX-4T-3
TIMAP 1-165	F: 5'-TGGGATCCATGGCCAGTCACGTGG-3' R: 5'-TTCTCGAGCTACGAGTTGACAGCAGGCA-3'	pGEX-4T-3

TIMAP 165-290	F: 5'-TAGGATCCGATGGGAACATGCCATATGA-3' R: 5'-AACTCGAGCTATGCACTGAGACTAGCTC-3'	pGEX-4T-3
TIMAP 35-165	F: 5'-TGGGATCCAAGAAATGGGCACAGTACG-3' R: 5'-TTCTCGAGCTACGAGTTGACAGCAGGCA-3'	pGEX-4T-3
TIMAP 52-165	F: 5'-TTGGATCCGAGCGGAAGCGCAGCA-3' R: 5'-TTCTCGAGCTACGAGTTGACAGCAGGCA-3'	pGEX-4T-3
TIMAP 67-165	F: 5'-TTGGATCCGAGGCCAGCGTGGC-3' R: 5'-TTCTCGAGCTACGAGTTGACAGCAGGCA-3'	pGEX-4T-3
TIMAP 291-567	F: 5'-TTGGATCCAGGACATCCATGGATGAGATG-3' R: 5'-CGCTCGAGTCCTAGGAGATACGGCAAC-3'	pGEX-4T-3
TIMAP 291-564	F: 5'-TTGGATCCAGGACATCCATGGATGAGATG-3' R: 5'-TTCTCGAGCTAACAGCCATGCACCTTCT-3'	pGEX-4T-3
TIMAP 331–567	F: 5'-TAGGATCCTCCTTGAGCCGGAGGACCTCCAG-3' R: 5'-CGCTCGAGTCCTAGGAGATACGGCAAC-3'	pGEX-4T-3
TIMAP 331–567 S333A/S337A	F: 5'-TAGGATCCTCCTTGGCTCGGAGGACCGCTAG-3' R: 5'-CGCTCGAGTCCTAGGAGATACGGCAAC-3'	pGEX-4T-3
TIMAP 331–567 S333D/S337D	F: 5'-TAGGATCCTCCTTGGACCGGAGGACCGACAG-3' R: 5'-CGCTCGAGTCCTAGGAGATACGGCAAC-3'	pGEX-4T-3
TIMAP WT FL	F: 5'-GGCTCGAGCTATGGCCAGTCACGTGGACCT-3' R: 5'-CGCGGATCCCTAGGAGATACGGCAACAGCC-3'	pEGFP-C1
TIMAP Δpp1c	F: 5'-GGCTCGAGCTATGAGCGTGGCCCTGCTGG-3' R: 5'-CGCGGATCCCTAGGAGATACGGCAACAGCC-3'	pEGFP-C1
EBP50 FL	F: 5'-GCCTCGAGTTATGAGCGCGGACGCGG-3' R: 5'-ATATGCGGCCGCTCAGAGGTTGCTGAAGAGTTC-3'	pCMV-Myc
EBP50 S288D/S310D	F1: 5'-GCCTCGAGTTATGAGCGCGGACGCGG-3' R1: 5'-GTGTCACTGGAGGCGGTTCTTGCCAGGGGTGGCATGG GGTCTC-3' F2: 5'-CAGTGACACCAGTGAGGAGCTGAATTCCCAAGACGACC CCA-3' R2: 5'-ATATGCGGCCGCTCAGAGGTTGCTGAAGAGTTC-3'	pCMV-Myc
RACK1 WT FL	F: 5'-GTGTCGACTATGACTGAGCAGATGACCCT-3' R: 5'-AAGCGGCCGCCTAGCGTGTGCCAATGGT-3'	pGEX-4T-2
RACK1 1–180	F: 5'-GTGTCGACTATGACTGAGCAGATGACCCT-3' R: 5'-AAGCGGCCGCCTAAGCCAGGTTCCATACCT-3'	pGEX-4T-2
RACK1 137–317	F: 5'-GTGTCGACTGTGTGCAAATACACTGTCCAG-3' R: 5'-AAGCGGCCGCCTAGCGTGTGCCAATGGT-3'	pGEX-4T-2

Table1. Oligonucleotides and vectors used for cloning

Recognition sequences of restriction endonucleases utilized in cloning are underlined. (F:forward primer, R: reverse primer, FL:full length)

RACK1 (GNB2L1)	F: 5'-GTGTCGACTATGACTGAGCAGATGACCCT-3' R: 5'-AAGCGGCCGCCTAGCGTGTGCCAATGGT-3'
TIMAP (PPP1RB16)	F: 5'-TGGGATCCGAGAATAAGGACCCTAACC-3' R: 5'-CGCTCGAGTCCTAGGAGATACGGCAAC-3'
PP2A B55 (PPP2R2A)	F: 5'-CAGCACCTTCCAGAGCCA-3' R: 5'-GGCAGATGCCCTCATGTC-3'

Table 2. Primers used for RT-PCR
(F: forward primer, R: reverse primer)

Methods

Cell cultures

Bovine pulmonary artery endothelial cells (BPAEC) (culture line-CCL 209) were obtained frozen at passage 8 (American Type Tissue Culture Collection, Rockville, MD), and were utilized at passages 17-22. MCF7 (catalogue No: 86012803) cells were obtained frozen at passage 11 (European Collection of Cell Cultures, Salisbury, UK). Cells were maintained at 37°C in a humidified atmosphere of 5% CO_2 and 95% air in MEM supplemented with 10% (v/v) fetal bovine serum (heat inactivated), 1% sodium pyruvate, 0.1 mM MEM non-essential amino acids solution. HeLa cells (catalogue No: 93021013) were obtained frozen at passage 4 (European Collection of Cell Cultures, Salisbury, UK) and maintained in DMEM supplemented with 10% (v/v) fetal bovine serum, 2 mM glutamine and 0.1 mM non-essential amino acids solution. Human Pulmonary Artery Endothelial Cells (HPAEC) (catalogue No: CC-2530) were obtained frozen at passage 3 (Lonza Group Ltd, Switzerland) and were cultured in EGM-2 Endothelial Cell Growth Medium-2 supplemented with 10% FBS and EGM-2 SingleQuots of Growth Factors. Cells were utilized at passages 5–7.

Cell synchronization

BPAEC were synchronized at G1/S phase using double thymidine block as follows. Cells were treated with 2mM thymidine for 16 h. After this first thymidine

block cells were released for 8 h and then treated with 2mM thymidine for 16 h again. G2/M phase cells were obtained by 14-16 h treatment with 80ng/ml nocodazole.

Transfection

To express recombinant wild type or mutant pCMV-myc EBP50, 1μg total DNA/3μl FuGENE® HD reagent was mixed and added to the culture plates containing cells at ~80% confluency according to the manufacturer's instruction. Cells were analyzed 24 h later.

HeLa cells were transfected with pEGFP-C1, pEGFP-C1 TIMAP WT or pEGFP-C1 TIMAP Δpp1c plasmids using Lipofectamine 2000 transfection reagent (Invitrogen Corporation, Carlsbad, CA) according to the manufacturer's instructions. After 24 hours cells were washed with PBS and used for immunoprecipitation.

Reverse transcription (RT) and polimerase chain reaction(PCR)

Total RNA was extracted from HPAEC using ZR RNA MicroPrep™ (Zymo Research Corporation, CA). cDNA was synthesized from 2μg of total RNA using 0.111μM oligo-dT primer and 200 U M-MLV reverse transcriptase (Promega Corporation, USA) with 5mM dNTP in 1x RT buffer. The reaction assay was incubated at 37°C for 1 hour.

Phire® or Phusion® High-Fidelity DNA Polymerases (Thermo Scientific, Inc.,Vantaa, Finland) were used for PCR. First step denaturation was set at 98°C for 1 minute. It was followed by 5 cycles of denaturation at 98°C for 10 sec, annealing for 10 sec, extension at 72°C for 30-60 sec, and by another 30 cycles, where the denaturation and extension was set at the same conditions, but the annealing temperature was changed. Different annealing temperatures were applied based on the actual melting points of primers to create the subcloning sites.

Coding regions of EBP50 (SLC9A3R1, NM_001077852), TIMAP (PPP1R16B, NM_015568), RACK1 (GNB2L1, NM_006098.4) were amplified using primer pairs as indicated in Table 2. The inserts were subcloned into the appropriate vectors then transformed into *E.coli* cells.

EBP50 S288D:S310D mutant was created using wild type EBP50 as a template and by oligonucleotides containing the mutant sequences. The PCR products were ligated using the Nmuci restriction site within the sequences, then subcloned into *E.coli*.

Restriction digestion

FastDigest restriction enzymes (Thermo Fisher Scientific, Inc., Waltham, USA) were employed. The amounts of restriction enzymes used were kept lower than 10% of the total reaction volume.
Recognition sites of the enzymes are as follows:
BamHI: G↓GATCC
Nmuci (Tsp45I): ↓GTSAC (S = G or C)
NotI: GC↓GGCCGC
SalI: G↓TCGAC
XhoI: C↓TCGAG

Agarose gel electrophoresis

To separate DNA fragments 0.8-1.2% agarose gels were used. Agarose was dissolved in 1xTAE by heating and 10 000X GelRed Nucleic Acid Gel Stain solution (Izinta, Hungary) was added to visualize the DNA. Samples were mixed with 6x DNA loading buffer (Promega Corporation, USA), loaded into the gel and the DNA fragments were separated at 80V in 1xTAE buffer. Fragments were cut out on an UV illuminator table (Hoefer Inc., Holliston, MA).

DNA extraction from agarose gel

DNA was extracted from agarose gel using GeneJET gel extraction kit (Thermo Fisher Scientific, Inc., Waltham) according to the manufacturer's protocol. Elution was done at 55°C in 30µl elution buffer. The purity and concentration of the DNA was evaluated by NanoDrop 2000 Spectrophotometer (Thermo Fisher Scientific, Inc., Waltham).

Competent cell preparation

A single colony of *E.coli* (JM109 or BL21(DE3)) was inoculated to 3ml LB medium and incubated at 37°C with shaking at 180 rpm overnight. Next day after 1:100 dilution of the culture were grown until OD_{600}=0.3-0.5, they were placed on ice for 5 minutes, which was followed by centrifugation at 5000 rpm for 5 minutes at 4°C. Cells were resuspended in 30ml 100mM $CaCl_2$ (pH 7.4), incubated on ice for 30 minutes then centrifuged again. The medium was removed then the pellett was resuspended in 3ml ice-cold 100mM $CaCl_2$ and 15% sterile glycerol was added. 400 µl aliquots were made and stored at -70°C.

Transformation

Plasmids were added to100µl competent cells thawed on ice. After 30 min incubation on ice, 45 sec heat shock was applied (42°C), then cells were replaced on ice. 900µl SOC medium was added to the samples and they were cultured at 180 rpm and 37°C for 45 min. After that bacteria were spread onto LB agar containing appropriate antibiotic. Controls were spread onto LB agar with and without the antibiotic. Plates were incubated for 16 h, at 37°C.

Plasmid preparation

One single colony of plasmid containing bacteria was inoculated into LB medium containing antibiotic and was grown at 37°C, 180 rpm for 16 h. GeneJET plasmid miniprep kit (Thermo Fisher Scientific, Inc., Waltham) was used to purify plasmid DNA. For larger scale plasmid preparation, the overnight culture was diluted 1:100 and further grown for 16 h and GeneJET plasmid maxiprep kit (Thermo Fisher Scientific, Inc., Waltham) was employed.

Immunofluorescence and microscopy

Cells were plated onto 0.2% gelatin coated glass coverslips and grown, washed once with 1x PBS and fixed with 3.7% paraformaldehyde in 1x PBS for 15 min. Between each following step, the cells were rinsed three times with 1x PBS. The cells were permeabilized with 0.5% Triton X-100 in PBS for 15 min, blocked with 2% BSA in PBS for 30 min, and incubated with primary then with secondary antibodies diluted in blocking solution for 1 h. Cover slips were rinsed and then mounted in ProLong Gold Antifade medium. All steps of the immunostaining were performed at room temperature.

Images were acquired with a Carl Zeiss Axioskope-20 microscope using Zeiss Plan-NEC FLUAR 63x 1.25 NA oil immersion objective and Axiocam color camera (Zeiss, model 412-312). Confocal images were acquired with an Olympus Fluoview FV1000 confocal microscope using UPLSAPO 60x 1.35 NA oil immersion objective on an inverted microscope (Olympus IX81) at 25°C. Images were processed using FV10-ASW v1.5 software.

Nonspecific binding of the secondary antibodies was checked in control experiments (not shown).

Immunoprecipitation

Cells with or without thymidine or nocodazole treatment grown in 100 mm tissue culture dishes were rinsed three times with 1x PBS and then collected and lysed with 600µl of immunoprecipitation (IP) buffer containing protease inhibitors. The lysate was centrifuged with 10,000 *g* for 15 min at 4°C. To avoid nonspecific binding, the supernatants were precleared with 50µl of protein G Sepharose (GE Healthcare, Piscataway, NJ) at 4°C for 3 h with end-over-end rotation. Protein G Sepharose was removed by centrifugation at 4°C for 10 min, and the supernatant was incubated with the appropriate volume of antibody at 4°C for 1 h and then with 50µl of fresh protein G Sepharose at 4°C overnight with gentle rotation. The resin was washed three times with 300µl of IP buffer and then resuspended in 150µl of 1x SDS sample buffer, boiled, and microcentrifuged for 5 minutes. The supernatant was analyzed by Western blot.

Subcellular fractionation

ProteoJET^{TM} Cytoplasmic and Nuclear Protein Extraction Kit (Thermo Fisher Scientific, Inc., Waltham) was used for subcellular fractionation. Cells were collected in cell lysis buffer, containing 0.01M DTT and protease inhibitors, vortexed and kept on ice for 10 min. Cytoplasmic fraction (CP1) was obtained by centrifugation at 500*g* for 7 min and further cleaned by centrifugation at 13,000*g* for 15 min at 4°C (CP2). Nuclear protein fraction (N) was obtained after washing the pellet from the first centrifugation two times with Nuclei washing buffer. The efficiency of fractionation was analyzed by immunoblotting using β-tubulin antibody as a cytoplasmic and lamin A/C antibody as a nuclear marker.

Membrane fraction was isolated using ProteoJET™ Membrane Protein Extraction Kit (Thermo Fisher Scientific, Inc., Waltham) according to the manufacturer's protocol. The efficiency of fractionation was analyzed by immunoblotting using CD31 antibody as a membrane marker.

siRNA transfection

RACK1 (GNB2L1) and TIMAP (PPP1R16B) were silenced using 50nM ON-TARGET plus SMARTpool siRNA, L-006876-00-0 HumanGNB2L1 and L-004065-00-0 HumanPP1R16B, respectively, (Thermo Fisher Scientific, Inc., Waltham) with DharmaFECT-4 transfection reagent (Thermo Fisher Scientific, Inc., Waltham) in serum-free medium. ON-TARGETplus siCONTROL nontargeting pool (D-001810-10-01-05; Thermo Fisher Scientific, Inc., Waltham) was used as an irrelevant control. After 6 h the medium was changed to complete medium. Cells were further incubated for 48-72 hours.

SDS-PAGE and Western blot

Protein samples were separated by 10-15% SDS-PAGE and transferred to 0.45μm pore sized Hybond ECL Nitrocellulose Membrane (GE Healthcare, Piscataway, NJ). Membranes were blocked with 5% low-fat dry milk powder in TBST and then

were incubated with primary antibody diluted in TBST containing 1% BSA for 1 hour or O/N at 4°C. After the washing steps (twice in TBST, once in TBS, 5 min each), the membranes were incubated with the HRP-conjugated secondary antibody diluted in 1% BSA-TBST for 1 hour. After washing, the membrane was incubated with Immobilon Western HRP Substrate (Millipore, Billerica, MA). Images were acquired using darkroom development techniques for chemiluminesence (Kodak Medical X-ray Developer) or using an Alpha Innotech FluorChem® FC2 Imager. Representative data of at least 3 independent experiments are shown.

GST pull-down assay

Escherichia coli BL21 (DE3) transformed with pGEX-4T-2/pGEX-4T-3 containing glutathione S-transferase (GST), pGEX-4T-3 containing TIMAP mutants or pGEX-4T-2 containing RACK1 or EBP50 constructs were induced with 1mM IPTG and grown at room temperature with shaking for 3h. Cells were harvested by centrifugation, sonicated in lysis buffer (50mM Tris-HCl (pH 7.5), 0.1% Tween 20, 0.2% 2-mercaptoethanol, protease inhibitors) and proteins were isolated by affinity chromatography on glutathione Sepharose 4B (GE Healthcare, Piscataway, NJ) according to the manufacturer's protocol. BPAEC grown in 100-mm culture flasks were washed twice with 1x ice-cold PBS, scraped, and lysed in 600µl lysis buffer. The lysates were incubated for 4 h at 4°C with GST or different GST-fused proteins coupled to glutathione Sepharose beads. The beads were washed three times with 1x PBS then the GST fusion proteins were eluted with 10mM glutathione and were tested for interacting proteins by SDS-PAGE and Western blot.

Anti-V5 Agarose Affinity Gel Chromatography

BPAEC grown in 6 well plates were transfected with pcDNA3.1 V5-His, pcDNA3.1 V5-His PP2A Bα, or pcDNA3.1 V5-His PP2A B'γ construct prepared in our laboratory. 24 h after transfection the cells were washed twice with 1x ice-cold PBS, scraped, and lysed in 600µl lysis buffer (50mM Tris-HCl (pH 7.5), 0.2% 2-mercaptoethanol and protease inhibitors). The cell lysates were sonicated then centrifuged at 10,000 *g* for 10 min at 4°C. The supernatant was added to 50µl Anti-V5

Agarose conjugate and rotated for 5 h at 4°C. Beads were washed 3 times with PBS then boiled with 1x SDS loading buffer and analyzed by Western blot.

ECIS measurements and in vitro wound healing assay

To study endothelial barrier function, wound healing, and cell migration ECIS (Electric cell-substrate impedance sensing) model Zθ, (Applied BioPhysics Inc. Troy, NY) was used. ECIS is a real-time, label-free, non-invasive, impedance-based method to study the activities of cells grown in tissue culture. To monitor transendothelial electric resistance [166], control or transfected cells were seeded onto type 8W10E arrays. With the wounding option, ECIS is able to apply high electric field to make a well-defined injury in a confluent cell monolayer and to screen the repopulation of this wounded area by noninvasive measurements [167, 168]. Wild type, mock, or mutant EBP50 transfected cells were seeded on type 8W10E arrays. After the cells achieved monolayer density (about 1000Ω impedance), an alternate current of 5 mA at 60 kHz frequency was applied for 30 sec duration to establish wounds in the cell layer, which led to the death and detachment of cells present on the small active electrode, then the impedance was measured for 5 h. The impedance in each wounded well increased gradually, until it reached a maximum plateau value.

LC-MS/MS analysis

Proteins were resolved by SDS-PAGE and stained with Blue Silver solution [169]. Liquid Chromatography with Tandem Mass Spectrometry Detection was performed by Dr. Tamás Janáky at the University of Szeged, Faculty of Medicine, Department of Medical Chemistry. Eluted peptides were analyzed by Data Dependent Aqusition and the three most abundant precursor ions were selected for MS/MS. Data were evaluated with ProteinLynx GlobalServer 2.4 software and Mascot 2.04 data browser.

Statistical analysis

Pearson correlation coefficient was determined as described in [170]. Analysis of Variance on Ranks was performed on Pearson coefficients using SigmaStat. Statistical significance was determined at $P<0.05$ by Dunn's Method, multiple comparisons versus control group (group of interphase cells).

Statistical analysis was done with Student's t-test. Significant changes are indicated by asterisks; * ($P<0.05$), ** ($P<0.01$), or *** ($P<0.001$). Densitometric analysis of immunoblots was done by Image J software.

Results

Localization of EBP50 in endothelial cells

Subcellular localization of EBP50 was investigated in endothelial cells. BPAEC were co-stained with anti-EBP50 and anti-β-tubulin antibody. Based on previous results of others on epithelial cells, we expected cytosolic/membrane localization of the protein. By confocal microscopy, EBP50 was detected mainly in the nucleus and in the perinuclear region (Fig. 7 a-c). Furthermore, EBP50 was also found in the nuclei of human umbilical vein endothelial cells (HUVEC) (Fig. 7 d-f), but in the cytoplasm of MCF7 human breast adenocarcinoma cell line (Fig. 7 j-l), an epithelial cell type. EBP50 shares high amino acid sequence homology with another adaptor protein within the NHERF family, namely NHERF2. To exclude the possibility of cross-reaction of the EBP50-specific antibody with NHERF2, BPAEC was stained with NHERF2 specific antibody as well. Our result clearly shows that NHERF2 localizes in the cytoplasm but not in the nucleus (Fig. 7 g-i), confirming the specificity of antibodies.

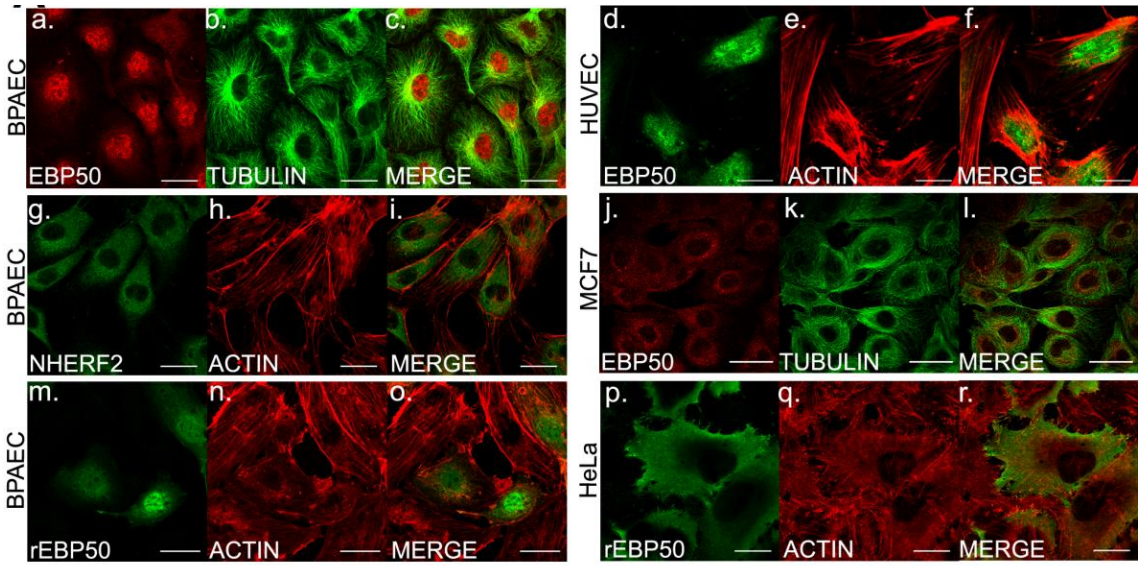

Figure 7. Nuclear localization of EBP50 in BPAEC.
Immunofluorescence staining of confluent BPAEC (a-c,g-i), HUVEC (d-f), MCF7 (j-l) and pCMV-myc EBP50 transfected BPAEC (m-o), or HeLa (p-r) cells was performed using anti-EBP50 (a,j: red, d: green), anti-tubulin (b,k: green), anti-NHERF2 (g: green), and monoclonal anti-c-myc (m,p: green) primary antibodies. Actin microfilaments were stained with Texas Red conjugated phalloidin (e,h, n,q: red). c,f,i,l,o and r are merged images of a-b, d-e, g-h, j-k, m-n, and p-q, respectively. Scale bars: 100 μm.

Recombinant protein expression was employed to verify our results. The coding region of bovine EBP50 was amplified by RT-PCR and cloned into a pCMV-Myc plasmid. Sequencing of the construct revealed one nucleotide deviance (at position 192) that did not cause amino acid change. Endothelial and epithelial cells were transfected with the construct, to verify this rather unique nuclear appearance of EBP50 in EC. Immunofluorescent staining with c-myc tag specific antibody showed that the recombinant EBP50 was in the nuclear and perinuclear region in EC (Fig. 7 m-o), however, it was present in the cytoplasm of the epithelial HeLa cells (Fig. 7 p-r).

Next, cytoplasmic and nuclear fractions of BPAEC and MCF7 cells were isolated to further strengthen our observation. Western blot analysis of the fractions proved that EBP50 is present in the nuclear fraction only in the endothelial cells. The efficiency of fractionations was confirmed using anti-β-tubulin antibody as a cytoplasmic and anti-lamin A/C antibody as a nuclear marker (Fig.8).

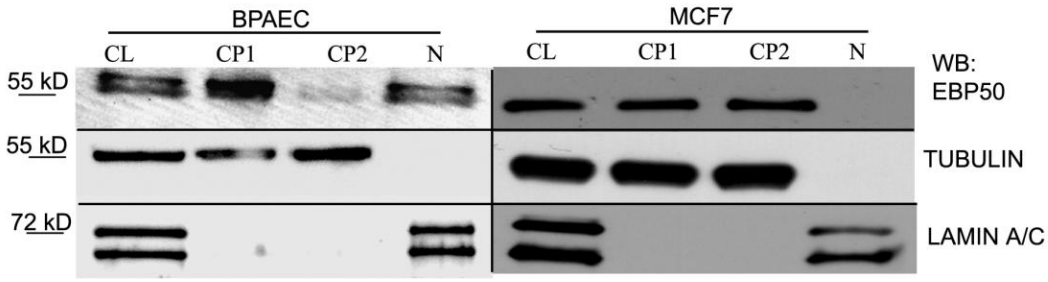

Figure 8. Cellular fractionations of BPAE and MCF7 cells.
The fractions were analyzed with anti-EBP50, anti-β-tubulin as a cytoplasmic and anti-lamin A/C antibodies as a nuclear marker. CL: cell lysate, CP1: cytoplasmic fraction 1, CP2: cytoplasmic fraction 2, N: nuclear fraction.

Phosphorylation dependent localization of EBP50

When BPAEC were co-stained with anti-EBP50 and anti-β-tubulin antibodies, we observed that EBP50 left the nuclear region in dividing cells. EBP50 was in the nucleus in interphase cells, however, during prophase its redistribution to the cytoplasm was apparent and we could detect its disappearance from the cytosol only in the phase of cytokinesis (Fig.9).

It was known from the literature, that phosphorylation of EBP50 is catalyzed by Cdk1 during mitosis and a mobility-shift upon SDS-PAGE was also observed [130]. Hence, we hypothesized that the varying localization of the protein during the cell cycle

can be related to its phosphorylation state. To prove our hypothesis first a phospho-mimic construct of bovine EBP50 was created by mutation of Ser^{288} and Ser^{310} side-chains to Asp to imitate phosphorylation. These side-chains in the bovine EBP50 referred to the human Ser-residues which were known to be phosphorylated in mitotic cells by Cdk1 [130]. BPAEC cells were transfected with the wild type and mutant EBP50. On SDS-PAGE the apparent size of EBP50 mutant shifted upward compared to the recombinant wild type EBP50 (Fig. 10 A). In addition, in aggreament with our hypothesis, the phospho-mimic mutant form of EBP50 showed cytoplasmic allocation but the wild-type recombinant protein was in the nucleus according to immunofluorescent staining (Fig. 10 B).

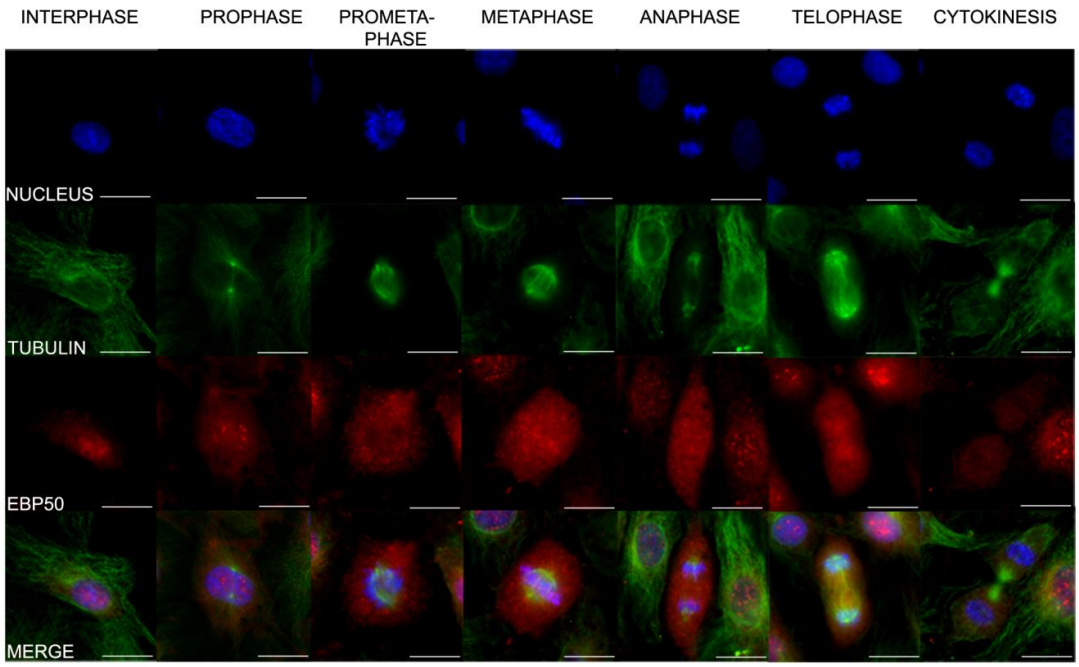

Figure 9. Localization of EBP50 during the phases of the cell cycle.
Immunofluorescence staining of BPAE cells was performed using anti-EBP50 (red) primary antibody. Phases of the cell cycle were identified by tubulin (green) and DAPI (blue) staining. Scale bar: 100 μm.

Next, BPAEC were synchronized to confirm the phosphorylation of the endogenous EBP50. Cells were arrested in G1/S phase using double thymidine block, and G2/M phase arrest was established using nocodazole treatment. EBP50 was detected as a 55 kDa band in the lysate of asynchronized cells. We also observed an additional pale band at a higher molecular mass that completely disappeared in the lysate of cells in G1/S, however, had a massive manifestation 8 h after releasing the cells from the thymidine block, as the majority of cells got near to the phase of mitosis (Fig. 11).

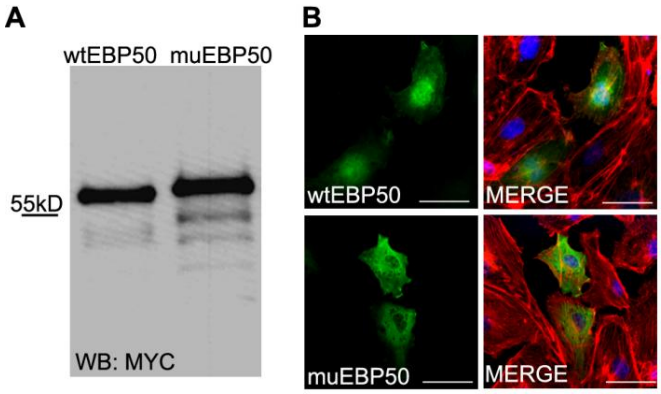

Figure 10. Localization of EBP50 is phosphorylation-dependent in BPAEC.
pCMV-Myc EBP50 wild type (wtEBP50) and pCMV-Myc EBP50 S288D:S310D phosphomimic mutant (muEBP50) proteins were analysed by Western blot (A) and immunofluorescence (B). Anti-myc (green) antibody was used for labeling of wild type and mutant EBP50 both in Western blot and immunofluorescent experiments. Actin microfilaments were stained with Texas Red conjugated phalloidin (red) and DAPI (blue) staining was used to visualize the nuclei. Scale bar: 100 μm.

Previously published data [130] and our results (Fig.10) together indicated that this higher molecular mass band could be the phosphorylated form of EBP50. Furthermore, these observations proved our hypothesis that the relocalization of EBP50 occurs in a phosphorylation-dependent manner.

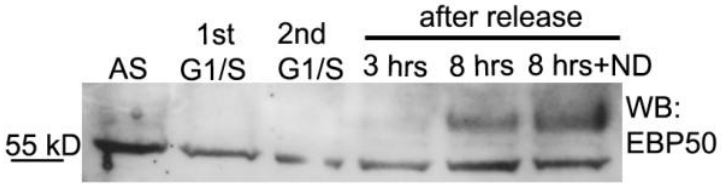

Figure 11. Phosphorylation level of EBP50 in synchronized BPAE cells.
Cells were arrested in G1/S phase using double thymidine block and in mitotic phase by nocodazole treatment. Samples of asynchronized cells (AS), 1st and 2nd thymidine block cells (G1/S), and cells after 3 or 8 h release of the thymidine block without or with addition of 80 ng/ml nocodazole (ND) were tested for EBP50 by Western blot.

Phospho-mimic EBP50 supports wound healing

Proliferation, cell division and migration are essential in wound healing [167, 171]. To further demonstrate the significance of the phosphorylation of EBP50 during the cell cycle, we compared the time course of wound healing of mock-transfected

BPAEC monolayer with the ones overexpressing wild type- or phospho-mimic EBP50 using electric cell impedance measurements, ECIS (Fig.12). The time from the beginning of wound healing to the time at 50% of the maximum impedance (effective time) was about the same for the mock-transfected control (1.9 h) and the sample overexpressing the wild type EBP50 (1.8 h). However, the phospho-mimic mutant form of EBP50 significantly accelerated the healing process (effective time =1.5 h).

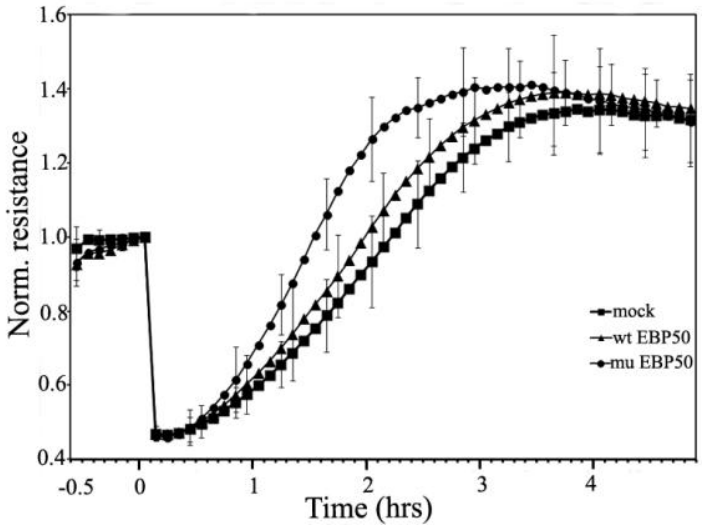

Figure 12. Phospho-mimic EBP50 supports wound healing.
BPAEC were transfected with pCMV-Myc EBP50 wild type (wt EBP50) and pCMV-Myc EBP50 S288D:S310D phosphomimic mutant (mu EBP50) and were plated onto two 8W10E arrays 24 h post-transfection. After cells achieved monolayer density (about 1000 Ω impedance) an alternate current of 5 mA at 60 kHz frequency was applied for 30 sec duration to establish wounds in the cell layer (0 h); after that the impedance was measured for 5 h. The average results from three independent experiments each made with two or three parallel measurements are shown. Error bars represent SD.

Identification of the protein phosphatase interacting with EBP50

Protein phosphorylation/dephosphorylation is a reversible process. We intended to identify the Ser/Thr specific protein phosphatase catalyzing the dephosphorylation of EBP50. BPAEC were arrested in mitotic phase and at the point of the release the media were implemented with specific protein phosphatase inhibitors. A specific PP2A inhibitor (5 nM okadaic acid) was able to maintain the phosphorylation state of EBP50 for 6 h after the release, suggesting that PP2A is involved in the dephosphorylation. On the other hand, 2 nM calyculin A, a specific inhibitor of PP1, had no effect on the above dephosphorylation process (data not shown).

Next, we examined protein-protein interactions between EBP50 and the protein phosphatases. Lysates from thymidine or nocodazole treated cells in S or M phase,

respectively, were prepared and the endogenous EBP50 was immunoprecipitated from each lysate using anti-EBP50 antibody. The immunoprecipitated complexes were probed in Western blot with antibodies raised against different protein phosphatase subunits. Our IP results clearly indicated protein-protein interactions between EBP50 and subunits of PP2A. EBP50 co-immunoprecipitated with the A (PP2Aa) and C (PP2Ac) subunits of PP2A, but no interaction of EBP50 was detected with PP1c α and δ isoforms. EBP50 was also observed in PP2Ac immunoprecipitates of lysates with thymidine or nocodazole treatments. The interaction between EBP50 and PP2A was clearly more pronounced in lysates of mitotic phase cells (Fig.13).

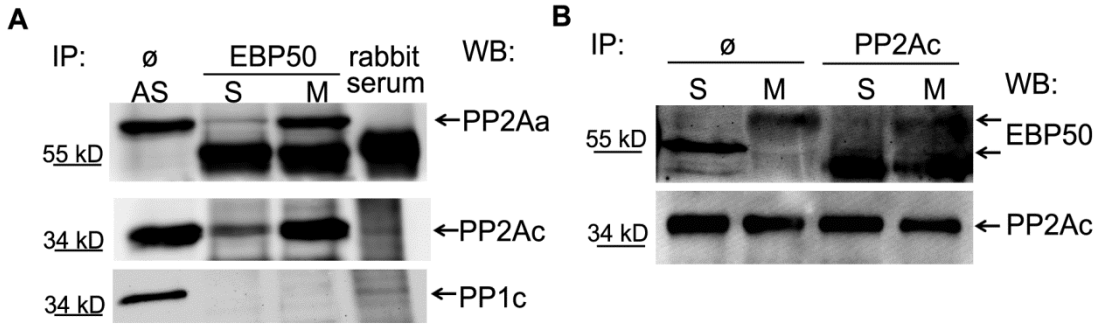

Figure 13. PP2A subunits associate with cellular EBP50.
EBP50 (panel A) or PP2A C subunit (panel B) was immunoprecipitated from lysates of thymidine or nocodazole treated BPAEC as described in Materials and Methods. The IP complexes were probed for PP2Aa, PP2Ac, and PP1c (α and δ) (A) or EBP50 and PP2Ac subunit (B). Ø: cell lysate without immunoprecipitation, AS: asynchonized cell lysate, S: early S phase cell lysate, M: mitotic phase lysate. Additional bands at 55kDa are IgG.

Identification of the third, variable B subunit of PP2A - which determines the substrate specificity and subcellular localization of the holoenzyme - in our system was not possible by immunoprecipitation, because the apparent size of the B subunits (about 55 kDa) is close to the size of IgG. To identify the B subunit present in PP2A holoenzyme interacting with EBP50, GST-tagged bacterial expression construct of EBP50 was created. Immobilized recombinant GST-EBP50 or GST protein, as a negative control, were incubated with or without BPAEC lysates in pull down experiments. The efficiency of the purification from the bacterial extract was analysed by Coomassie staining (Fig.14A). The total cell lysates and the eluted proteins were tested using antibodies against different PP2A subunits by Western blot (Fig.14B). The results indicate the presence of B subunit in the GST-EBP50 pull-down along with A

and C subunits of PP2A (Fig.14B). In the same set of experiment B' subunit of PP2A was not detectable.

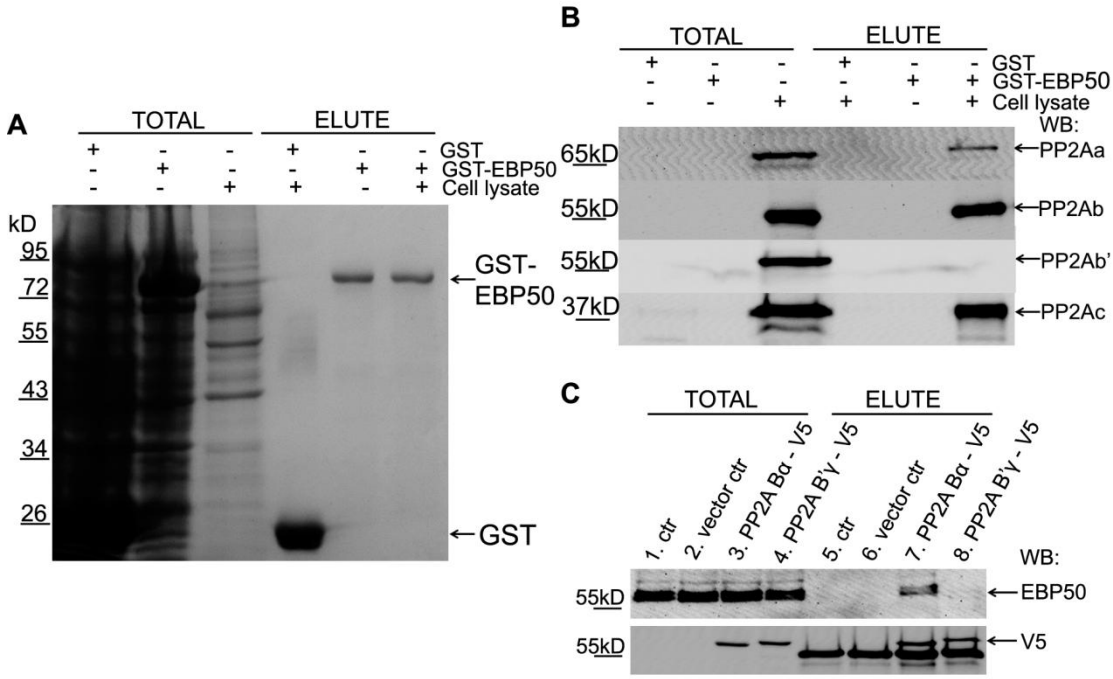

Figure 14. Bα subunit of PP2A interacts with EBP50.
Panels *A* and *B*: Bacterially expressed glutathione S-transferase (GST) and GST-tagged wild-type EBP50 were loaded onto glutathione-Sepharose. After a washing step the resin samples were incubated with BPAEC lysate or cell lysis buffer. Non-binding proteins were washed out and the bound proteins were eluted with 10 mM glutathion. Coomassie staining *(A)* and Western blot probed with PP2A A, B, B', or C specific antibodies *(B)* of the bacterial and endothelial cell lysates (Total) and the eluted fractions after the pull-down are shown. Panel *C*: BPAEC monolayers were transfected with pcDNA3.1 V5-His (vector ctr), pcDNA3.1 V5-His PP2A Bα (PP2A Bα–V5) and pcDNA3.1 V5-His B'γ (PP2A B'γ–V5) plasmids. Lysates of the transfected cells were incubated with Anti-V5 Agarose Affinity Gel as described in Materials and Methods, and the bound proteins were eluted by boiling the resin in 1X SDS sample buffer. Western blot analysis of the lysates of transfected cells (Total) and eluted samples were done using EBP50 (upper panel) and V5-tag (lower panel) specific antibodies. Additional bands at 55kD are IgG.

Subsequently, we confirmed the specific interaction between EBP50 and the α isoform of PP2A B subunit using overexpressed B subunits in mammalian cells with Anti-V5 Affinity Gel. BPAEC were transfected with expression contructs containing the coding sequence of PP2A Bα or B'γ subunits and the overexpressed proteins were bound to anti-V5 antibody immobilized on the resin. The eluted recombinants and the presence of EBP50 in the eluted fractions were analyzed by Western blot (Fig.14C). Even though the amount of Bα and B'γ subunits appears the same, the binding of endogenous EBP50 was detectable only to Bα. Taken together, data of immunoprecipitations demonstrate that endogenous EBP50 and endogenous PP2A

physically associate, moreover, our results indicate that EBP50 interacts with the holoenzyme form of PP2A containing Bα.

Co-localization of EBP50 and PP2A

In the immunoprecipiation experiments (Fig. 13) we detected the highest level of interaction between EBP50 and PP2A in the mitotic phase. Also, the size shift of EBP50 suggesting its phosphorylation and the cytosolic localization of EBP50 was correlated with the M phase. This led us to search possible co-localization of EBP50 with PP2A during mitosis. For that reason, BPAEC were co-stained with anti-EBP50 and anti-PP2Ac antibodies (Fig. 15A). While EBP50 has nuclear and perinuclear distribution in interphase cells, PP2Ac appears to be present mainly in the cytoplasm, therefore, merge of parallel images emphasizes no overlap of staining. On the other hand, in agreement with our immunoprecipitation experiments which indicated strong protein-protein interaction between EBP50 and PP2A, we detected co-localization of EBP50 and PP2Ac in pro-, prometa-, meta-, ana-, and telophase. We also observed that the two proteins still co-localize at the beginning of cytokinesis, when EBP50 still showed cytoplasmic appearance. Conversely, no co-localization could be observed in the late cytokinesis, when EBP50 was found mostly in the nucleus again. To quantify the extent of association, the Pearson's correlation coefficient was determined at the different phases of the cell cycle. Positive value of the coefficient indicates co-localization/association of the studied proteins. Significant co-localization was found from the prophase till the early cytokinesis, but not in late cytokinesis, compared to interphase (Fig.15B).

To confirm that the EBP50-PP2A interaction is specific and phosphorylation dependent, the same analysis of cells co-stained with PP2Ac and NHERF2 specific primary antibodies was performed. NHERF2 has the highest amino acid sequence homology with EBP50 in the NHERF family, but there is no possible Cdk1 phosphorylation site in NHERF2. Both PP2Ac and NHERF2 are in the cytoplasm of interphase cells, however neither co-localization nor interaction between these proteins in interphase or any other phase of the observed cells could be detected (Fig.15C).

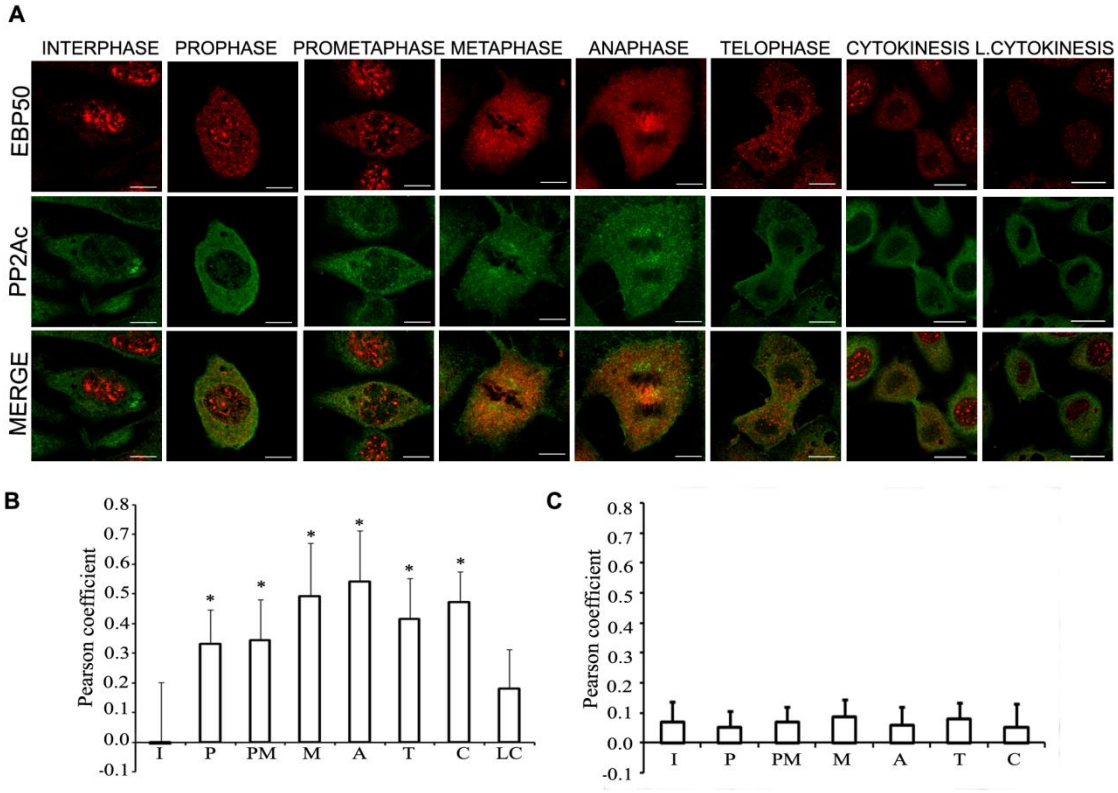

Figure 15. Co-localization of EBP50 and PP2Ac during mitosis in BPAEC.
(A) Immunofluorescence staining of BPAEC was performed using anti-EBP50 (anti-SLC9A3R1 antibody, Abgent) (red) and anti-PP2Ac (green) primary antibodies. Phases of the cell cycle were identified using DAPI staining (not shown). Scale bars: 100 µm. Co-localization of EBP50 (B) or NHERF2 (C) and PP2Ac was evaluated by determination of Pearson cross-correlation coefficient. The results are presented as means ± SD from 50-100 (B) or 25-30 (C) independent cells for each studied phase of the cell cycle. Statistical analysis was done with ANOVA on ranks. Significant changes compared to the interphase cells are indicated by * (P <0.05). I: interphase, P: prophase, PM: prometaphase, M: metaphase, A: anaphase, T: telophase, C: cytokinesis, LC: late cytokinesis.

Identification of RACK1 as a novel TIMAP interacting protein

TIMAP protein is abundant in EC. The involvement of TIMAP in EC barrier regulation has been shown [92] and it is accepted that TIMAP regulates PP1 as its regulatory subunit. However, the number of known protein partners of TIMAP is low.
To identify new interacting partners of TIMAP in endothelial cells, GST pull-down assay was performed. GST-tagged recombinant full length TIMAP protein immobilized on glutathione Sepharose was incubated with BPAEC lysate. GST protein incubated with the cell lysate and GST-TIMAP incubated with the lysis buffer were used as negative controls. After the required washing steps the eluted proteins were separated on SDS-PAGE stained with BlueSilver solution and the pattern of the protein bands in

the three samples were compared. An extra band at about 34 kDa was identified in the sample of GST-TIMAP incubated with BPAEC lysate (Fig. 16). It was cut from the gel and was further analyzed by LC-MS/MS (Dr. Janáky, University of Szeged). Bovine RACK1 (Gene: GNB2L1, Accession number: P63243) was identified using Swissprot and Uniprot TREMBL database. This result was supported by Western blot analysis of the pull-down samples using anti-RACK1 antibody (Fig. 16B). The specific band of RACK1 can be seen in the total cell lysate (positive control) and in the GST-TIMAP sample which was incubated with the cell lysate, conversely, no RACK1 signal was detectable in the two negative control samples suggesting a specific interaction between TIMAP and RACK1.

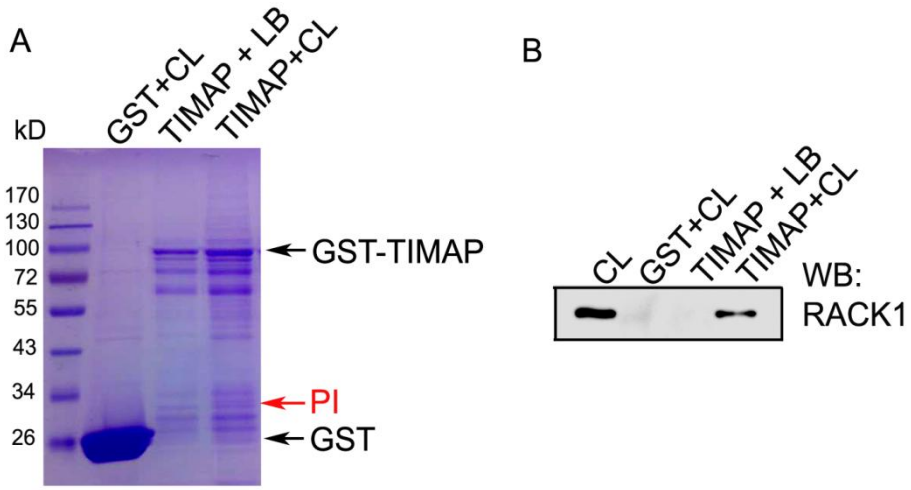

Figure 16. Detection of TIMAP-RACK1 interaction by pull-down.
Bacterially expressed glutathione S-transferase (GST) and GST-tagged wild-type TIMAP were loaded onto glutathione-Sepharose. After a washing step the resin samples were incubated with BPAEC lysate (CL) or cell lysis buffer (LB). Non-binding proteins were washed out and the bound proteins were eluted with 10 mM glutathion. Blue silver staining of the endothelial cell lysate (CL) and the eluted fractions after the pull-down are shown (A). Red arrow points the band of a possible interacting protein (PI) appearing only in the TIMAP sample incubated with EC cell lysate (TIMAP+CL). That band was cut from the gel and was identified by LC-MS/MS as RACK1 which was confirmed by Western blot (B).

RACK1 binds TIMAP-PP1c complex in endothelial cells

To verify the interaction of the endogenous proteins in endothelial cells immunoprecipitation experiments were utilized. RACK1 was shown to be present in the immunoprecipitate (IP) of TIMAP and vice versa, TIMAP co-immunoprecipitated with RACK1 (Fig. 17A).

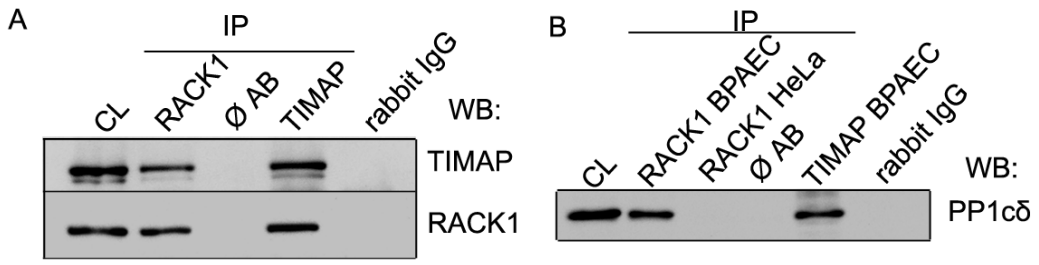

Figure 17. RACK1 interacts with TIMAP in endothelial cells.
RACK1 or TIMAP was immunoprecipitated from lysates of BPAEC (*A*) and BPAEC or HeLa (*B*) cells as described in Materials and Methods. IP complexes were probed for TIMAP and RACK1 (*A*) or PP1cδ (*B*). CL: cell lysate, Ø AB: control of IP from BPAEC without the addition of antibody.

Since our group has shown earlier that TIMAP has a strong interaction with PP1cδ [92, 93], the presence of PP1cδ in the TIMAP-RACK1 complexes was also studied. PP1c was present in both the RACK1 and the TIMAP IP complexes (Fig. 17B). To test whether RACK1 binds PP1c directly without the presence of TIMAP, immunoprecipitation was made with RACK1 antibody from HeLa cells that do not express endogenous TIMAP [91]. No interaction was detected between RACK1 and PP1cδ in HeLa cells (Fig. 17B), therefore one may conclude that RACK1 interacts with PP1cδ via TIMAP. To further confirm this result, RACK1 was immunoprecipitated from control, non-siRNA and TIMAP specific siRNA transfected EC. When TIMAP was depleted PP1cδ was not detected in the RACK1 IP (Fig. 18A).

Furthermore, mammalian constructs were created to express recombinant wild type and truncated TIMAP in HeLa cells. The truncated form does not contain the PP1c binding motif, as the first 68 amino acids are deleted; consequently it is expected not to bind the phosphatase. HeLa were transfected with empty pEGFP, wild type TIMAP/pEGFP (GFP-TIMAP wt) or truncated TIMAP/pEGFP (GFP-TIMAP ΔPP1c) plasmids. GFP or the endogenous RACK1 were immunoprecipitated and the IP complexes were probed for RACK1, GFP and PP1cδ (Fig. 18B). Our results indicate that although HeLa contains PP1cδ, the phosphatase was not present in the RACK1 IP except in wild type TIMAP over-expressing HeLa. Furthermore, PP1cδ was not detectable with the truncated form of TIMAP in the RACK1-GFP-TIMAP ΔPP1c complex, only in the RACK1-GFP-TIMAP wt complex. These results imply that PP1cδ is present in the latter complex due to its interaction with TIMAP, but there is no direct binding between PP1cδ and RACK1; furthermore, the presence of this phosphatase is not a requirement for TIMAP-RACK1 interaction.

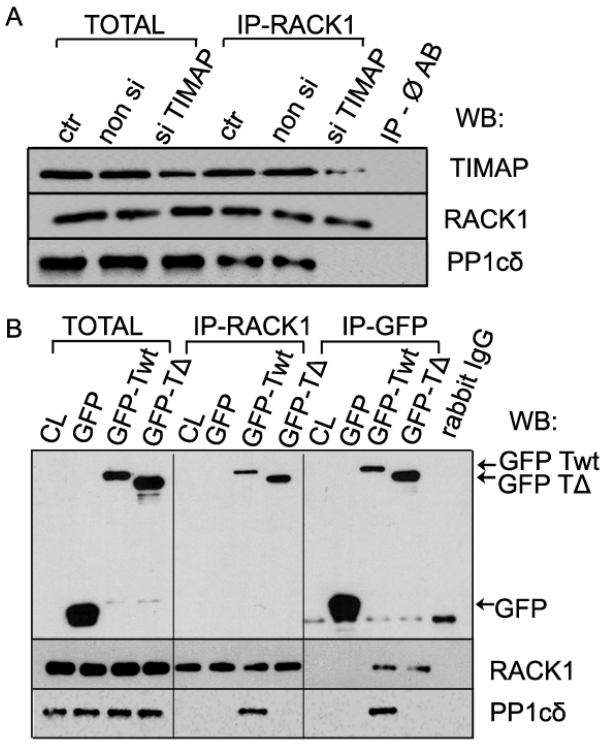

Figure 18. RACK1 interacts with PP1cδ via TIMAP.
RACK1 was immunoprecipitated from *(A)*: non transfected (ctr), non-siRNA, TIMAP specific siRNA (si TIMAP) transfected BPAEC cell lysates or *(B)* RACK1 and GFP were immunoprecipitated from pEGFP-C1 (GFP), pEGFP-C1 TIMAP WT (GFP-Twt) or pEGFP-C1 TIMAPΔpp1c (GFP-TΔ) transfected HeLa cell lysates. IP complexes were probed for GFP, RACK1 or PP1cδ.

Mapping the TIMAP-RACK1 interaction domains

Besides the PP1c binding motif, several additional domains were identified within the sequence of TIMAP. Therefore further deletion mutants of TIMAP were created to identify its domains concerned in the RACK1 interaction (Fig. 19). The interface between bacterially expressed TIMAP and endogenous RACK1 was mapped by GST pull-down assays. First two shortened mutants (N-terminal (TIMAP 1-290) and a C-terminal (TIMAP 291-567)) truncated mutants of TIMAP were created. Surprisingly, RACK1 was able to bind both to the TIMAP 1-290 mutant containing the nuclear localization signal (NLS), the PP1c-binding motif and the five ANK repeats, as well as to the TIMAP 291-567 mutant with the earlier identified PKA (Ser337) and GSK3β (Ser333) phosphorylation sites [172] and the C-terminal CAAX prenylation motif. The latter one was excluded as a significant region of TIMAP in the interaction,

since the shortened C-terminal fragment missing the CAAX box (TIMAP 291-563) did not bind less RACK1 than TIMAP 291-567. To further specify the interacting region in the N-terminal section of the protein, additional shorter recombinants were tested. When the N-terminal fragment was shortened (TIMAP 1-165) we still could detect binding. The mutants containing only ANK4-5 and a region with unidentified function (TIMAP 165-290) or ANK1-3 (TIMAP 67-165) did not bind to RACK1. Therefore it was concluded that none of the ANK repeats are concerned. The very N-terminal region of TIMAP (spanning amino acids 1- 34) does not affect the binding either. The short region of the potential NLS, however, appeared to be essential by the comparison of the binding ability of TIMAP 35-165 and TIMAP 52-165 to endogenous RACK1 as the only difference between these two fragments is the presence or absence of the NLS motif, respectively.

Taken together, these results indicate that two regions of TIMAP are capable to bind RACK1: the NLS motif in the N-terminal half of the molecule and a region in the C-terminal half.

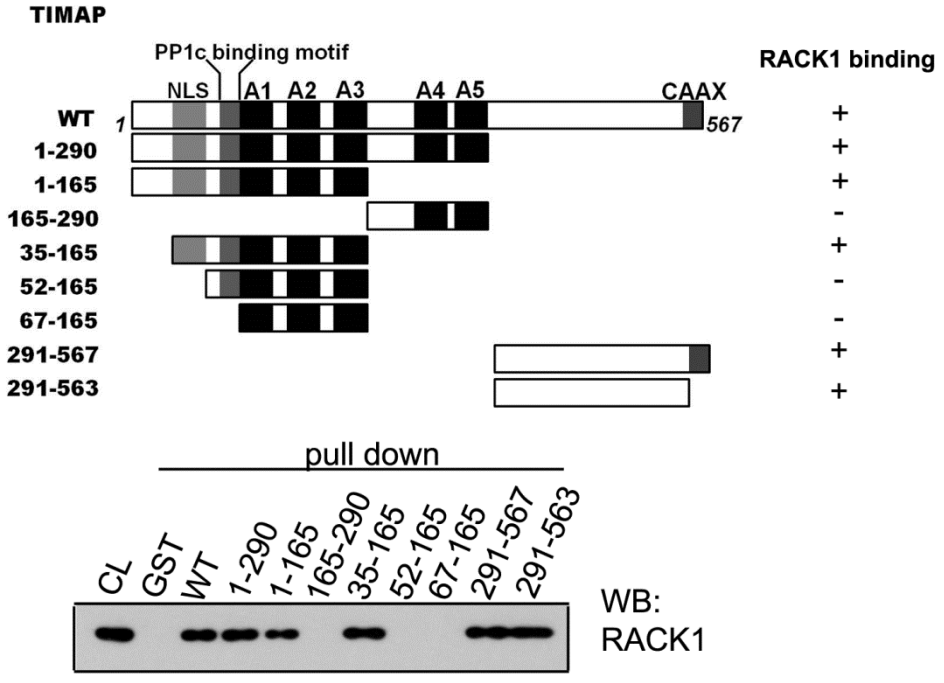

Figure 19. Domain mapping of TIMAP-RACK1 interaction.
GST-TIMAP pull-down of endogenous RACK1. GST, recombinant GST-TIMAP WT or additional GST-TIMAP fragments (depicted in the upper part of panel *A*) were loaded onto glutathione-Sepharose as described in Materials and Methods. The immobilized protein samples were incubated with BPAEC lysate. Western blot of the pull-down eluates probed with anti-RACK1 antibody is shown. CL: total cell lysate.

Due to its seven WD repeats the β-propeller structure of RACK1 offers multiple docking sites for several interactions. The association of native TIMAP to bacterially expressed full length GST-RACK1, N-terminal (1-180) or C-terminal (137-317) GST-RACK1 truncated forms were studied in GST pull-down assays (Fig.20). Our results clearly demonstrate that only the N-terminal half of RACK1 (WD repeats 1-4) is involved in the RACK1-TIMAP interaction.

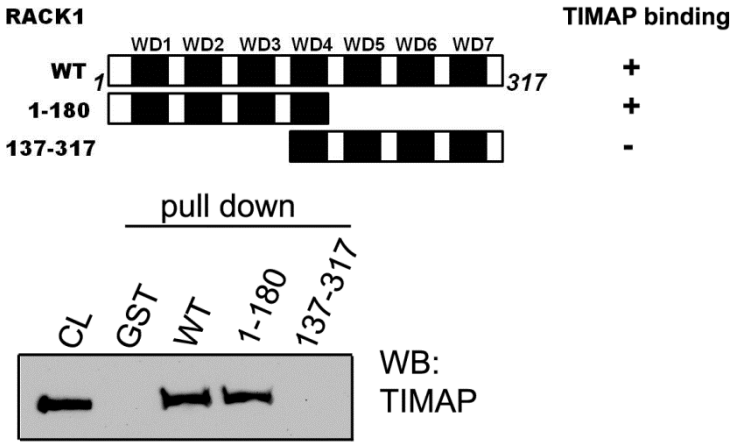

Figure 20. Domain mapping of RACK1-TIMAP interaction.
GST-RACK1 pull-down of endogenous TIMAP. GST, recombinant RACK1 WT or GST-RACK1 fragments (depicted in the upper part of panel *B*) were tested in pull-down assay. The immobilized samples were incubated with BPAEC lysate. Western blot of the pull-down eluates was probed with anti-TIMAP antibody.

Forskolin treatment attenuates the RACK1-TIMAP interaction

Phosphorylation of a protein may change its conformation and eventually may affect its protein-protein interactions. RACK1 (reviewed in [149]) and TIMAP [93, 172] are recognized to be related to several kinases, and upon the activation of certain kinases changes in their protein-protein interactions were described. Namely, PKCs and RACK1 mutually influence each other, but RACK1 may participate in the cAMP/PKA pathway as well [137, 139, 173]. Recent results indicate that TIMAP is a target for PKA-primed GSK-3β mediated phosphorylation on sites Ser337 and Ser333, respectively [93, 172]. Therefore we next tested the effect of the activation of PKC and PKA on the TIMAP-RACK1 interaction challenging EC with PMA and forskolin, respectively.

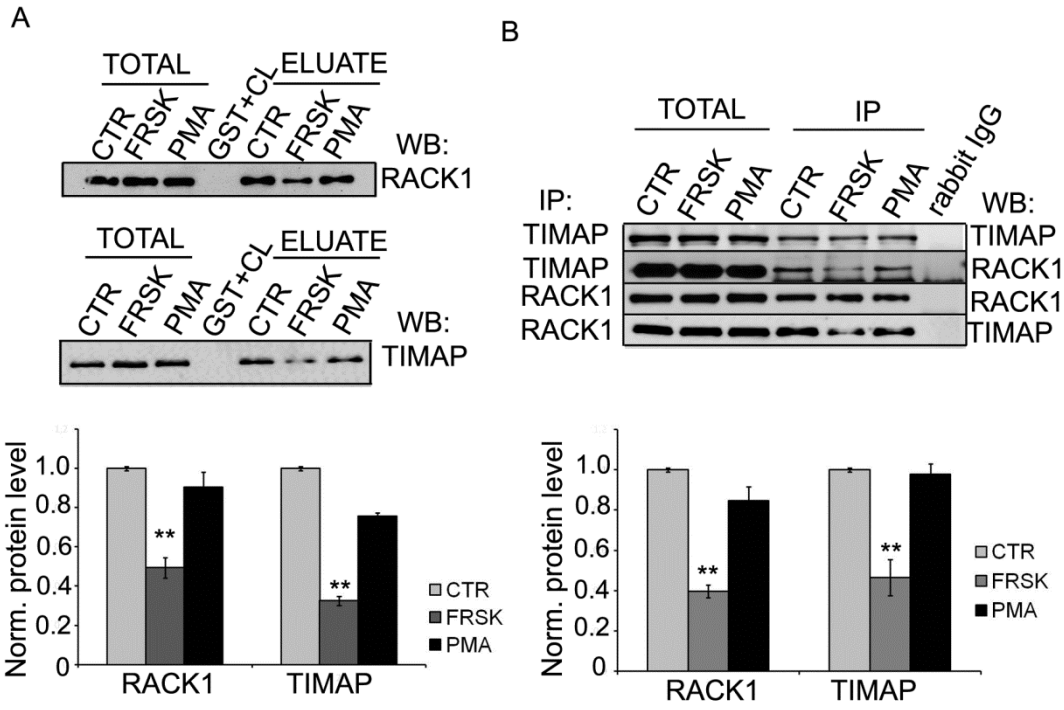

Figure 21. TIMAP-RACK1 interaction is attenuated by the cAMP/PKA pathway.
(A) GST, full-length GST-TIMAP (upper part) or GST-RACK1(middle part) were immobilized on glutathione-Sepharose and incubated with cell lysates of non treated (ctr), forskolin (50 μM for 30 min) (FRSK) or PMA (1 μM for 30 min) treated BPAEC. The eluted proteins were tested by Western blot using anti-RACK1 and anti-TIMAP antibodies. *(B)* Endogenous TIMAP or RACK1 was immunoprecipitated from BPAEC lysates after the same treatments described for panel A. IP complexes were probed for TIMAP and RACK1. Shown are representative data of means ± SE from at least 3 independent experiments. Protein levels were quantified by densitometric analysis. Eluted proteins were normalized against total protein levels. Significant changes are indicated by asterisks ** ($P<0.01$).

The attenuative or restorative effects of PMA or forskolin treatment on the interaction were established by GST pull-down assays first. Equal amounts of bacterially expressed GST-TIMAP or GST-RACK1 were loaded onto glutation Sepharose 4B and untreated, forskolin or PMA challenged endothelial cell lysates were added to the resin. Bound proteins in the eluates were analyzed by Western blot (Fig. 21A). The amount of RACK1-TIMAP complex was considerably lower after the activation of the cAMP/PKA pathway (forskolin). On the other hand PMA treatment of EC had no significant effect on the interaction. These findings were further strengthened with endogenous proteins only, when IP complexes of RACK1 and TIMAP drawn from EC after the same treatments were analyzed by Western blot (Fig. 21B). Our results suggest that forskolin induces PKA and PKA-primed GSK3β phosphorylation of TIMAP which attenuates the RACK1-TIMAP binding. Truncated wild type, S333A/S337A phosphorylation deficient, and S333D/S337D phosphomimic mutants of a TIMAP

fragment spanning amino acids 331–567 were overexpressed in *E. coli* and were utilized in pull-down experiments. Consistent with the above described findings, the amount of RACK1 bound to the phospomimic TIMAP fragment was decreased compared to the amount of RACK1 bound to wild type TIMAP or the phosphorylation deficient fragment (Fig. 22). These data suggest that the phosphorylation state of TIMAP is an important factor in its interaction with RACK1.

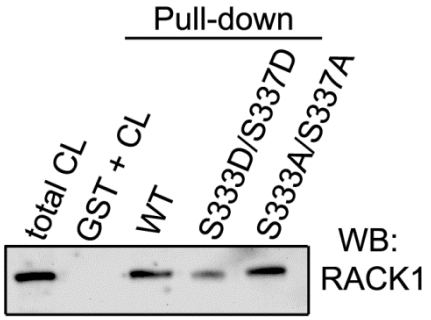

Figure 22. Phosphomimic mutation of TIMAP attenuates RACK1 binding.
GST, recombinant GST-tagged truncated wild type, S333A/S337A, and S333D/S337D mutants of a TIMAP fragment (amino acids 331–567) were loaded onto glutathione-Sepharose as described in Materials and Methods. The immobilized protein samples were incubated with BPAEC lysate. Western blot of the pull-down eluates probed with anti-RACK1 antibody is shown. CL: cell lysate. Representative data of at least 3 independent experiments are shown.

Activation of the cAMP/PKA pathway affects localization of TIMAP

TIMAP localizes to the cell membrane and it is also present in the nucleus and in the cytoplasm surrounding the nucleus in HPAEC monolayer [92]. We investigated whether the RACK1-TIMAP complex formation has any effect on the subcellular localization of TIMAP and RACK1. To modulate the interaction, HPAEC monolayers were subjected to agents affecting the phosphorylation level of TIMAP and the subcellular localization was detected by immunofluorescence studies of the monolayers (Fig. 23-24) or by Western blot of subcellular fractions (Fig 25). Forskolin was employed to indicate the cAMP/PKA pathway. AR-A014418 and H89 were utilized to inhibit GSK3β and PKA, respectively.

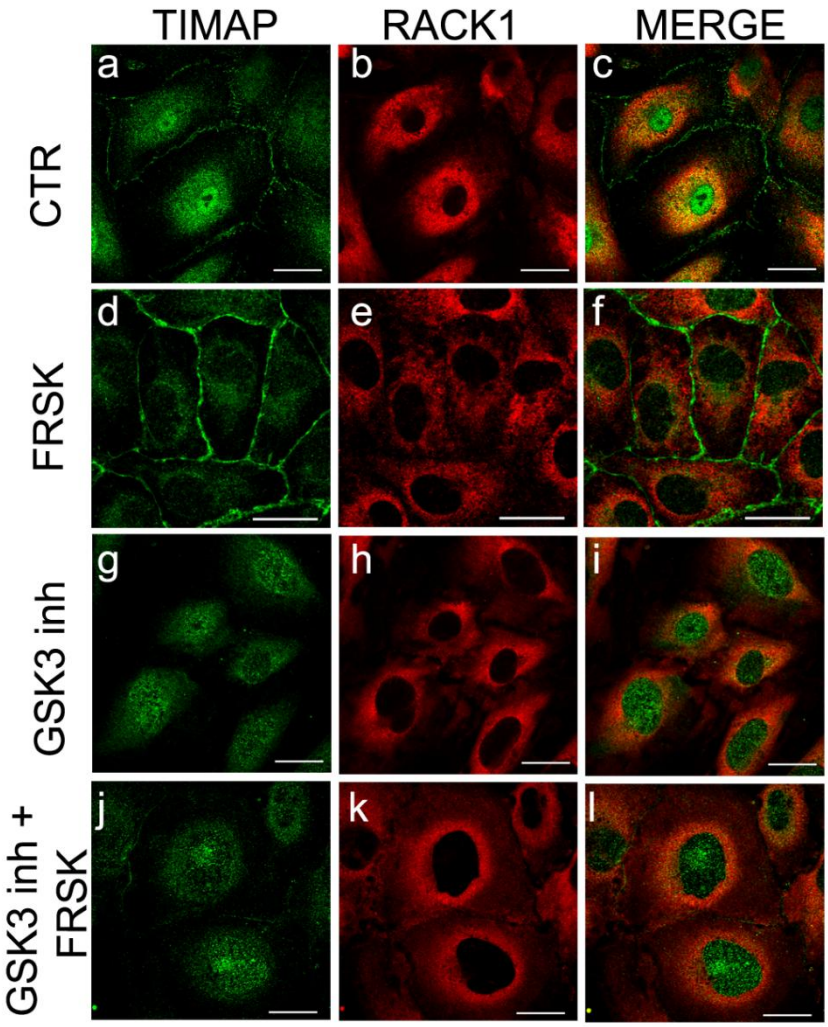

Figure 23. GSK3β inhibitor results in loss of membrane localized TIMAP.
Immunofluorescence staining of confluent HPAEC without (a-c) (CTR), or with various treatments as follows: 50 μM forskolin (FRSK) for 30 min (d-f); 20 μM GSK3β inhibitor, AR-A014418, (GSK3 inh) for 4 hrs (g-i); or 20 μM GSK3β inhibitor for 4 hrs followed by 50 μM forskolin for 30 min (j-l) using anti-TIMAP (a,d,g,j: green) and anti-RACK1 (b,e,h,k: red) primary antibodies was performed. Representative data of at least three independent experiments are shown. Scale bars: 100 μm.

The applied effectors did not change the cytoplasmic localization of RACK1 as shown on confocal images (Fig. 23 b,e,h,k). On the other hand, upon forskolin treatment, the amount of nuclear TIMAP decreased parallel with its more pronounced appearance in the cell membrane (Fig. 23 d) compared to the untreated sample (Fig. 23 a). Since PKA phosphorylation of TIMAP on Ser337 primes its GSK3β phosphorylation on Ser333 [93, 172], AR-A014418, a selective GSK-3β inhibitor [174], was employed alone or as pretreatment before addition of forskolin to prevent PKA primed phosphorylation of TIMAP by GSK-3β. Without forskolin, no TIMAP was detected in the plasma membrane when GSK-3β was inhibited (Fig.23 g); also, the effect of forskolin was strongly attenuated in the presence of AR-A014418 (Fig.23 j). Merged images indicate

co-localization of RACK1 and TIMAP in the region of cytoplasm that is rather close to the nucleus in control and GSK-3β inhibited cells (Fig. 23 c,i,l), but co-localization was not detectable in cells treated exclusively with forskolin (Fig. 23 f). When cells were pretreated with a PKA inhibitor, H89, no translocation of TIMAP to the cell membrane was observed upon forskolin challenge, proving the involvement of PKA activity (Fig. 24).

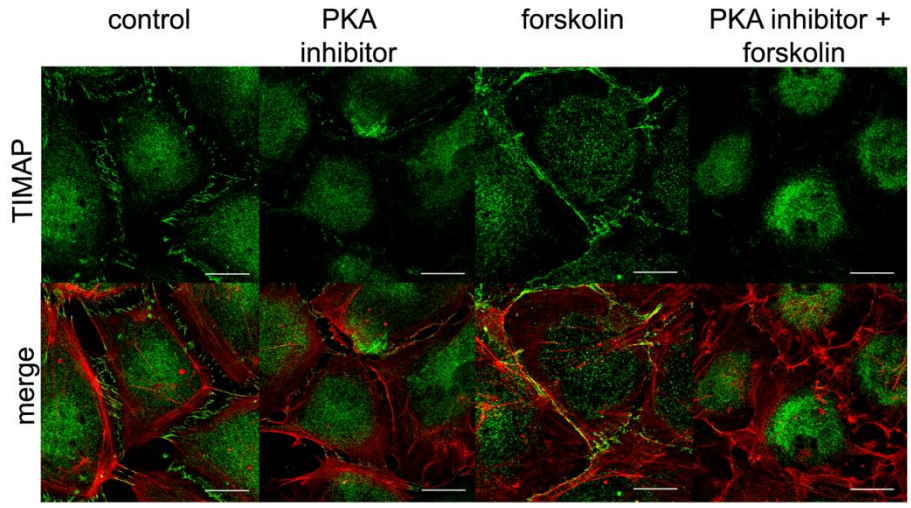

Figure 24. Effect of PKA inhibition on the localization of TIMAP.
Immunofluorescence staining of confluent HPAEC without (control), or with various treatments as follows: 10 μM H89 (PKA inhibitor) for 30 min; 50 μM forskolin for 30 min; or 10 μM H89 for 30 min followed by 50 μM forskolin for 30 min using anti-TIMAP antibody and Texas-Red Phalloidin. Scale bars: 100 μm.

Membrane and nuclear fractions of HPAEC were isolated by cell fractionation and the amount of TIMAP in the fractions was detected by Western blot (Fig. 25A).The amount of TIMAP increased in the membrane fraction after forskolin, but it was significantly lowered in the presence of GSK-3β inhibitor compared to the control, parallel with the results of the immunofluorescent staining. Forskolin challenge in GSK-3β inhibited cells caused significant increase in the TIMAP level in the membrane fraction compared to the extremely faint signal found in the same fraction of cells treated only with the kinase inhibitor. Furthermore, Western blot analysis of the nuclear fractions, as expected, demonstrated opposite trends for the changes. The least amount of TIMAP was detected in the nuclear fraction of the forskolin treated cells, while inhibition of GSK-3β caused a large increase, however, forskolin significantly moderated this effect of the inhibitor.

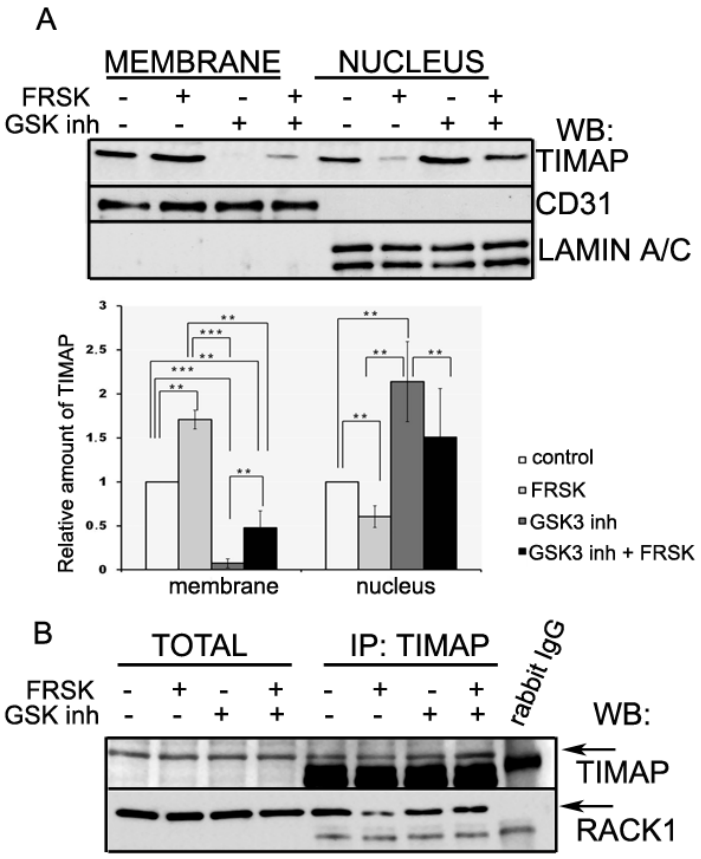

Figure 25. GSK3β inhibitor results in loss of membrane localized TIMAP.
Subcellular fractionations of HPAEC cells trated with 10 μM H89 (PKA inhibitor) for 30 min; 50 μM forskolin for 30 min; or 10 μM H89 for 30 min followed by 50 μM forskolin for 30 min. The fractions were analyzed with anti-TIMAP, anti-CD31 as membrane, anti-lamin A/C as nuclear and anti-β-tubulin (not shown) as cytoplasmic marker antibody. Quantitative analysis of TIMAP signals is also shown. CD31 or lamin A/C bands were used for protein level normalization. The results are presented as means ± SE from 3 independent experiments. Statistical analysis was done with Student's t-test. Significant changes are indicated by asterisks; * ($P<0.05$), ** ($P<0.01$), or *** ($P<0.001$). (*B*) TIMAP was immunoprecipitated from HPAEC after the same set of treatments as listed in panel (*A*). Total cell lysates and the IP complexes were probed for TIMAP and RACK1. Additional bands in IP samples correspond to IgG.

There was no significant change in the amount of RACK1 in TIMAP IP of GSK-3β inhibited cells compared to control. As expected, less RACK1 was associated to TIMAP after forskolin challenge, but no effect of forskolin was detectable after AR-A014418 pretreatment of EC (Fig. 25B). These results suggest that interaction of TIMAP with RACK1 may exist in the cytoplasm of EC and it is affected by double phosphorylation (PKA and GSK-3β) of TIMAP.

Effect of RACK1 depletion on TIMAP

RACK1 was depleted in HPAEC cells using silencing RNA duplexes specific for RACK1 (GNB2L1). The efficiency of silencing was confirmed both at mRNA and protein level of RACK1 by RT-PCR and Western blot (Fig. 26A,B).

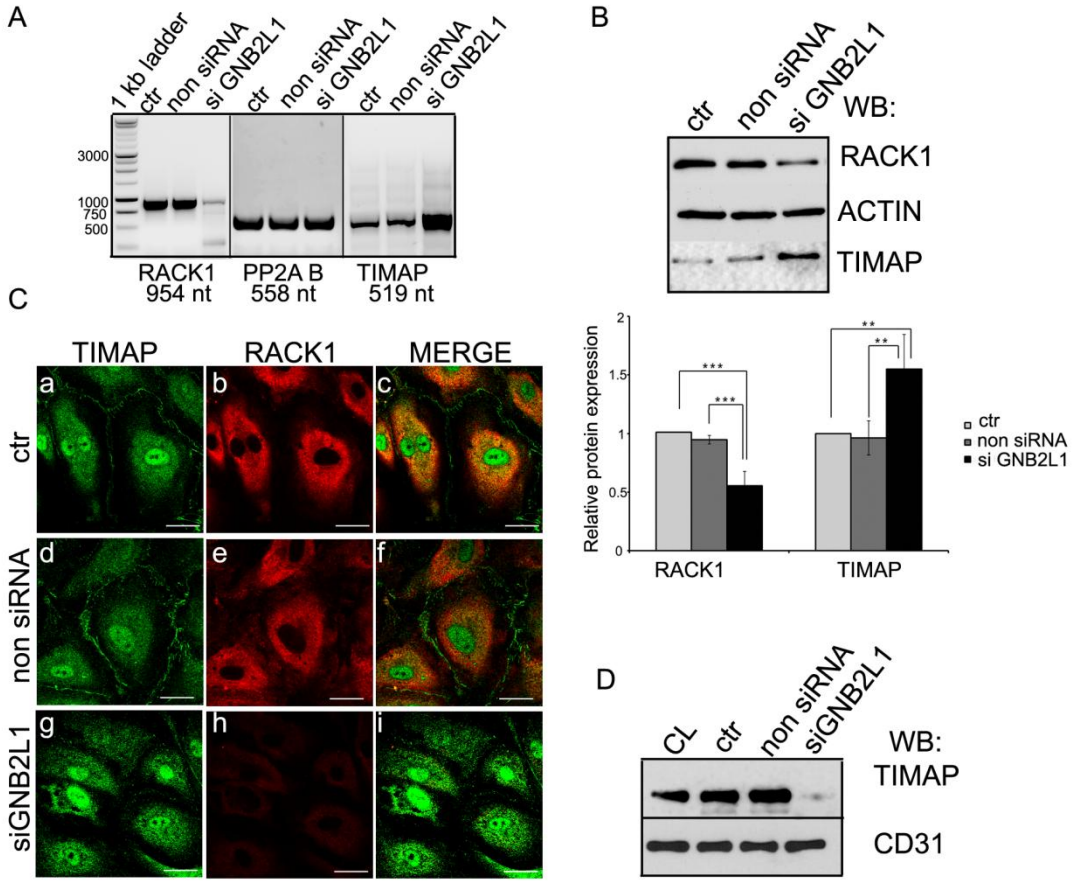

Figure 26. RACK1 depletion modulates mRNA and protein levels of TIMAP and affects the membrane localization of TIMAP.

(*A*) HPAEC grown on 6-well plate was transfected with small interfering RNA (siRNA). Total RNA was isolated from non transfected (ctr), non silencing RNA, or RACK1 specific siRNA (siGBN2L1) transfected cells and analyzed by RT-PCR using specific primer pairs for RACK1, PP2A B (irrelevant control) or TIMAP. (*B*) Western blot analysis of non transfected (ctr), non silencing RNA, or siGBN2L1 transfected cells using RACK1, TIMAP and actin specific antibodies. Actin was tested as loading control. The amount of RACK1 or TIMAP signal was expressed as ratio of RACK1/TIMAP:β-actin signal density. The error bars correspond to SE from 3 independent transfections. Statistical analysis was done with Student's t-test. Significant changes are indicated by asterisks; ** ($P<0.01$), or *** ($P<0.001$). *(C)* Immunofluorescence staining of confluent non transfected (ctr) (a-c), non silencing RNA (d-f) or siGBN2L1 treated (g-i) HPAEC using anti-TIMAP (a,d,g: green) and anti-RACK1 (b,e,h: red) primary antibodies is presented. Scale bars: 100μm. *(D)* Membrane fractions of non transfected (ctr), non silencing RNA or siGBN2L1 transfected HPAEC were isolated as described in Materials and Methods. Total cell lysate (CL) was also loaded as control. The fractions were analyzed with anti-TIMAP and anti-CD31 antibodies.

We detected about 70-80% and 50% decrease in the mRNA and protein level of RACK1, respectively, in the depleted cells compared to the control or non silencing RNA transfected cells. Primers for B55, the regulatory subunit of protein phosphatase 2A, were used as endogenous control of RT-PCR. In the same set of experiments the mRNA and protein level of TIMAP were evaluated as well; interestingly, both increased in the RACK1 depleted HPAEC (Fig. 26A,B). This observation may suggest that RACK1 may be involved in the regulation of TIMAP transcription, but elaboration of this assumption would require further examination.

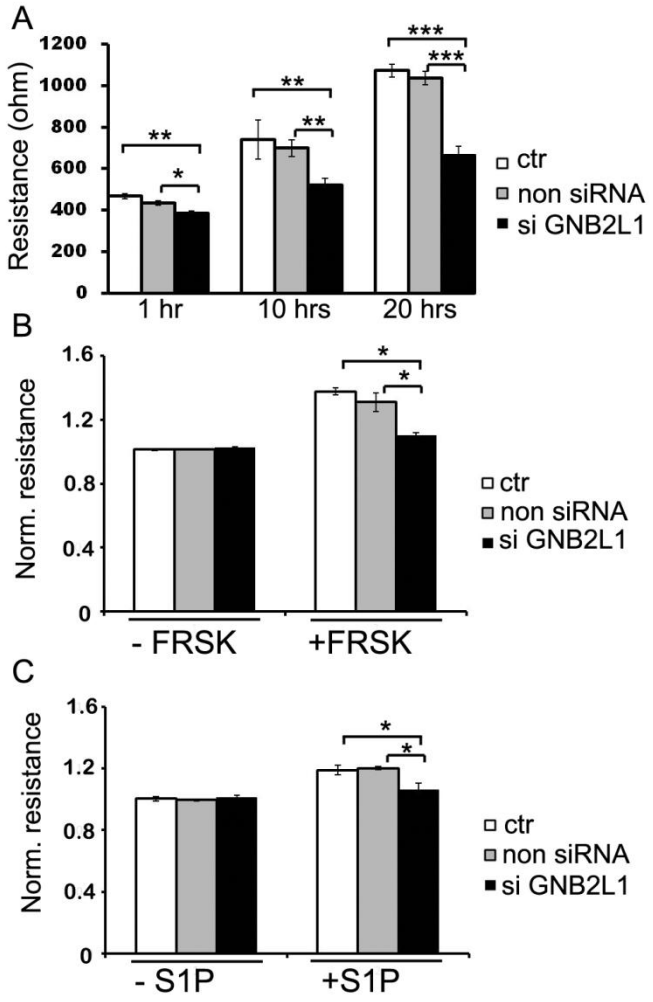

Figure 27. RACK1 depletion attenuates EC barrier function.
Non transfected (ctr), non silencing or RACK1 specific silencing RNA transfected HPAEC were plated (5×10^5 cells/well) onto two 8W10E arrays 48 h post-transfection. (A): The initial resistance values at the beginning of the measurement were about 300 Ω and the impedance was measured for 20 hrs after the seeding. (B,C): After overnight incubation and basal TER monitoring (900–1200 Ω), HPAEC monolayers were treated with 50 μM forskolin (B) or 1 μM sphingosine 1-phosphate (S1P) (C). Relative resistances that were detected at the time of maximal TER increase of forskolin/S1P treated cells are shown for each sample. The results are presented as means ± SEM at least of four chambers for each treatment.

Immunofluorescent staining and Western blot analysis of the membrane fraction of RACK1 siRNA transfected HPAEC revealed loss of TIMAP in the plasma membrane (Fig. 26C, D). This offers another plausible interpretation of the increased amount of TIMAP, namely, RACK1 silenced cells simply try to compensate for the lowered membrane localized TIMAP. More importantly, the loss of TIMAP at the membrane in the absence of RACK1 led us to the conclusion that the adaptor protein RACK1 assists the traffic of TIMAP to the cell membrane.

Previous results of our group showed the involvement of TIMAP in EC barrier regulation. Therefore, it was tested whether the barrier function of EC monolayers could be affected by RACK1 depletion as a consequence of loss of TIMAP in the plasma membrane. Endothelial barrier formation (attachment and spreading of EC) of control and RACK1 depleted HPAEC were followed by ECIS measurements (Fig. 27A). The number of control and siRNA transfected cells inoculated in ECIS wells was identical; also there was no notable difference in the cell density of the samples and no dead cells were observed in the wells after the ECIS measurements. The impedance values measured at 1 h after the start of the measurement were significantly lower for the RACK1 silenced sample. During the 20 hours of the experiment, this difference became more pronounced, implying that the formation of endothelial barrier was damaged in the absence of RACK1. In addition, the effect of forskolin and sphingosin 1-phosphate, two barrier enhancing agonists, was strongly attenuated in RACK1 depleted EC (Fig. 27B,C).

RACK1 aids farnesylation/membrane transport of TIMAP

Since co-localization of TIMAP and RACK1 was not detected in our previous experiments in the cell membrane, we could exclude that RACK1 would be directly involved in the transport of TIMAP. Yet, we hypothesized that the prenylation of TIMAP leading to its movement to the plasma membrane may require the anchoring property of RACK1. Indeed, we detected interaction of farnesyl transferase with RACK1 in pull-down assay, the binding region in RACK1 is in the N-terminal WD1-4 region (Fig. 28A). Most importantly, TIMAP and farnesyl transferase co-immunoprecipitated from HPAEC with normal RACK1 level only, but not from

RACK1 depleted cells (Fig. 28B), suggesting a pivotal role of RACK1 in TIMAP prenylation.

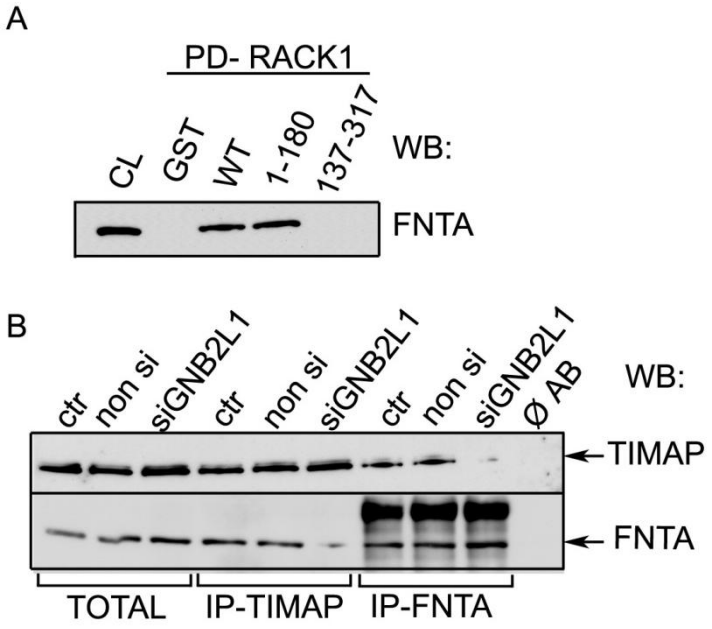

Figure 28. TIMAP interacts with farnesyl transferase via RACK1.
(*A*) GST-RACK1 pull-down of endogenous farnesyl transferase (FNTA). GST, recombinant RACK1 WT or GST-RACK1 fragments were tested in pull-down assay. The immobilized samples were incubated with BPAEC lysate. Western blot of the pull-down eluates was probed with anti-FNTA antibody. (*B*) TIMAP or FNTA was immunoprecipitated from non transfected (ctr), non silencing RNA or siGBN2L1 transfected HPAEC. Total cell lysates and the IP complexes were probed for TIMAP and FNTA. Additional bands in IP samples correspond to IgG.

Discussion

EBP50 is a well characterized protein in epithelium, yet little is known about its role in other cell types. It is expressed at high levels in the kidney, liver, small intestine, and placenta, but also expressed at lower levels in the brain and lung [116, 117]. Studies made on epithelial cells revealed that EBP50 is localized at the plasma membrane and the cytoplasm, and it is accepted that its primary function is to act as a scaffold protein linking transmembrane proteins to various cytoskeletal proteins. In polarized cells such as kidney proximal tubule cells it is localized primarily in the apical region [175] where its association with proteins like cystic fibrosis transmembrane conductance regulator, podocalyxin, G-protein coupled- or tyrosine kinase receptors was found [176-178].

In interphase endothelial cells (BPAEC and HUVEC) we detected EBP50 in the nucleus and in the perinuclear region in contrast with the above mentioned cytoplasmic location found by others in epithelial cells. Our results were verified by immunofluorescent staining, subcellular fractionation, and recombinant protein expression. The amino acid sequence deduced from the DNA coding the endothelial EBP50 (SLC9A3R1) is identical with the published bovine sequence in the database (NM_001077852). Hence the varying location of EBP50 in endothelial and epithelial cells may be the consequence of different interactive protein partners suggesting diverse function of EBP50 in the two cell types. EBP50 and NHERF2 are the most similar members of the NHERF family (49% amino acid identity), therefore the localization of the two proteins in BPAEC was also compared. Results of immunoflurescence clearly excluded the possibility of non-specific binding of the primary antibodies; EBP50 and NHERF2 appeared at different locations in BPAEC. In addition, by recombinant protein expression we detected the same pattern of localization of the overexpressed EBP50, as well. Only a few studies [179, 180] have reported nuclear localization of EBP50 but only in cancer cell lines not in normal cells. It was shown that EBP50 is overexpressed in hepatocellular carcinoma cell lines and it is localized in the cytoplasm and in the nucleus [123]. Recent studies revelaed that EBP50 expression levels and location were affected by active blastocysts and decidualization during the window of implantation. At the implantation site on day 5 of pregnancy, EBP50 was mainly expressed in the nuclei of stroma cells, whereas from day 6 to 8 of pregnancy, the expression of EBP50 was noted in the cytoplasm of decidual cells [181]. In addition, cell cycle dependent

shuttling between the nucleus and the cytoplasm of merlin, an ERM-like tumor suppressor protein, was described [182] in glioma and osteosarcoma cells. Interestingly, others also detected ERM proteins in the nucleus of MDCK and HeLa cells [183].

It is known that EBP50 can be phoshorylated by protein kinases on multiple sites. During mitosis it is phosphorylated by Cdk1 at Ser279 and Ser301 and this phosphorylation inhibits its oligomerization [130]. The SPX(K/R) preferred phosphorylation motifs of Cdk1 are conserved in EBP50 of different species, thus Ser279 and Ser301 residues in the rabbit protein referred in [130] correspond to Ser288 and Ser310 in the bovine EBP50. Therefore, we concluded that the cell cycle dependent localization change and mobility shift on SDS-PAGE of the endothelial EBP50 are in parallel with the phosphorylation and possibly the oligomerization state of the protein. Furthermore, the phospho-mimic mutant (S288D:S310D) form of EBP50 showed mobility shift on SDS-PAGE and cytoplasmic localization, as did the endogenous EBP50 in dividing cells.

The nuclear envelope offers a selective barrier between the nuclear compartment and the cytoplasm. At the transition from prophase to prometaphase of mitosis the breakdown of the nuclear envelope leads to combination of the two compartments [184]. However, we could detect EBP50 in the cytoplasm in cells in early prophase to late cytokinesis, suggesting an active transporting mechanism. A number of proteins required for nucleocytoplasmic transport have important functions during mitosis [185], still the significance of the varying location of EBP50 is not clear yet. Recent studies showed that phosphorylation, one of the major posttranslational modifications, strongly regulates the interaction of EBP50 with several proteins, like moesin and ezrin [122, 132]. Further investigations are necessary to clarify what is the function(s) of EBP50 in the nucleus and cytoplasm and what are the targeted proteins in these compartments.

Phospho-mimic mutant (S288D:S310D) form of EBP50 significantly accelerated the wound healing of BPAEC indicating the physiological significance of the phosphorylation of the protein. In vascular smooth muscle cells siRNA mediated depletion of EBP50 increased cell migration and induced cell morphology changes, moreover, binucleated cells were observed as the defect of cytokinesis [186]. *NHERF1/EBP50* gene mutations were identified in cancer cells [187], in addition knockdown of EBP50 increased cellular proliferation and migration of cancer cell lines suggesting that EBP50 acts as a tumor suppressor [188]. Our findings in normal cells

underline the importance of EBP50 in cell division via the cyclin dependent kinase phosphorylation and PP2A dependent dephosphorylation of the protein.

Experiments made with phosphatase inhibitors suggested that the dephosphorylation of the Cdk1 (mitosis) -specific phosphoserine side chains in HeLa cells is mediated by PP1 or PP2A phosphatases, but not by PP2B [130]. Our attempts to verify the involvement of PP1 in the dephosphorylation of EBP50 in BPAEC have failed, since specific inhibitor (calyculin A, 2 nM) of PP1 had no effect on the phosphorylation state of EBP50 arrested in G2/M phase, moreover, immunoprecipitation experiments did not show protein-protein interaction between EBP50 and PP1. On the other hand, our results indicated that PP2A interacts and co-localizes with EBP50 in a cell cycle dependent manner. We did detect remarkable amount of PP2A A and C subunits in the immunoprecipitate of EBP50 and definite co-localization of the C subunit and EBP50 in mitotic phase BPAEC. Furthermore, we identified Bα (also named as PR55)[89], besides the AC dimer, with pull-down assays as the third subunit in the PP2A holoenzyme interacting with EBP50.

Our results do not specify which subunit(s) of the PP2A heterotrimer is/are directly interacting with EBP50 and no PDZ binding domain was identified in the PP2A subunits. A C-terminal motif was described in several peptides and proteins, which was shown to be responsible for binding to the PDZ domains in EBP50 [176, 189]. We compared the sequence of the four amino acids at the C-terminal of the PP2A subunits (LSLA for A, DYFL for C and DKVN for Bα subunit) with this DS/TxL motif. Although none of these tetrapeptides seem to be optimal, still we cannot exclude any subunit of PP2A as a potential binding partner for EBP50, as the results of others [176, 189] with peptide bonding indicate broad variations in the motif.

The location change and the co-localization of EBP50 with PP2Ac during the course of mitosis were parallel, with the highest levels of co-localization during the phases from metaphase to early cytokinesis. We also observed that the ratio of dividing cells was higher in cells expressing the phospho-mimic mutant (S288D:S310D) compared to those expressing the wild type EBP50. Since we could not detect the phosphorylated form of EBP50 in the lysate of interphase cells, these results suggest that the dephosphorylation of P-Ser288 and P-Ser310 is necessary for the mitotic exit and it is catalyzed by PP2A. Dephosphorylation of the Cdk1 substrates by PP1 and

PP2A as an element of the exit from mitosis in vertebrate cells was described earlier [190-192].

Our results show that a protein thought to be a linker between the plasma membrane and cytoplasmic/cytoskeletal proteins may be involved in nuclear events as well. We provide evidences for cell cycle dependent localization and phosphorylation of EBP50, and its interaction with PP2A during mitosis. Our results indicate that EBP50 may have a significant role in the course of the cell cycle and that PP2A can be the phosphatase dephosphorylating P-Ser288 and P-Ser310 of EBP50 in BPAEC.

In a search for partners of TIMAP we recognized and proved by different methods that TIMAP binds the adaptor protein, RACK1.

RACK1 is known as a scaffolding protein which belongs to the WD-repeat containing proteins. It seems that RACK1 has no preference for a common structural feature in its binding partners. Among the RACK1 interacting proteins some contain Src homology (SH2) domains [141], pleckstrin homology (PH) domains like dynamin [173, 193], C2 and V5 domains in PKCs [135, 136] or PDZ domains [194]; but there is also example for a whole specific structural conformation requirement on the partner's side [195]. Our results indicate that RACK1 binds to the NLS region at the N-terminal of TIMAP, but there is/are further association site(s) within the C-terminal half region of TIMAP suggesting a more complex surface for the interaction. It should be noted that the PKA/GSK-3β phosphorylation sites, Ser337/333 of TIMAP are present in this region. Site directed mutations revealed that the phosphorylation state of TIMAP is an important factor of the interaction. Moreover, we showed that the site/region in RACK1 responsible for TIMAP binding is within the N-terminal half (WD 1-4) of the protein. RACK1 forms homodimers via the fourth WD repeat [153], therefore both the N- and C-terminal mutants tested were designed to contain WD 4 as described by others [196]. Thus the binding region can be further narrowed to WD 1-3, but elucidation of the exact binding sites in TIMAP and RACK1 requires additional research. Another PP1 related protein, CPI17 (PKC potentiated PP1 inhibitor), was recognized as binding partner of RACK1 by yeast two-hybrid screening [197]. Interestingly, binding of the dimer form (catalytic and scaffolding subunit) of PP2A, another major Ser/Thr protein phosphatase, was shown to a C-terminal WD repeat in RACK1 [196, 198]. The mutual or exclusive binding of the two subunits of PP2A was not resolved. We found that PP1cδ is present

in the RACK1-TIMAP complex as TIMAP is its regulatory/targeting subunit, but does not bind directly to RACK1.

Although RACK1 and PKC are intimately related to each other (for review see [149]), that seems irrelevant in the TIMAP-RACK1 relation, as PKC activation of EC did not change their binding. On the other hand, activation of the cAMP/PKA pathway had significant effect not only on the interaction, but also on the localization of TIMAP. The second messenger cAMP is known as endothelial barrier stabilizer [199, 200]. Upon cAMP/PKA activation of EC, we detected enrichment of TIMAP in the plasma membrane and its translocation from the nucleus. Since parallel translocation of RACK1 did not happen from the cytoplasm of EC either to the membrane or to the nucleus, this suggests that separate signaling pathways regulating nuclear export and membrane traffic of TIMAP could be initiated simultaneously.

RACK1 is connected to the cAMP/PKA signaling pathway through its interaction with cAMP phosphodiesterases [139, 155]. Similar to our results, in hippocampal neurons dissociation of RACK1 from its binding partner, Fyn kinase, occurs upon activation of the PKA pathway [156]. RACK1 translocated to the nucleus in glioma and neuroblastoma cell lines upon PKA activation by forskolin [154] to mediate the expression of a brain-derived neurotrophic factor. In contrast, no translocation of RACK1 upon forskolin treatment of EC was observed in our experiments. However, it was revealed recently that phosphorylation by PKA or sequential phosphorylation by PKA and GSK-3β only slightly modulated the binding of TIMAP to PP1cδ [93]. The dissociation constant of the complex was about the same, only the rate of dissociation decreased to a small extent. *In vitro* phosphatase assays indicated that double phosphorylated form of TIMAP allowed PP1c activity toward phospho-moesin substrate, but mono- or non-phosphorylated form of TIMAP inhibited the phosphatase. PKA/GSK-3β phosphorylation sites, Ser337/333 of TIMAP are present in the C-terminal region which was shown to bind RACK1, thus the phosphorylation of these side chains may affect not only the regulatory effect of TIMAP on PP1cδ, but the binding of TIMAP to RACK1 as well. The phosphorylation may directly impair the connection by inducing conformation change of TIMAP, or may initiate interactions with other binding partners leading to the loss of RACK1-TIMAP complex. Our results clearly demonstrate that significant loss in TIMAP-RACK1 complex follows PKA primed GSK-3β phosphorylation of TIMAP.

On the contrary, when the TIMAP-RACK1 interaction was diminished by depletion of RACK1, TIMAP was not found in the plasma membrane of the silenced cells suggesting a pivotal role of RACK1 in prenylation/membrane localization of TIMAP. Significance of RACK1 in membrane localization of a Vang protein was also recognized by RACK1 knockdown recently [201]. Prenylation of TIMAP at the C-terminal CAAX box [91] by farnesyl transferase [202] is required for its membrane localization. Eventually, deficiency of membrane anchored TIMAP may be the result of the lack of its prenylation. Our results indicated that both TIMAP and farnesyl transferase bind to the N-terminal half of RACK1 and the interaction between TIMAP and farnesyl transferase was diminished in RACK1 depleted cells. These confirm the assumption of RACK1 being the anchoring surface for the prenylation of TIMAP. Since TIMAP is involved in the regulation of EC barrier function [92], RACK1 should also be regarded as a participant in maintaining barrier integrity, through the regulation of TIMAP prenylation.

The pulmonary vascular endothelium functions as a semi-selective barrier between blood and surrounding tissues and controls biological processes such as protein and fluid transport or inflammation. Endothelial barrier dysfunction is the primary cause of vascular leak and pulmonary edema in sepsis and is an essential component of angiogenesis, tumor metastasis, and atherosclerosis. Therefore, the maintenance of vascular EC barrier integrity may have profound clinical importance. In agreement with the conclusion that RACK1 is involved in the maintenance of barrier integrity, we found decelerated barrier formation in RACK1 depleted EC. Consistent with this, it was shown by others that RACK1 regulates cell adhesion [203], moreover, silencing of RACK1 inhibited cell proliferation and decreased migration and adhesion capability of carcinoma cells [204]. A recent paper [205] described the involvement of RACK1 in Gβγ-mediated adherens junction assembly in EC. They studied the function of Gβγ in re-annealing of adherens junctions after thrombin challenge/protease-activated receptor activation. RACK1, normally bond to Gβγ, is released after thrombin and that triggers Fyn activation via the focal adhesion kinase. In RACK1 depleted cells, they detected slower recovery of TER after thrombin. Our transendothelial electric resistance (TER) measurement with thrombin treated RACK1 depleted cells showed the same result (not shown). Still, the positive effect of cAMP/PKA activation (forskolin treatment) on TER was significantly attenuated in RACK1 silenced EC. Moreover, sphingosin-1-

phosphate, a well-known vascular stabilizer [206, 207], had also failed to increase TER in RACK1 depleted cells. It seems, that RACK1 may be involved in multiple signaling pathways concerned in EC barrier regulation.

Taken together, both EBP50 and TIMAP are related to the ERM proteins which play a major role in EC cytoskeleton regulation and EC barrier maintenance. Our results revealed that subcellular localization of EBP50 in EC is different from that of in epithelium, e.g. it localizes in the nucleus in interphase EC and EBP50 seems to be involved in the regulation of cell cycle in EC. Our most recent results suggest that EBP50 and the closely related NHERF2 have different binding specificity to ERM in EC, implying their different roles in the regulation of ERM proteins. We also found that the scaffolding protein, RACK1, aids prenylation and consequently cell membrane localization of TIMAP, where PP1c-TIMAP may dephosphorylate the ERM proteins. Furthermore, our newly initiated investigations indicate the significance of TIMAP in angiogenesis, as well.

Summary

Vascular endothelial cell monolayer acts as a semiselective barrier between blood and the interstitium. Phosphorylation level of many cytoskeleton and cytoskeleton-associated proteins playing crucial role in the EC barrier function is critical to tissue and organ function. ERM-binding phosphoprotein 50 (EBP50) is a phosphorylatable PDZ domain-containing adaptor protein that is abundantly expressed in epithelium but was not yet studied in the endothelium. We found unusual nuclear localization of EBP50 in bovine pulmonary artery endothelial cells (BPAEC). Immunofluorescent staining and cellular fractionation demonstrated that EBP50 is present in the nuclear and perinuclear region in interphase cells. In the prophase of mitosis EBP50 redistributes to the cytoplasmic region in a phosphorylation dependent manner and during mitosis EBP50 co-localizes with protein phosphatase 2A. Furthermore, *in vitro* wound healing of BPAEC expressing phospho-mimic mutant of EBP50 was accelerated indicating that EBP50 is involved in the regulation of the cell division. Cell cycle dependent specific interactions were detected between EBP50 and the subunits of PP2A (A, C, and Bα) with immunoprecipitation and pull-down experiments. The interaction of EBP50 with the Bα containing form of PP2A suggests that this holoenzyme of PP2A can be responsible for the dephosphorylation of EBP50 in cytokinesis. Moreover, our results underline the significance of EBP50 in cell division via reversible phosphorylation of the protein with cyclin dependent kinase and PP2A in normal cells.

TIMAP, TGF-β inhibited membrane-associated protein, is most abundant in endothelial cells with a regulatory effect on the endothelial barrier function, yet little is known about its interacting partners. RACK1, receptor for activated protein kinase C, serves as an anchor in multiple signaling pathways. We found that RACK1 binds to the TIMAP-PP1c complex in endothelial cells. WD1-4 repeats of RACK1 were identified as critical regions of the interaction both with TIMAP and farnesyl transferase. Phosphorylation of TIMAP by activation of the cAMP/PKA pathway reduced the amount of TIMAP-RACK1 complex and enhanced translocation of TIMAP to the cell membrane in vascular endothelial cells. However, both membrane localization of TIMAP and transendothelial resistance were attenuated after RACK1 depletion. Farnesyl transferase, the enzyme responsible for prenylation and consequent membrane

localization of TIMAP, is present in the RACK1-TIMAP complex in control cells, but it does not co-immunoprecipitate with TIMAP after RACK1 depletion. Our results suggest that transient parallel linkage of TIMAP and farnesyl transferase to RACK1 could ensure prenylation and transport of TIMAP to the plasma membrane where it may attend in maintaining the endothelial barrier as a phosphatase regulator.

Összefoglalás

A vaszkuláris endotél sejtek szemiszelektív barrierként választják el a keringő vért a környező szövetektől. A jól működő endotél barrier funció fenntartásában számos citoszkeletális és citoszkeleton asszociált fehérje foszforilációja fontos szerepet játszik. Az EBP50 (ezrin-radixin-moesin-binding phosphoprotein 50), egy olyan foszforilálható adaptor fehérje, mely epitél sejtekben magas expressziós szinttel rendelkezik azonban endotél sejtekben még nem vizsgálták. Immunfluoreszcens festéssel, valamint sejtfrakcionálással az EBP50 fehérjét az interfázisban lévő endotél sejtek magi régiójában detektáltuk. A mitózis profázisában foszforiláció-függő módon a sejtek citoplazmájába transzlokálódott és kolokalizáció volt megfigyelhető a protein foszfatáz 2A enzimmel. Az EBP50 foszforilációt utánzó mutánsát expresszáló sejtek gyorsabb *in vitro* sebgyógyálást mutattak, ami az EBP50 sejtosztódásban betöltött szabályozó szerepére utal. Immunprecipitációs és pull down kísérletekkel sikerült igazolnuk az EBP50 és a PP2A (A, C, és Bα) alegységei közötti sejtciklus függő kölcsönhatást. Eredményeink arra utalnak, hogy a PP2A enzim szerepet játszik az EBP50 fehérje defoszforilálásában normál sejtekben a sejtciklus során.

A TIMAP (TGFβ inhibited membrane-associated protein) endotél sejtekben rendelkezik a legmagasabb expressziós szinttel, szerepéről és kölcsönható partnereiről azonban csak keveset tudunk. A RACK1 (Receptor for Activated C Kinase 1) adaptor fehérje, számos jelátviteli útvonalban játszik szerepet. Eredményeink alapján endotél sejtekben a RACK1 a TIMAP-PP1c komplexhez kötődik. A kölcsönhatásban a RACK1 WD1-4 doménjei vesznek részt, melyhez kötődik továbbá a farnezil-transzferáz enzim is. A cAMP/PKA útvonal aktiválásával elért TIMAP foszforiláció csökkentette a RACK1-TIMAP komplex mennyiségét, valamint a TIMAP membránban való feldúsulásához vezetett. A RACK1 depléciójával a TIMAP membránlokalizációja valamint a farnezil-transzferáz enzimmel való kölcsönhatása is megszűnt. Eredményeink alapján a RACK1 adaptor fehérje biztosítja a TIMAP prenilációját az ehhez szükséges farnezil-transzferáz enzimmel való kölcsönhatással.

References

1. Komarova, Y. and A.B. Malik, *Regulation of endothelial permeability via paracellular and transcellular transport pathways.* Annu Rev Physiol, 2010. **72**: p. 463-93.
2. Mehta, D. and A.B. Malik, *Signaling mechanisms regulating endothelial permeability.* Physiol Rev, 2006. **86**(1): p. 279-367.
3. Dejana, E., *Endothelial cell-cell junctions: happy together.* Nat Rev Mol Cell Biol, 2004. **5**(4): p. 261-70.
4. Mangialardi, G., et al., *Diabetes Causes Bone Marrow Endothelial Barrier Dysfunction by Activation of the RhoA-Rho-Associated Kinase Signaling Pathway.* Arterioscler Thromb Vasc Biol, 2013. **33**(3): p. 555-64.
5. Johansson, B.B. and L.E. Linder, *Reversibility of the blood-brain barrier dysfunction induced by acute hypertension.* Acta Neurol Scand, 1978. **57**(4): p. 345-8.
6. McQuaid, K.E. and A.K. Keenan, *Endothelial barrier dysfunction and oxidative stress: roles for nitric oxide?* Exp Physiol, 1997. **82**(2): p. 369-76.
7. Maniatis, N.A. and S.E. Orfanos, *The endothelium in acute lung injury/acute respiratory distress syndrome.* Curr Opin Crit Care, 2008. **14**(1): p. 22-30.
8. Raghavendran, K. and L.M. Napolitano, *Definition of ALI/ARDS.* Crit Care Clin, 2011. **27**(3): p. 429-37.
9. Kubo, K., *[Basis and clinical aspects of ALI/ARDS]*. Nihon Naika Gakkai Zasshi, 2005. **94**(9): p. 1956-63.
10. Caldwell, R.B., et al., *Vascular endothelial growth factor and diabetic retinopathy: role of oxidative stress.* Curr Drug Targets, 2005. **6**(4): p. 511-24.
11. Hashizume, H., et al., *Openings between defective endothelial cells explain tumor vessel leakiness.* Am J Pathol, 2000. **156**(4): p. 1363-80.
12. Shore, A.C., *The microvasculature in type 1 diabetes.* Semin Vasc Med, 2002. **2**(1): p. 9-20.
13. Tooke, J.E., *Microvascular function in human diabetes. A physiological perspective.* Diabetes, 1995. **44**(7): p. 721-6.
14. Dudek, S.M. and J.G. Garcia, *Cytoskeletal regulation of pulmonary vascular permeability.* J Appl Physiol, 2001. **91**(4): p. 1487-500.
15. Yuan, S.Y., *Protein kinase signaling in the modulation of microvascular permeability.* Vascul Pharmacol, 2002. **39**(4-5): p. 213-23.
16. Manning, G., et al., *The protein kinase complement of the human genome.* Science, 2002. **298**(5600): p. 1912-34.
17. Aitken, A., *Protein consensus sequence motifs.* Methods Mol Biol, 2003. **211**: p. 465-85.
18. Gaudreault, N., et al., *Counter regulatory effects of PKCbetaII and PKCdelta on coronary endothelial permeability.* Arterioscler Thromb Vasc Biol, 2008. **28**(8): p. 1527-33.
19. Brautigan, D.L., *Phosphatases as partners in signaling networks.* Adv Second Messenger Phosphoprotein Res, 1997. **31**: p. 113-24.
20. Wera, S. and B.A. Hemmings, *Serine/threonine protein phosphatases.* Biochem J, 1995. **311 (Pt 1)**: p. 17-29.
21. Cohen, P.T., *Novel protein serine/threonine phosphatases: variety is the spice of life.* Trends Biochem Sci, 1997. **22**(7): p. 245-51.

22. Zhang, Z., et al., *Expression and characterization of rat protein phosphatases-1 alpha, -1 gamma 1, -1 gamma 2, and -1 delta.* Arch Biochem Biophys, 1993. **303**(2): p. 402-6.
23. Andreassen, P.R., et al., *Differential subcellular localization of protein phosphatase-1 alpha, gamma1, and delta isoforms during both interphase and mitosis in mammalian cells.* J Cell Biol, 1998. **141**(5): p. 1207-15.
24. Goldberg, J., et al., *Three-dimensional structure of the catalytic subunit of protein serine/threonine phosphatase-1.* Nature, 1995. **376**(6543): p. 745-53.
25. Egloff, M.P., et al., *Crystal structure of the catalytic subunit of human protein phosphatase 1 and its complex with tungstate.* J Mol Biol, 1995. **254**(5): p. 942-59.
26. Egloff, M.P., et al., *Structural basis for the recognition of regulatory subunits by the catalytic subunit of protein phosphatase 1.* EMBO J, 1997. **16**(8): p. 1876-87.
27. Maynes, J.T., et al., *Crystal structure of the tumor-promoter okadaic acid bound to protein phosphatase-1.* J Biol Chem, 2001. **276**(47): p. 44078-82.
28. Kita, A., et al., *Crystal structure of the complex between calyculin A and the catalytic subunit of protein phosphatase 1.* Structure, 2002. **10**(5): p. 715-24.
29. Terrak, M., et al., *Structural basis of protein phosphatase 1 regulation.* Nature, 2004. **429**(6993): p. 780-4.
30. Virshup, D.M. and S. Shenolikar, *From promiscuity to precision: protein phosphatases get a makeover.* Mol Cell, 2009. **33**(5): p. 537-45.
31. Barford, D., A.K. Das, and M.P. Egloff, *The structure and mechanism of protein phosphatases: insights into catalysis and regulation.* Annu Rev Biophys Biomol Struct, 1998. **27**: p. 133-64.
32. Cohen, P.T., *Protein phosphatase 1--targeted in many directions.* J Cell Sci, 2002. **115**(Pt 2): p. 241-56.
33. Wakula, P., et al., *Degeneracy and function of the ubiquitous RVXF motif that mediates binding to protein phosphatase-1.* J Biol Chem, 2003. **278**(21): p. 18817-23.
34. Bollen, M., *Combinatorial control of protein phosphatase-1.* Trends Biochem Sci, 2001. **26**(7): p. 426-31.
35. Garcia, A., et al., *Serine/threonine protein phosphatases PP1 and PP2A are key players in apoptosis.* Biochimie, 2003. **85**(8): p. 721-6.
36. Xing, H., Y. Hong, and K.D. Sarge, *Identification of the PP2A-interacting region of heat shock transcription factor 2.* Cell Stress Chaperones, 2007. **12**(2): p. 192-7.
37. Bollag, B., et al., *JC virus small T antigen binds phosphatase PP2A and Rb family proteins and is required for efficient viral DNA replication activity.* PLoS One, 2010. **5**(5): p. e10606.
38. Stone, S.R., J. Hofsteenge, and B.A. Hemmings, *Molecular cloning of cDNAs encoding two isoforms of the catalytic subunit of protein phosphatase 2A.* Biochemistry, 1987. **26**(23): p. 7215-20.
39. Zhou, J., H.T. Pham, and G. Walter, *The formation and activity of PP2A holoenzymes do not depend on the isoform of the catalytic subunit.* J Biol Chem, 2003. **278**(10): p. 8617-22.
40. Baharians, Z. and A.H. Schonthal, *Autoregulation of protein phosphatase type 2A expression.* J Biol Chem, 1998. **273**(30): p. 19019-24.

41. Wadzinski, B.E., et al., *NH2-terminal modification of the phosphatase 2A catalytic subunit allows functional expression in mammalian cells.* J Biol Chem, 1992. **267**(24): p. 16883-8.
42. Hemmings, B.A., et al., *alpha- and beta-forms of the 65-kDa subunit of protein phosphatase 2A have a similar 39 amino acid repeating structure.* Biochemistry, 1990. **29**(13): p. 3166-73.
43. Wang, S.S., et al., *Alterations of the PPP2R1B gene in human lung and colon cancer.* Science, 1998. **282**(5387): p. 284-7.
44. Ruediger, R., H.T. Pham, and G. Walter, *Alterations in protein phosphatase 2A subunit interaction in human carcinomas of the lung and colon with mutations in the A beta subunit gene.* Oncogene, 2001. **20**(15): p. 1892-9.
45. Ruediger, R., et al., *Identification of binding sites on the regulatory A subunit of protein phosphatase 2A for the catalytic C subunit and for tumor antigens of simian virus 40 and polyomavirus.* Mol Cell Biol, 1992. **12**(11): p. 4872-82.
46. Ruediger, R., et al., *Molecular model of the A subunit of protein phosphatase 2A: interaction with other subunits and tumor antigens.* J Virol, 1994. **68**(1): p. 123-9.
47. Janssens, V. and J. Goris, *Protein phosphatase 2A: a highly regulated family of serine/threonine phosphatases implicated in cell growth and signalling.* Biochem J, 2001. **353**(Pt 3): p. 417-39.
48. Yang, S.I., et al., *Control of protein phosphatase 2A by simian virus 40 small-t antigen.* Mol Cell Biol, 1991. **11**(4): p. 1988-95.
49. Cho, U.S. and W. Xu, *Crystal structure of a protein phosphatase 2A heterotrimeric holoenzyme.* Nature, 2007. **445**(7123): p. 53-7.
50. Groves, M.R., et al., *The structure of the protein phosphatase 2A PR65/A subunit reveals the conformation of its 15 tandemly repeated HEAT motifs.* Cell, 1999. **96**(1): p. 99-110.
51. Strack, S., et al., *Protein phosphatase 2A holoenzyme assembly: identification of contacts between B-family regulatory and scaffolding A subunits.* J Biol Chem, 2002. **277**(23): p. 20750-5.
52. Mayer, R.E., et al., *Structure of the 55-kDa regulatory subunit of protein phosphatase 2A: evidence for a neuronal-specific isoform.* Biochemistry, 1991. **30**(15): p. 3589-97.
53. Healy, A.M., et al., *CDC55, a Saccharomyces cerevisiae gene involved in cellular morphogenesis: identification, characterization, and homology to the B subunit of mammalian type 2A protein phosphatase.* Mol Cell Biol, 1991. **11**(11): p. 5767-80.
54. Zolnierowicz, S., et al., *Diversity in the regulatory B-subunits of protein phosphatase 2A: identification of a novel isoform highly expressed in brain.* Biochemistry, 1994. **33**(39): p. 11858-67.
55. Strack, S., et al., *Cloning and characterization of B delta, a novel regulatory subunit of protein phosphatase 2A.* FEBS Lett, 1999. **460**(3): p. 462-6.
56. Millward, T.A., S. Zolnierowicz, and B.A. Hemmings, *Regulation of protein kinase cascades by protein phosphatase 2A.* Trends Biochem Sci, 1999. **24**(5): p. 186-91.
57. McCright, B. and D.M. Virshup, *Identification of a new family of protein phosphatase 2A regulatory subunits.* J Biol Chem, 1995. **270**(44): p. 26123-8.
58. Csortos, C., et al., *High complexity in the expression of the B' subunit of protein phosphatase 2A0. Evidence for the existence of at least seven novel isoforms.* J Biol Chem, 1996. **271**(5): p. 2578-88.

59. Tehrani, M.A., M.C. Mumby, and C. Kamibayashi, *Identification of a novel protein phosphatase 2A regulatory subunit highly expressed in muscle.* J Biol Chem, 1996. **271**(9): p. 5164-70.
60. Tanabe, O., et al., *Molecular cloning of a 74-kDa regulatory subunit (B" or delta) of human protein phosphatase 2A.* FEBS Lett, 1996. **379**(1): p. 107-11.
61. McCright, B., et al., *The B56 family of protein phosphatase 2A (PP2A) regulatory subunits encodes differentiation-induced phosphoproteins that target PP2A to both nucleus and cytoplasm.* J Biol Chem, 1996. **271**(36): p. 22081-9.
62. Zolnierowicz, S., et al., *The variable subunit associated with protein phosphatase 2A0 defines a novel multimember family of regulatory subunits.* Biochem J, 1996. **317 (Pt 1)**: p. 187-94.
63. Nagase, T., et al., *Tissue and subcellular distributions, and characterization of rat brain protein phosphatase 2A containing a 72-kDa delta/B" subunit.* J Biochem, 1997. **122**(1): p. 178-87.
64. McCright, B., A.R. Brothman, and D.M. Virshup, *Assignment of human protein phosphatase 2A regulatory subunit genes b56alpha, b56beta, b56gamma, b56delta, and b56epsilon (PPP2R5A-PPP2R5E), highly expressed in muscle and brain, to chromosome regions 1q41, 11q12, 3p21, 6p21.1, and 7p11.2 --> p12.* Genomics, 1996. **36**(1): p. 168-70.
65. Creyghton, M.P., et al., *PR72, a novel regulator of Wnt signaling required for Naked cuticle function.* Genes Dev, 2005. **19**(3): p. 376-86.
66. Creyghton, M.P., et al., *PR130 is a modulator of the Wnt-signaling cascade that counters repression of the antagonist Naked cuticle.* Proc Natl Acad Sci U S A, 2006. **103**(14): p. 5397-402.
67. Voorhoeve, P.M., E.M. Hijmans, and R. Bernards, *Functional interaction between a novel protein phosphatase 2A regulatory subunit, PR59, and the retinoblastoma-related p107 protein.* Oncogene, 1999. **18**(2): p. 515-24.
68. Hendrix, P., et al., *Structure and expression of a 72-kDa regulatory subunit of protein phosphatase 2A. Evidence for different size forms produced by alternative splicing.* J Biol Chem, 1993. **268**(20): p. 15267-76.
69. Moreno, C.S., et al., *WD40 repeat proteins striatin and S/G(2) nuclear autoantigen are members of a novel family of calmodulin-binding proteins that associate with protein phosphatase 2A.* J Biol Chem, 2000. **275**(8): p. 5257-63.
70. Klee, C.B., T.H. Crouch, and M.H. Krinks, *Calcineurin: a calcium- and calmodulin-binding protein of the nervous system.* Proc Natl Acad Sci U S A, 1979. **76**(12): p. 6270-3.
71. Klee, C.B., H. Ren, and X. Wang, *Regulation of the calmodulin-stimulated protein phosphatase, calcineurin.* J Biol Chem, 1998. **273**(22): p. 13367-70.
72. Wang, M.G., et al., *Calcineurin A alpha (PPP3CA), calcineurin A beta (PPP3CB) and calcineurin B (PPP3R1) are located on human chromosomes 4, 10q21-->q22 and 2p16-->p15 respectively.* Cytogenet Cell Genet, 1996. **72**(2-3): p. 236-41.
73. Rusnak, F. and P. Mertz, *Calcineurin: form and function.* Physiol Rev, 2000. **80**(4): p. 1483-521.
74. Verin, A.D., et al., *Characterization of the protein phosphatase 1 catalytic subunit in endothelium: involvement in contractile responses.* J Cell Biochem, 2000. **79**(1): p. 113-25.
75. Hartshorne, D.J. and K. Hirano, *Interactions of protein phosphatase type 1, with a focus on myosin phosphatase.* Mol Cell Biochem, 1999. **190**(1-2): p. 79-84.

76. Totsukawa, G., et al., *Distinct roles of ROCK (Rho-kinase) and MLCK in spatial regulation of MLC phosphorylation for assembly of stress fibers and focal adhesions in 3T3 fibroblasts.* J Cell Biol, 2000. **150**(4): p. 797-806.
77. Alessi, D., et al., *The control of protein phosphatase-1 by targetting subunits. The major myosin phosphatase in avian smooth muscle is a novel form of protein phosphatase-1.* Eur J Biochem, 1992. **210**(3): p. 1023-35.
78. Shimizu, H., et al., *Characterization of the myosin-binding subunit of smooth muscle myosin phosphatase.* J Biol Chem, 1994. **269**(48): p. 30407-11.
79. Machida, H., et al., *Molecular cloning and analysis of the 5'-flanking region of the human MYPT1 gene.* Biochim Biophys Acta, 2001. **1517**(3): p. 424-9.
80. Okubo, S., et al., *A regulatory subunit of smooth muscle myosin bound phosphatase.* Biochem Biophys Res Commun, 1994. **200**(1): p. 429-34.
81. Ito, M., et al., *Myosin phosphatase: structure, regulation and function.* Mol Cell Biochem, 2004. **259**(1-2): p. 197-209.
82. Ichikawa, K., et al., *Interactions and properties of smooth muscle myosin phosphatase.* Biochemistry, 1996. **35**(20): p. 6313-20.
83. Toth, A., et al., *Phosphorylation of MYPT1 by protein kinase C attenuates interaction with PP1 catalytic subunit and the 20 kDa light chain of myosin.* FEBS Lett, 2000. **484**(2): p. 113-7.
84. Patil, S.B. and K.N. Bitar, *RhoA- and PKC-alpha-mediated phosphorylation of MYPT and its association with HSP27 in colonic smooth muscle cells.* Am J Physiol Gastrointest Liver Physiol, 2006. **290**(1): p. G83-95.
85. Eto, M., et al., *A novel protein phosphatase-1 inhibitory protein potentiated by protein kinase C. Isolation from porcine aorta media and characterization.* J Biochem, 1995. **118**(6): p. 1104-7.
86. Fujioka, M., et al., *A new isoform of human myosin phosphatase targeting/regulatory subunit (MYPT2): cDNA cloning, tissue expression, and chromosomal mapping.* Genomics, 1998. **49**(1): p. 59-68.
87. Arimura, T., et al., *Identification, characterization, and functional analysis of heart-specific myosin light chain phosphatase small subunit.* J Biol Chem, 2001. **276**(9): p. 6073-82.
88. Tan, I., et al., *Phosphorylation of a novel myosin binding subunit of protein phosphatase 1 reveals a conserved mechanism in the regulation of actin cytoskeleton.* J Biol Chem, 2001. **276**(24): p. 21209-16.
89. Csortos, C., I. Kolosova, and A.D. Verin, *Regulation of vascular endothelial cell barrier function and cytoskeleton structure by protein phosphatases of the PPP family.* Am J Physiol Lung Cell Mol Physiol, 2007. **293**(4): p. L843-54.
90. Skinner, J.A. and A.R. Saltiel, *Cloning and identification of MYPT3: a prenylatable myosin targetting subunit of protein phosphatase 1.* Biochem J, 2001. **356**(Pt 1): p. 257-67.
91. Cao, W., et al., *TIMAP, a novel CAAX box protein regulated by TGF-beta1 and expressed in endothelial cells.* Am J Physiol Cell Physiol, 2002. **283**(1): p. C327-37.
92. Csortos, C., et al., *TIMAP is a positive regulator of pulmonary endothelial barrier function.* Am J Physiol Lung Cell Mol Physiol, 2008. **295**(3): p. L440-50.
93. Czikora, I., et al., *Characterization of the effect of TIMAP phosphorylation on its interaction with protein phosphatase 1.* Biochimie, 2011. **93**(7): p. 1139-1145.

94. Kim, K., et al., *The protein phosphatase-1 targeting subunit TIMAP regulates LAMR1 phosphorylation.* Biochem Biophys Res Commun, 2005. **338**(3): p. 1327-34.
95. Adyshev, D.M., I.A. Kolosova, and A.D. Verin, *Potential protein partners for the human TIMAP revealed by bacterial two-hybrid screening.* Mol Biol Rep, 2006. **33**(2): p. 83-9.
96. Pato, M.D., et al., *Smooth-muscle caldesmon phosphatase is SMP-I, a type 2A protein phosphatase.* Biochem J, 1993. **293**(Pt 1): p. 35-41.
97. Cairns, J., et al., *Dephosphorylation of the small heat shock protein Hsp27 in vivo by protein phosphatase 2A.* J Biol Chem, 1994. **269**(12): p. 9176-83.
98. Yamamoto, H., et al., *Dephosphorylation of fetal-tau and paired helical filaments-tau by protein phosphatases 1 and 2A and calcineurin.* J Biochem (Tokyo), 1995. **118**(6): p. 1224-31.
99. Ambach, A., et al., *The serine phosphatases PP1 and PP2A associate with and activate the actin-binding protein cofilin in human T lymphocytes.* Eur J Immunol, 2000. **30**(12): p. 3422-31.
100. Witt, C.J., et al., *Interrelationship between protein phosphatase-2A and cytoskeletal architecture during the endothelial cell response to soluble products produced by human head and neck cancer.* Otolaryngol Head Neck Surg, 2000. **122**(5): p. 721-7.
101. Tar, K., et al., *Role of protein phosphatase 2A in the regulation of endothelial cell cytoskeleton structure.* J Cell Biochem, 2006. **98**(4): p. 931-53.
102. Takizawa, N., N. Niiro, and M. Ikebe, *Dephosphorylation of the two regulatory components of myosin phosphatase, MBS and CPI17.* FEBS Lett, 2002. **515**(1-3): p. 127-32.
103. Lontay, B., et al., *Okadaic acid induces phosphorylation and translocation of myosin phosphatase target subunit 1 influencing myosin phosphorylation, stress fiber assembly and cell migration in HepG2 cells.* Cell Signal, 2005. **17**(10): p. 1265-75.
104. Verin, A.D., et al., *Role of Ca2+/calmodulin-dependent phosphatase 2B in thrombin-induced endothelial cell contractile responses.* Am J Physiol, 1998. **275**(4 Pt 1): p. L788-99.
105. Kolozsvari, B., et al., *Role of calcineurin in thrombin-mediated endothelial cell contraction.* Cytometry A, 2009. **75**(5): p. 405-11.
106. Verin, A.D., et al., *Role of Ca2+/calmodulin-dependent phosphatase 2B in thrombin-induced endothelial cell contractile responses.* Am J Physiol, 1998. **275**(4 Pt 1): p. L788-99.
107. Kolozsvari, B., et al., *Calcineurin regulates endothelial barrier function by interaction with and dephosphorylation of myosin phosphatase.* Cardiovasc Res, 2012. **96**(3): p. 494-503.
108. Morais Cabral, J.H., et al., *Crystal structure of a PDZ domain.* Nature, 1996. **382**(6592): p. 649-52.
109. Fanning, A.S. and J.M. Anderson, *Protein-protein interactions: PDZ domain networks.* Curr Biol, 1996. **6**(11): p. 1385-8.
110. Shenolikar, S., et al., *N-terminal PDZ domain is required for NHERF dimerization.* FEBS Lett, 2001. **489**(2-3): p. 233-6.
111. Li, J., A. Mahajan, and M.D. Tsai, *Ankyrin repeat: a unique motif mediating protein-protein interactions.* Biochemistry, 2006. **45**(51): p. 15168-78.
112. Mosavi, L.K., et al., *The ankyrin repeat as molecular architecture for protein recognition.* Protein Sci, 2004. **13**(6): p. 1435-48.

113. van der Voorn, L. and H.L. Ploegh, *The WD-40 repeat.* FEBS Lett, 1992. **307**(2): p. 131-4.
114. Sondek, J., et al., *Crystal structure of a G-protein beta gamma dimer at 2.1A resolution.* Nature, 1996. **379**(6563): p. 369-74.
115. Donowitz, M., et al., *NHERF family and NHE3 regulation.* J Physiol, 2005. **567**(Pt 1): p. 3-11.
116. Weinman, E.J., et al., *Characterization of a protein cofactor that mediates protein kinase A regulation of the renal brush border membrane Na(+)-H+ exchanger.* J Clin Invest, 1995. **95**(5): p. 2143-9.
117. Reczek, D., M. Berryman, and A. Bretscher, *Identification of EBP50: A PDZ-containing phosphoprotein that associates with members of the ezrin-radixin-moesin family.* J Cell Biol, 1997. **139**(1): p. 169-79.
118. Weinman, E.J., et al., *Structure-function of recombinant Na/H exchanger regulatory factor (NHE-RF).* J Clin Invest, 1998. **101**(10): p. 2199-206.
119. LaLonde, D.P., D. Garbett, and A. Bretscher, *A regulated complex of the scaffolding proteins PDZK1 and EBP50 with ezrin contribute to microvillar organization.* Mol Biol Cell, 2010. **21**(9): p. 1519-29.
120. Fievet, B., D. Louvard, and M. Arpin, *ERM proteins in epithelial cell organization and functions.* Biochim Biophys Acta, 2007. **1773**(5): p. 653-60.
121. Ingraffea, J., D. Reczek, and A. Bretscher, *Distinct cell type-specific expression of scaffolding proteins EBP50 and E3KARP: EBP50 is generally expressed with ezrin in specific epithelia, whereas E3KARP is not.* Eur J Cell Biol, 2002. **81**(2): p. 61-8.
122. Baeyens, N., et al., *Identification and functional implication of a Rho kinase-dependent moesin-EBP50 interaction in noradrenaline-stimulated artery.* Am J Physiol Cell Physiol, 2010. **299**(6): p. C1530-40.
123. Shibata, T., et al., *EBP50, a beta-catenin-associating protein, enhances Wnt signaling and is over-expressed in hepatocellular carcinoma.* Hepatology, 2003. **38**(1): p. 178-186.
124. Fouassier, L., et al., *Evidence for ezrin-radixin-moesin-binding phosphoprotein 50 (EBP50) self-association through PDZ-PDZ interactions.* J Biol Chem, 2000. **275**(32): p. 25039-45.
125. Bhattacharya, S., et al., *A conformational switch in the scaffolding protein NHERF1 controls autoinhibition and complex formation.* J Biol Chem, 2010. **285**(13): p. 9981-94.
126. Lau, A.G. and R.A. Hall, *Oligomerization of NHERF-1 and NHERF-2 PDZ domains: differential regulation by association with receptor carboxyl-termini and by phosphorylation.* Biochemistry, 2001. **40**(29): p. 8572-80.
127. Cunningham, R., et al., *Role of NHERF and scaffolding proteins in proximal tubule transport.* Urol Res, 2010. **38**(4): p. 257-62.
128. Fouassier, L., et al., *Protein kinase C regulates the phosphorylation and oligomerization of ERM binding phosphoprotein 50.* Exp Cell Res, 2005. **306**(1): p. 264-73.
129. Hall, R.A., et al., *G protein-coupled receptor kinase 6A phosphorylates the Na(+)/H(+) exchanger regulatory factor via a PDZ domain-mediated interaction.* J Biol Chem, 1999. **274**(34): p. 24328-34.
130. He, J., et al., *Phosphorylation and cell cycle-dependent regulation of Na+/H+ exchanger regulatory factor-1 by Cdc2 kinase.* J Biol Chem, 2001. **276**(45): p. 41559-65.

131. Voltz, J.W., et al., *Phosphorylation of PDZ1 domain attenuates NHERF-1 binding to cellular targets.* J Biol Chem, 2007. **282**(46): p. 33879-87.
132. Garbett, D., D.P. LaLonde, and A. Bretscher, *The scaffolding protein EBP50 regulates microvillar assembly in a phosphorylation-dependent manner.* J Cell Biol, 2010. **191**(2): p. 397-413.
133. Raghuram, V., H. Hormuth, and J.K. Foskett, *A kinase-regulated mechanism controls CFTR channel gating by disrupting bivalent PDZ domain interactions.* Proc Natl Acad Sci U S A, 2003. **100**(16): p. 9620-5.
134. Ron, D., et al., *Cloning of an intracellular receptor for protein kinase C: a homolog of the beta subunit of G proteins.* Proc Natl Acad Sci U S A, 1994. **91**(3): p. 839-43.
135. Ron, D., J. Luo, and D. Mochly-Rosen, *C2 region-derived peptides inhibit translocation and function of beta protein kinase C in vivo.* J Biol Chem, 1995. **270**(41): p. 24180-7.
136. Stebbins, E.G. and D. Mochly-Rosen, *Binding specificity for RACK1 resides in the V5 region of beta II protein kinase C.* J Biol Chem, 2001. **276**(32): p. 29644-50.
137. Rigas, A.C., et al., *The scaffolding protein RACK1 interacts with androgen receptor and promotes cross-talk through a protein kinase C signaling pathway.* J Biol Chem, 2003. **278**(46): p. 46087-93.
138. Birikh, K.R., et al., *Interaction of "readthrough" acetylcholinesterase with RACK1 and PKCbeta II correlates with intensified fear-induced conflict behavior.* Proc Natl Acad Sci U S A, 2003. **100**(1): p. 283-8.
139. Yarwood, S.J., et al., *The RACK1 signaling scaffold protein selectively interacts with the cAMP-specific phosphodiesterase PDE4D5 isoform.* J Biol Chem, 1999. **274**(21): p. 14909-17.
140. Okano, K., et al., *RACK1 binds to Smad3 to modulate transforming growth factor-beta1-stimulated alpha2(I) collagen transcription in renal tubular epithelial cells.* J Biol Chem, 2006. **281**(36): p. 26196-204.
141. Chang, B.Y., R.A. Harte, and C.A. Cartwright, *RACK1: a novel substrate for the Src protein-tyrosine kinase.* Oncogene, 2002. **21**(50): p. 7619-29.
142. Sondek, J. and D.P. Siderovski, *Ggamma-like (GGL) domains: new frontiers in G-protein signaling and beta-propeller scaffolding.* Biochem Pharmacol, 2001. **61**(11): p. 1329-37.
143. Del Vecchio, I., et al., *Functional mapping of the promoter region of the GNB2L1 human gene coding for RACK1 scaffold protein.* Gene, 2009. **430**(1-2): p. 17-29.
144. Wang, S., et al., *Cloning, expression and genomic structure of a novel human GNB2L1 gene, which encodes a receptor of activated protein kinase C (RACK).* Mol Biol Rep, 2003. **30**(1): p. 53-60.
145. Chou, Y.C., et al., *Structure and genomic organization of porcine RACK1 gene.* Biochim Biophys Acta, 1999. **1489**(2-3): p. 315-22.
146. Al-Reefy, S., et al., *Evidence for a pro-apoptotic function of RACK1 in human breast cancer.* Oncogene, 2010. **29**(41): p. 5651; author reply 5652.
147. Al-Reefy, S. and K. Mokbel, *The role of RACK1 as an independent prognostic indicator in human breast cancer.* Breast Cancer Res Treat, 2010. **123**(3): p. 911; author reply 912.
148. Nagashio, R., et al., *Expression of RACK1 is a novel biomarker in pulmonary adenocarcinomas.* Lung Cancer, 2010. **69**(1): p. 54-9.

149. Adams, D.R., D. Ron, and P.A. Kiely, *RACK1, A multifaceted scaffolding protein: Structure and function.* Cell Commun Signal, 2011. **9**: p. 22.
150. Chang, B.Y., M. Chiang, and C.A. Cartwright, *The interaction of Src and RACK1 is enhanced by activation of protein kinase C and tyrosine phosphorylation of RACK1.* J Biol Chem, 2001. **276**(23): p. 20346-56.
151. Chang, B.Y., et al., *RACK1, a receptor for activated C kinase and a homolog of the beta subunit of G proteins, inhibits activity of src tyrosine kinases and growth of NIH 3T3 cells.* Mol Cell Biol, 1998. **18**(6): p. 3245-56.
152. Arimoto, K., et al., *Formation of stress granules inhibits apoptosis by suppressing stress-responsive MAPK pathways.* Nat Cell Biol, 2008. **10**(11): p. 1324-32.
153. Thornton, C., et al., *Spatial and temporal regulation of RACK1 function and N-methyl-D-aspartate receptor activity through WD40 motif-mediated dimerization.* J Biol Chem, 2004. **279**(30): p. 31357-64.
154. Yaka, R., et al., *Pituitary adenylate cyclase-activating polypeptide (PACAP(1-38)) enhances N-methyl-D-aspartate receptor function and brain-derived neurotrophic factor expression via RACK1.* J Biol Chem, 2003. **278**(11): p. 9630-8.
155. Bird, R.J., G.S. Baillie, and S.J. Yarwood, *Interaction with receptor for activated C-kinase 1 (RACK1) sensitizes the phosphodiesterase PDE4D5 towards hydrolysis of cAMP and activation by protein kinase C.* Biochem J, 2010. **432**(1): p. 207-16.
156. Yaka, R., et al., *NMDA receptor function is regulated by the inhibitory scaffolding protein, RACK1.* Proc Natl Acad Sci U S A, 2002. **99**(8): p. 5710-5.
157. O'Donovan, H.C., P.A. Kiely, and R. O'Connor, *Effects of RACK1 on cell migration and IGF-I signalling in cardiomyoctes are not dependent on an association with the IGF-IR.* Cell Signal, 2007. **19**(12): p. 2588-95.
158. Hermanto, U., et al., *RACK1, an insulin-like growth factor I (IGF-I) receptor-interacting protein, modulates IGF-I-dependent integrin signaling and promotes cell spreading and contact with extracellular matrix.* Mol Cell Biol, 2002. **22**(7): p. 2345-65.
159. Besson, A., T.L. Wilson, and V.W. Yong, *The anchoring protein RACK1 links protein kinase Cepsilon to integrin beta chains. Requirements for adhesion and motility.* J Biol Chem, 2002. **277**(24): p. 22073-84.
160. Yang, J., et al., *Receptor for activated C kinase 1 (RACK1) inhibits function of transient receptor potential (TRP)-type channel Pkd2L1 through physical interaction.* J Biol Chem, 2012. **287**(9): p. 6551-61.
161. Isacson, C.K., et al., *RACK1 is a BKCa channel binding protein.* Am J Physiol Cell Physiol, 2007. **292**(4): p. C1459-66.
162. Link, A.J., et al., *Direct analysis of protein complexes using mass spectrometry.* Nat Biotechnol, 1999. **17**(7): p. 676-82.
163. Ji, H., et al., *Coordinated assembly of human translation initiation complexes by the hepatitis C virus internal ribosome entry site RNA.* Proc Natl Acad Sci U S A, 2004. **101**(49): p. 16990-5.
164. Coyle, S.M., W.V. Gilbert, and J.A. Doudna, *Direct link between RACK1 function and localization at the ribosome in vivo.* Mol Cell Biol, 2009. **29**(6): p. 1626-34.
165. Nilsson, J., et al., *Regulation of eukaryotic translation by the RACK1 protein: a platform for signalling molecules on the ribosome.* EMBO Rep, 2004. **5**(12): p. 1137-41.

166. Giaever, I. and C.R. Keese, *A morphological biosensor for mammalian cells.* Nature, 1993. **366**(6455): p. 591-2.
167. Keese, C.R., et al., *Electrical wound-healing assay for cells in vitro.* Proc Natl Acad Sci U S A, 2004. **101**(6): p. 1554-9.
168. Hsu, C.C., et al., *Effects of negative pressures on epithelial tight junctions and migration in wound healing.* Am J Physiol Cell Physiol, 2010. **299**(2): p. C528-34.
169. Candiano, G., et al., *Blue silver: a very sensitive colloidal Coomassie G-250 staining for proteome analysis.* Electrophoresis, 2004. **25**(9): p. 1327-33.
170. Vereb, G., et al., *Cholesterol-dependent clustering of IL-2Ralpha and its colocalization with HLA and CD48 on T lymphoma cells suggest their functional association with lipid rafts.* Proc Natl Acad Sci U S A, 2000. **97**(11): p. 6013-8.
171. Sharma, G.D., J. He, and H.E. Bazan, *p38 and ERK1/2 coordinate cellular migration and proliferation in epithelial wound healing: evidence of cross-talk activation between MAP kinase cascades.* J Biol Chem, 2003. **278**(24): p. 21989-97.
172. Li, L., et al., *Phosphorylation of TIMAP by glycogen synthase kinase-3beta activates its associated protein phosphatase 1.* J Biol Chem, 2007. **282**(35): p. 25960-9.
173. Rodriguez, M.M., et al., *RACK1, a protein kinase C anchoring protein, coordinates the binding of activated protein kinase C and select pleckstrin homology domains in vitro.* Biochemistry, 1999. **38**(42): p. 13787-94.
174. Bhat, R., et al., *Structural insights and biological effects of glycogen synthase kinase 3-specific inhibitor AR-A014418.* J Biol Chem, 2003. **278**(46): p. 45937-45.
175. Wade, J.B., et al., *Differential renal distribution of NHERF isoforms and their colocalization with NHE3, ezrin, and ROMK.* Am J Physiol Cell Physiol, 2001. **280**(1): p. C192-8.
176. Hall, R.A., et al., *A C-terminal motif found in the beta2-adrenergic receptor, P2Y1 receptor and cystic fibrosis transmembrane conductance regulator determines binding to the Na+/H+ exchanger regulatory factor family of PDZ proteins.* Proc Natl Acad Sci U S A, 1998. **95**(15): p. 8496-501.
177. Schmieder, S., et al., *Podocalyxin activates RhoA and induces actin reorganization through NHERF1 and Ezrin in MDCK cells.* J Am Soc Nephrol, 2004. **15**(9): p. 2289-98.
178. Weinman, E.J., et al., *The association of NHERF adaptor proteins with g protein-coupled receptors and receptor tyrosine kinases.* Annu Rev Physiol, 2006. **68**: p. 491-505.
179. Fouassier, L., et al., *Ezrin-radixin-moesin-binding phosphoprotein (EBP50), an estrogen-inducible scaffold protein, contributes to biliary epithelial cell proliferation.* Am J Pathol, 2009. **174**(3): p. 869-80.
180. Shibata, T., et al., *EBP50, a beta-catenin-associating protein, enhances Wnt signaling and is over-expressed in hepatocellular carcinoma.* Hepatology, 2003. **38**(1): p. 178-86.
181. Li, X., et al., *Temporal and Spatial Regulation of Ezrin-Radixin-Moesin-Binding Phosphoprotein-50-kDa (EBP50) during Embryo Implantation in Mouse Uterus.* Int J Mol Sci, 2012. **13**(12): p. 16418-29.
182. Muranen, T., et al., *Cell cycle-dependent nucleocytoplasmic shuttling of the neurofibromatosis 2 tumour suppressor merlin.* Oncogene, 2005. **24**(7): p. 1150-8.

183. Batchelor, C.L., A.M. Woodward, and D.H. Crouch, *Nuclear ERM (ezrin, radixin, moesin) proteins: regulation by cell density and nuclear import.* Exp Cell Res, 2004. **296**(2): p. 208-22.
184. Kutay, U. and M.W. Hetzer, *Reorganization of the nuclear envelope during open mitosis.* Curr Opin Cell Biol, 2008. **20**(6): p. 669-77.
185. Nigg, E.A., *Nucleocytoplasmic transport: signals, mechanisms and regulation.* Nature, 1997. **386**(6627): p. 779-87.
186. Baeyens, N., et al., *EBP50 is involved in the regulation of vascular smooth muscle cell migration and cytokinesis.* J Cell Biochem, 2011. **112**(9): p. 2574-84.
187. Dai, J.L., et al., *NHERF (Na+/H+ exchanger regulatory factor) gene mutations in human breast cancer.* Oncogene, 2004. **23**(53): p. 8681-7.
188. Pan, Y., L. Wang, and J.L. Dai, *Suppression of breast cancer cell growth by Na+/H+ exchanger regulatory factor 1 (NHERF1).* Breast Cancer Res, 2006. **8**(6): p. R63.
189. Wang, S., et al., *Peptide binding consensus of the NHE-RF-PDZ1 domain matches the C-terminal sequence of cystic fibrosis transmembrane conductance regulator (CFTR).* FEBS Lett, 1998. **427**(1): p. 103-8.
190. Schmitz, M.H., et al., *Live-cell imaging RNAi screen identifies PP2A-B55alpha and importin-beta1 as key mitotic exit regulators in human cells.* Nat Cell Biol, 2010. **12**(9): p. 886-93.
191. Wu, J.Q., et al., *PP1-mediated dephosphorylation of phosphoproteins at mitotic exit is controlled by inhibitor-1 and PP1 phosphorylation.* Nat Cell Biol, 2009. **11**(5): p. 644-51.
192. Mochida, S., et al., *Regulated activity of PP2A-B55 delta is crucial for controlling entry into and exit from mitosis in Xenopus egg extracts.* EMBO J, 2009. **28**(18): p. 2777-85.
193. Koehler, J.A. and M.F. Moran, *RACK1, a protein kinase C scaffolding protein, interacts with the PH domain of p120GAP.* Biochem Biophys Res Commun, 2001. **283**(4): p. 888-95.
194. Liedtke, C.M. and X. Wang, *The N-terminus of the WD5 repeat of human RACK1 binds to airway epithelial NHERF1.* Biochemistry, 2006. **45**(34): p. 10270-7.
195. Bourd-Boittin, K., et al., *RACK1, a new ADAM12 interacting protein. Contribution to liver fibrogenesis.* J Biol Chem, 2008. **283**(38): p. 26000-9.
196. Kiely, P.A., et al., *Insulin-like growth factor I controls a mutually exclusive association of RACK1 with protein phosphatase 2A and beta1 integrin to promote cell migration.* Mol Cell Biol, 2006. **26**(11): p. 4041-51.
197. Chiba, Y., et al., *A functional interaction between CPI-17 and RACK1 proteins in bronchial smooth muscle cells.* Biochem Biophys Res Commun, 2010. **401**(3): p. 487-90.
198. Kiely, P.A., et al., *Tyrosine 302 in RACK1 is essential for insulin-like growth factor-I-mediated competitive binding of PP2A and beta1 integrin and for tumor cell proliferation and migration.* J Biol Chem, 2008. **283**(34): p. 22952-61.
199. Birukova, A.A., et al., *Protein kinase A attenuates endothelial cell barrier dysfunction induced by microtubule disassembly.* Am J Physiol Lung Cell Mol Physiol, 2004. **287**(1): p. L86-93.
200. Baumer, Y., et al., *Role of Rac 1 and cAMP in endothelial barrier stabilization and thrombin-induced barrier breakdown.* J Cell Physiol, 2009. **220**(3): p. 716-26.

201. Li, S., et al., *Rack1 is required for Vangl2 membrane localization and planar cell polarity signaling while attenuating canonical Wnt activity.* Proc Natl Acad Sci U S A, 2011. **108**(6): p. 2264-9.
202. Casey, P.J., *Biochemistry of protein prenylation.* J Lipid Res, 1992. **33**(12): p. 1731-40.
203. Dalby, M.J., A. Hart, and S.J. Yarwood, *The effect of the RACK1 signalling protein on the regulation of cell adhesion and cell contact guidance on nanometric grooves.* Biomaterials, 2008. **29**(3): p. 282-9.
204. Li, J., et al., *Receptor for activated C kinase 1 (RACK1): a regulator for migration and invasion in oral squamous cell carcinoma cells.* J Cancer Res Clin Oncol, 2012. **138**(4): p. 563-71.
205. Knezevic, N., et al., *The G protein betagamma subunit mediates reannealing of adherens junctions to reverse endothelial permeability increase by thrombin.* J Exp Med, 2009. **206**(12): p. 2761-77.
206. Belvitch, P. and S.M. Dudek, *Role of FAK in S1P-regulated endothelial permeability.* Microvasc Res, 2012. **83**(1): p. 22-30.
207. Paik, J.H., et al., *Sphingosine 1-phosphate receptor regulation of N-cadherin mediates vascular stabilization.* Genes Dev, 2004. **18**(19): p. 2392-403.

Keywords

Adaptor proteins

Barrier function

ECIS (electrical cellsubstrate impedence sensing)

Endothelium

Protein phosphatases

RACK1

TIMAP

Acknowledgement

I am particularly grateful to my supervisor Dr. Csilla Csortos for her support and guidance during the years of my Ph.D. education.

I would also like to thank Prof. László Virág and Prof. Pál Gergely, our current and previous heads of the Department of Medical Chemistry for giving me all the support for my work.

Many thanks to Mrs. Andrea Farkas Tanka, Mrs. Ella Kovács Dembrovszki, Mrs. Erzsébet Herbály and Mrs. Ágota Szántó Kelemen for their excellent technical assistance.

Experimental work was performed by the support of the TÁMOP-4.2.2.A-11/1/KONV-2012-0025 project. The doctoral training program was supported by the TÁMOP-4.2.2/B-10/1-2010-0024 project. The projects are co-financed by the European Union and the European Social Fund.

Appendix

The thesis is based on the following publications:

Boratkó A, Gergely P, Csortos C (2012) Cell Cycle Dependent Association of EBP50 with Protein Phosphatase 2A in Endothelial Cells. PLoS ONE 7(4): e35595. doi:10.1371/journal.pone.0035595

IF: 4.092 (2011)

Boratkó A, Gergely P, Csortos C (2013) RACK1 is involved in endothelial barrier regulation via its two novel interacting partners, Cell Commun Signal. 2013 Jan 11;11(1):2. doi: 10.1186/1478-811X-11-2.

IF: 5.5 (2011)

Register Number: DEENKÉTK/171/2013.
Item Number:
Subject: Ph.D. List of Publications

Candidate: Anita Boratkó

Neptun ID: GIHJDJ

Doctoral School: Doctoral School of Molecular Medicine

List of publications related to the dissertation

1. **Boratkó, A.**, Gergely, P., Csortos, C.: RACK1 is involved in endothelial barrier regulation via its two novel interacting partners.
   Cell Commun Signal. 11 (2), 1-14, 2013.
   DOI: http://dx.doi.org/10.1186/1478-811X-11-2
   IF:5.5 (2011)

2. **Boratkó, A.**, Gergely, P., Csortos, C.: Cell cycle dependent association of EBP50 with protein phosphatise 2A in endothelial cells.
   PLoS One. 7 (4), e35595, 2012.
   DOI: http://dx.doi.org/10.1371/journal.pone.0035595
   IF:4.092 (2011)

List of other publications

3. Szilágyi, O., **Boratkó, A.**, Panyi, G., Hajdú, P.: The role of PSD-95 in the rearrangement of Kv1.3 channels to the immunological synapse.
Pflugers Arch. Epub ahead of print (2013)
DOI: http://dx.doi.org/10.1007/s00424-013-1256-6
IF:4.463 (2011)

Total IF: 14.055

Total IF (publications related to the dissertation): 9.592

The Candidate's publication data submitted to the Publication Database of the University of Debrecen have been validated by Kenezy Life Sciences Library on the basis of Web of Science, Scopus and Journal Citation Report (Impact Factor) databases.

07 May, 2013